State-of-the-art review on water-based nanofluids for low temperature solar thermal collector application

Fazlay Rubbi[a,*], Likhan Das[a], Khairul Habib[a,*], Navid Aslfattahi[b], R. Saidur[c,d], Md Tauhidur Rahman[e]

[a] Department of Mechanical Engineering, Universiti Teknologi PETRONAS, 32610, Bandar Seri Iskandar, Perak Darul Ridzuan, Malaysia

[b] Department of Mechanical Engineering, Faculty of Engineering, University of Malaya, Kuala Lumpur, 50603, Malaysia

[c] Research Centre for Nano-Materials and Energy Technology (RCNMET), School of Science and Technology, Sunway University, No. 5, Jalan Universiti, Bandar Sunway, 47500, Petaling Jaya, Malaysia

[d] Department of Engineering, Lancaster University, Lancaster, LA1 4YW, UK

[e] Department of Petroleum Engineering, Universiti Teknologi PETRONAS, 32610, Bandar Seri Iskandar, Perak Darul Ridzuan, Malaysia

*Corresponding author: Fazlay Rubbi (mdfrs22@gmail.com) and Khairul Habib (khairul.habib@utp.edu.my)

Abstract

In the last decade, nanofluids have set significant milestones as efficient working fluids in the field of solar energy conversion to meet rising energy demand. Research on thermophysical properties, long-term stability, and rheology is progressing to achieve effective practical deployment of nanofluids in renewable solar photo-thermal energy conversion sectors (i.e., solar collectors). Nonetheless, researchers and engineers are having a difficult time coping with nearly infinite culpable variables influencing the output of various types of nanofluids. This paper aims to provide an up-to-date analysis of the developments and challenges of widely used water-based nanofluids, with a focus on formulation methods, main properties (thermophysical, stability, and rheological), and effective implementation in low temperature solar collector systems. Previous experimental and numerical studies on the subject have been compiled and thoroughly scrutinized, providing crucial phenomena, mechanisms, flaws, and responsible parameters for achieving stable and optimized thermal properties that integrate with heat transfer performance. It has been discovered that optimizing the critical factors leads to superior behavior of the nanofluids, which results in improved thermal efficiency of the solar collectors. Finally, emerging concerns are identified, as are potential recommendations to resolve existing problems in the field for future advancement that would mobilize rapid progress and practical engineering use of water based nanofluids on solar collectors.

Keywords: Nanofluids, Thermophysical Properties, Stability, Rheology, Solar Collectors.

Nomenclature

Abbreviations

NF	Nanofluid	DSC	Dynamic Scanning Calorimetry
NP	Nanoparticle	DLVO	Derjaguin Landau Vewey and Overbeek
BF	Base Fluid	ZP	Zeta potential (mV)
HTF	Heat Transfer Fluid	EDL	Electrical double layer
SC	Solar Collector	IEP	Isoelectric Point
TC	Thermal conductivity	FPSC	Flat plate solar collector
d_p	Particle diameter (nm)	ETSC	Evacuated tube solar collector
ECS	Energy Conversion System	DASC	Direct absorber solar collector
CNT	Carbon Nanotube	PV/T	Photovoltaic/thermal solar collector
SWCNT	Single-walled carbon nanotube	UV-Vis	Ultraviolet–visible spectroscopy
MWCNT	Multi-walled carbon nanotube	MDS	Molecular dynamic simulation
EG	Ethylene glycol		
SDS	Sodium Dodecyl Sulphate	***Greek Letters***	
SDBS	Sodium Dodecyl Benzene Sulphonate	μ	Dynamic viscosity (Pa.s)
CTAB	Cetyl Trimethyl Ammonium Bromide	φ	Particle concentration (%)
CTAC	Cetrimonium chloride	ζ	Zeta potential (mV)
GA	Gum Arabic	α	Absorptivity
PVP	Polyvinylpyrrolidone	ε	Dielectric Constant
DDC	Distearyl Dimethylammonium Chloride	***Subscripts***	
PLS	Potassium Lauryl Sulphate		
k	Thermal conductivity (W/m.K)	nf	Nanofluid
c_p	Specific heat capacity (Kj/kg.K)	bf	Base Fluid
T	Temperature (K)	np	Nanoparticle

1. Introduction

1.1. Overview on nanofluid

Nanofluids (NFs) are superior colloids formed by dispersing nanoscale (1-100 nm) materials in pure base fluid (BF), which is usually a liquid. Masuda, et al. [1] synthesized nanoscale suspensions for the first time experimentally in 1993, and Choi and Eastman [2] named them as ‘nanofluid’ in 1995. Due to remarkably extra-large surface area and dominant characteristics of dispersed solid particles of nanomaterials relative to BFs, NFs convey superior heat transfer properties [3]. The surfaces of nanoparticles (NPs) regulate their properties rather than their volume, providing efficient and flexible thermal, optical, mechanical, and electrical properties

[4]. The addition of very low weight concentration of these NPs into conventional heat transfer fluids (HTFs) remarkably enriches essential thermo-physical, optical, and chemical features of the fluids. The important thermo-physical properties of HTFs, such as conductive heat transport and specific heat capacity, have a significant impact on the thermal energy efficiency of cooling fluid-based thermal energy storage and energy conversion systems. Numerous studies have confirmed a considerable escalation in thermal conductivity, specific heat capacity and heat transfer characteristics of nanofluids in comparison with their BFs [5-7]. Beyond all the promising NF characteristics, colloidal stability of suspended NPs in main fluid emerges as the most difficult barrier to overcome, as particles appear to congregate over time. The primary factor in the sustainable use of NFs in various heating and cooling applications is the maintenance of a long suspension period [8]. Furthermore, the excellent properties and suspension stability of NFs are dependent on key parameters such as suspension stability, as well as types of BFs, NPs, particle concentration (φ) and morphology that can cause significant divergence in thermal characteristics.

Water based nanosuspensions are the most researched and used class of nanosuspensions due to the numerous advantages of water as a BF, including higher thermal conductivity and heat capacity than other BFs (i.e., oils and glycols), extreme availability, simplicity, and commercial prospects. Water-based NFs are suitable for low-temperature thermal applications up to 90°C, and they are particularly well-suited for use as HTF in solar energy harvesting due to their advanced photo-thermal properties, relatively good thermal stability, and sustainable nature as compared to other traditional toxic liquids such as ethylene glycol, ionic liquids, and so on. Aside from regular NF (i.e., dispersion of a single distinct nanomaterial in the BF), the hybrid category of NF (i.e., dispersion of two distinct nanomaterials) has piqued the interest of researchers for further advancement [9]. Extensive research articles have been published in recent years that investigate the properties, factors, and future potential of water-adopted NFs in practical fields such as solar thermal collectors. **Fig. 1** represents previous publications reported on water-based NF, which considerably outnumbers other variants of NF in recent years (2015-2020), indicating huge interest in water-based due to its unique properties.

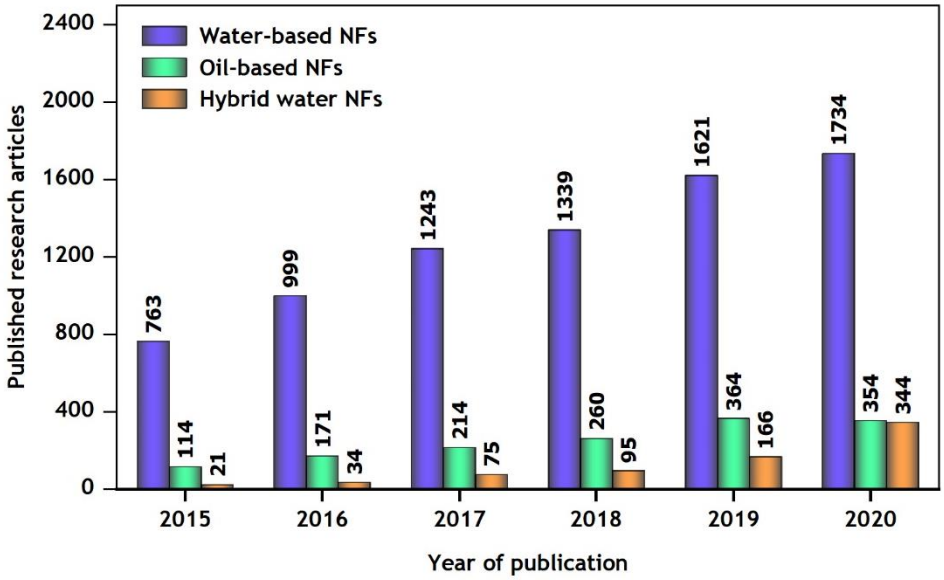

Fig. 1. Published research articles on water, oil and hybrid based nanofluids from year 2015 to 2020 (Source of data: Scopus, using keywords: Water nanofluids, Oil nanofluids and Hybrid water nanofluids).

1.2. Application of nanofluids on solar thermal collectors

Various water based NFs are commonly applied in thermal and thermo-electric heating-cooling systems, including but not limited to heat exchangers [10], automobile cooling [11], photovoltaic cooling [12], building heating [13], industrial process heating, thermo-electric cooling [14], refrigeration systems [15].

However, the dearth of sustainable energy resources has become a sophisticated challenge to meet the ever-growing global energy demand alongside depletion of carbon-based fossil energy resources and their constant threat to the environment. In this context, experts are focusing on the search for alternative renewable energy sources that will be adequate to meet the massive energy demand in the future. Since the energy demand will keep escalating in the future, one way to compensate for the energy scarcity is by utilizing sustainable renewable energy sources. Solar energy is one of the most convenient, pollutant-free, sustainable, renewable and abundantly available energy resources to harvest clean thermal energy [16]. A plethora of research is being conducted on solar energy systems by substituting traditional HTFs with NFs to advance the thermal energy conversion efficiency [17-19]. Solar collector (SC) systems are one of the emerging renewable energy sectors that is rapidly expanding due to the development of NFs as advanced working fluids [20, 21]. SCs are engineered systems to harness solar radiation and produce sustainable energy that can be utilized in different domestic and

industrial heating and cooling processes [22]. Mahian, et al. [23] recently published a review on the advancement of NF-based renewable energy conversion systems (i.e., solar thermal collectors) and their environmental effects. Over the last few years, research and development have resulted in a significant increase in the energy efficiency of various SC systems operated with NFs replacing traditional BFs [17].

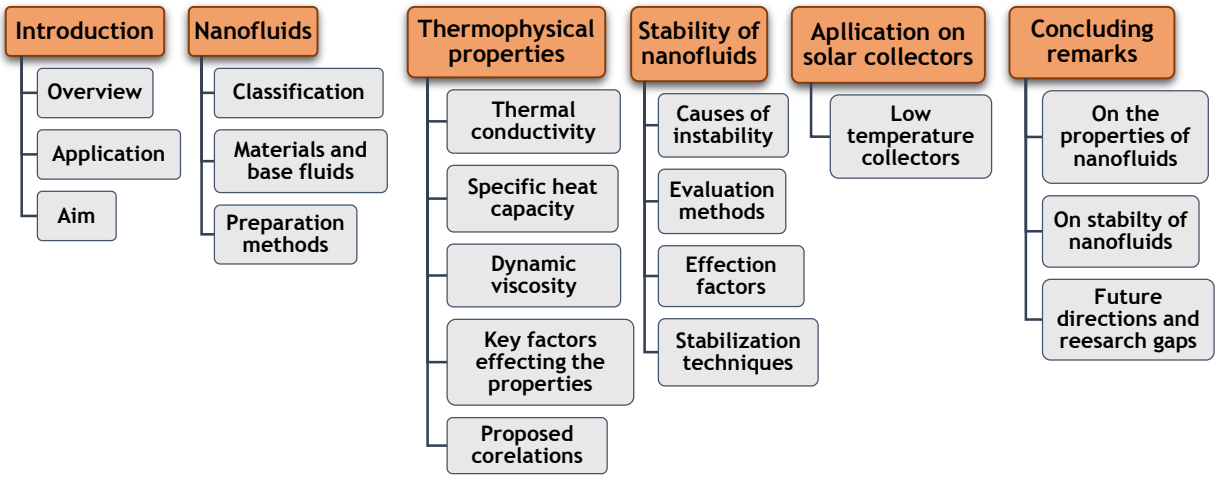

Fig. 2. Overview of layout of this review paper.

1.3. Aim of this review

The aim of this paper is to provide a detailed state-of-the-art analysis on research developments in thermo-physical properties of water-based NFs, as well as suspension stability, and potential implementation in low temperature SC technologies. A few articles [24, 25], attempted to provide a general overview of different properties (thermal and optical) and applications of NFs on SCs, while others while others [8, 26] endeavored to address NF stability issues. Yet, there are no comprehensive review that particularly intends to articulate overall advances on most frequently applied water-based NFs characteristics, stability mechanisms, limitations, and applications on SCs. Therefore, the authors are inspired to provide a much needed, detailed, and up-to-date analysis of the thermo-physical properties (thermal conductivity, cp, and rheology), stability behavior (mechanism, critical parameter, and evaluation techniques), and implementation of the NFs on low temperature thermal SCs to assess their effectiveness. Since water-based NFs are best suited for low-temperature solar collectors, the detailed NF characterization is thoroughly analyzed and compiled from preparation to implementation on SCs to provide a clear understanding of the topic based on extensive previous research. Furthermore, potential properties of NFs are comprehensively discussed, providing causes and effects of several critical parameters and insights of suspension stability are reported. The

application section critically examines the performance of several water-based NF-operated SCs, scrutinizing influential factors to assess the overall impact of the NFs on system performance. Based on the review of extensive experimental and numerical studies, challenging issues and research gaps are identified, important conclusions are drawn based on present developments and recommendations are rendered for further advancement in the field. This study offers an essential step towards robust development and understanding of water-based NFs for implementation in photothermal ECS i.e., SCs. The layout of the article is demonstrated in **Fig. 2**.

2. Nanofluids

2.1. Base fluid and nanomaterials

NFs are developed diffusing nanostructured materials at nanoscale range into pure conventional working fluids. The NF classification based on extensively used BFs and nanomaterials is depicted in **Fig. 3**. Water, oils (thermal, synthetic, and vegetable), glycols (ethylene and propylene), and ionic liquids have all been used as dispersion medium in the formulation of NFs based on thermal systems and working temperature ranges. Each of the fluids has some advantages and drawbacks on their own while implemented on thermal systems. Water-based NFs are superior to other BFs in low temperature applications due to their superior thermo-physical properties, low cost, and availability. In contrast, for medium to high temperature thermal systems, other fluids (oils, glycols, and liquid salts) are generally utilized.

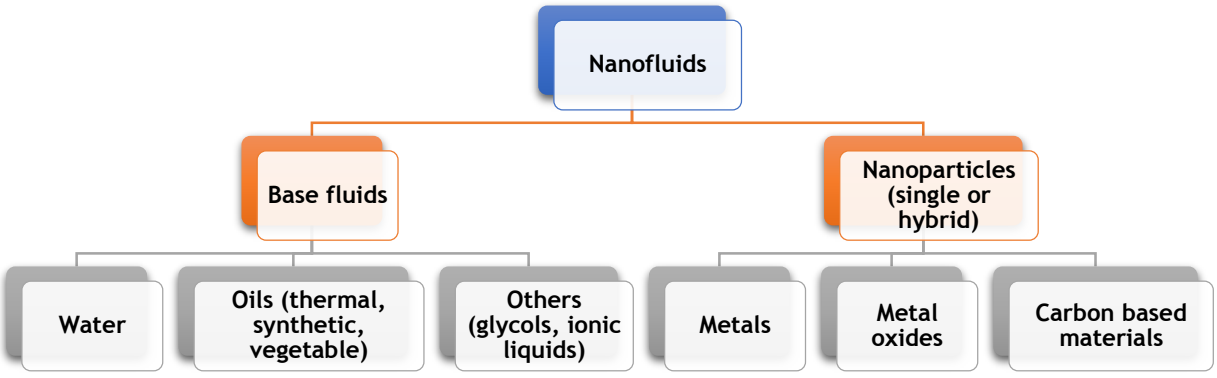

Fig. 3. Classification of nanofluids in terms of base fluids and nanoparticles.

Suspended nanomaterials are the most distinctive feature of NFs as these particles possess unique thermal and optical properties and significantly impact the characteristics of BFs. Nanomaterials have at least one dimension in the nanometer range with high conductive surface

to volume ratio, superior physical, chemical, and mechanical properties relative to their bulk form. Nanomaterials can be metallic (e.g., Ag, Cu, Ti, Fe, Al), polymers, ceramics, non-metallic (CuO, TiO_2, Al_2O_3, SiO_2) and carbon-based (SWCNT, MWCNT, graphene, MXene) materials which are formed in various geometrical shapes such as spherical, cylindrical, rod-like, and pate-like. In terms of their dimensions at the nanoscale, nanostructured materials can be divided into four categories: (a) zero-dimensional (0-D) nanomaterials with no dimensions, such as nanoparticles and graphene/carbon quantum dots; (b) one-dimensional (1-D) nanomaterials with one dimension at the nanoscale range, such as nanotubes and nanowires; (c) Two-dimensional (2-D) nanomaterials with layered nanofilms such as graphene and MXene nanoflakes; (d) Bulk three-dimensional (3-D) nanomaterials that are confined at nanoscale dimensions such as bulk powder, composite nanomaterials and multi-nanolayers. **Fig. 4** represents an illustration of nanostructured materials based on their dimensions at nanoscale length. Colloidal suspension comprises of a BF and one of those types of particles defined as NF. If the suspension is made up of more than one type of dispersed particle in fluid, it is referred to as hybrid NF [27]. Many studies have been published in the literature in which various types of nanomaterials are combined with water to characterize their potency in practical applications. The specifics of the NFs formulation and characterization will be covered in subsequent parts of this study.

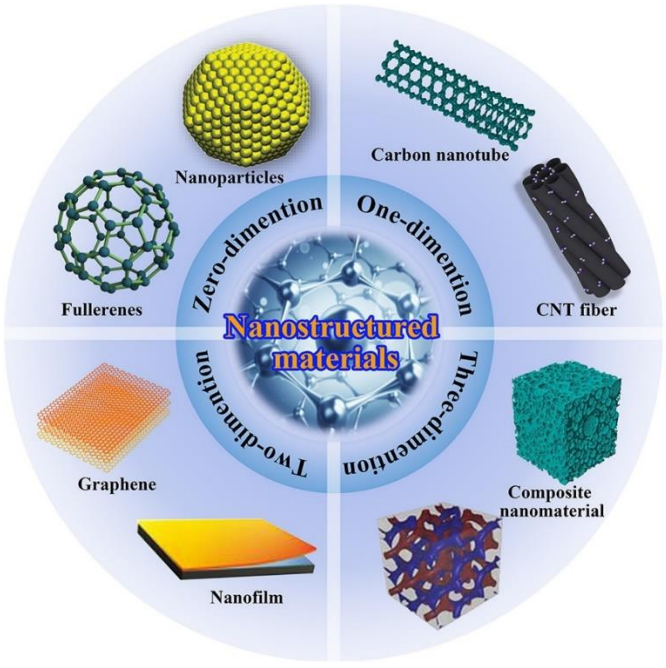

Fig. 4. Demonstration of nanomaterials with unique dimensions at the nanoscale range [4].

2.2. Formulation of nanofluids

NFs are considered advanced thermo-fluids due to their enhanced thermophysical properties, including conductive heat transfer coefficient, thermal conductivity, thermal diffusivity, and heat storage capability, as compared to conventional working fluids such as water and oils. Exceptional properties of NFs are depicted in **Fig. 5**, which are considered necessary in various applications and to perform efficiently according to their advantages over microfluids. The formulation of NF suspension is an important step because it can influence a few main parameters, including suspension stability and thermo-optical properties. The first stage of NF formulation includes the synthesis of nanostructured materials, which are later combined with BF to produce a solid-liquid suspension. In nanotechnology, many physical, chemical, and physiochemical techniques are frequently used to synthesize NPs. Furthermore, during the synthesis process, NPs are assessed using various systematic approaches such as transmission microscopy, infrared spectroscopy, X-ray diffraction, and Raman spectroscopy.

To prepare stable NFs, two standard methods are used: the single-step method, which incorporates two separate procedures of nanoparticle fabrication and dispersion into BF concurrently, and the two-step method, which integrates two separate processes of particle fabrication followed by dispersion using several stabilization techniques for uniform dispersion of solid particles. Both fundamental approaches possess several advantages and drawbacks in terms of flexibility, thermophysical characterization, and economics. The major challenge in nano powder dispersion technology is NP sedimentation over time. Although the single-step technique is stated to generate stable NFs, it is discovered that thermal properties are more predominant when fluids are fabricated in two steps [28]. The following sections address these methods in greater detail.

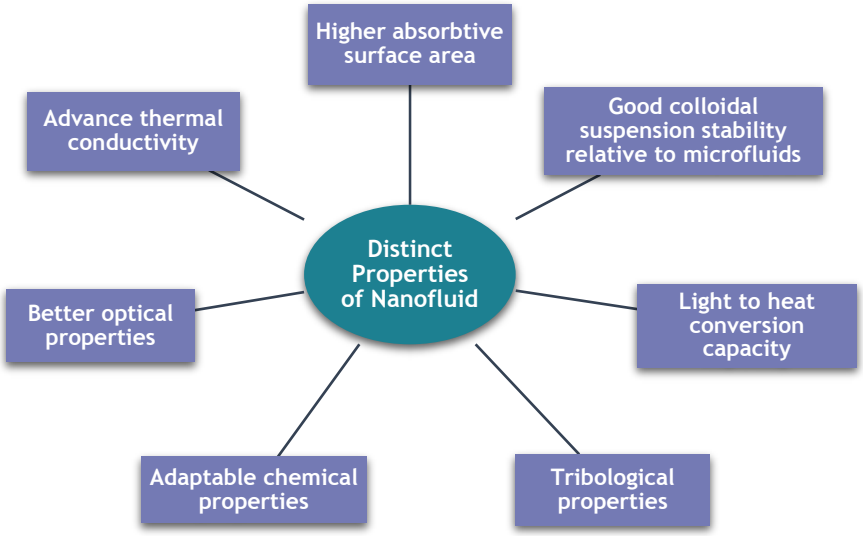

Fig. 5. Distinct advanced properties of nanofluids relative to microfluids.

2.2.1. Two-step technique

The two-step (also recognized as top-down/dispersion) method is the simplest, cost-effective, and scalable technique where solid nanomaterials are independently synthesized and subsequently suspended into a pure fluid and stabilized using chemical dispersants and/or mechanical, physical treatments to formulate stable NF. In the first step, bulk materials are broken down into suitable nano range using several approaches, such as wet-chemical etching and/or physical procedures. The synthesis step also includes a few intermediate processes such as drying of the particles, storage, and the dispersion of the particles. **Fig. 6(a)** categorizes various nanomaterial synthesis techniques. The stabilization step comprises multifarious techniques, for instance, chemical (electrostatic, steric, and electro-steric), and/or physical (ultrasonication, high pressure homogenization and ball milling) treatments. **Fig. 6(b)** construes formulation of NF using the two-step method. Clustering of dry NPs is, however, unavoidable during the drying phase, storage time, and dispersion into BF in this system of NF formulation [29]. The primary drawback of the two-step technique is that the high surface energy of the NPs results in nonhomogeneous particle dispersion, which results in short-term suspension stability and unpredictable thermophysical properties. This shortcoming can be compensated for by repeated physical or chemical treatments that break down the aggregation and maintain the consistency of the mixture over a longer period of time. Sarsam, et al. [30] formulated water-based graphene NFs employing several surfactants (SDBS, SDS and, CTAB) along with ultrasonication as a physical stabilization technique. The study revealed that pristine GNPs are not consistently dispersed in water without dispersants. Inclusion of various surfactants and then performing the ultrasonication for 60 minutes delivered considerably stable suspension for over two months. The addition of different surfactants, followed by ultrasonication for 60 minutes, resulted in a significantly stable suspension for more than two months. Two-step methods are the predominant techniques to formulate NFs due to their simple production procedures, flexibility with parameters and scalable production for industrial usage. This technique is frequently used to formulate carbon-based, metallic, and oxide-based NFs in various base fluids including water. In essence, the two-step method is the suitable technique to formulate and obtain thermo-physical, chemical, and optically enriched NFs at large scale production.

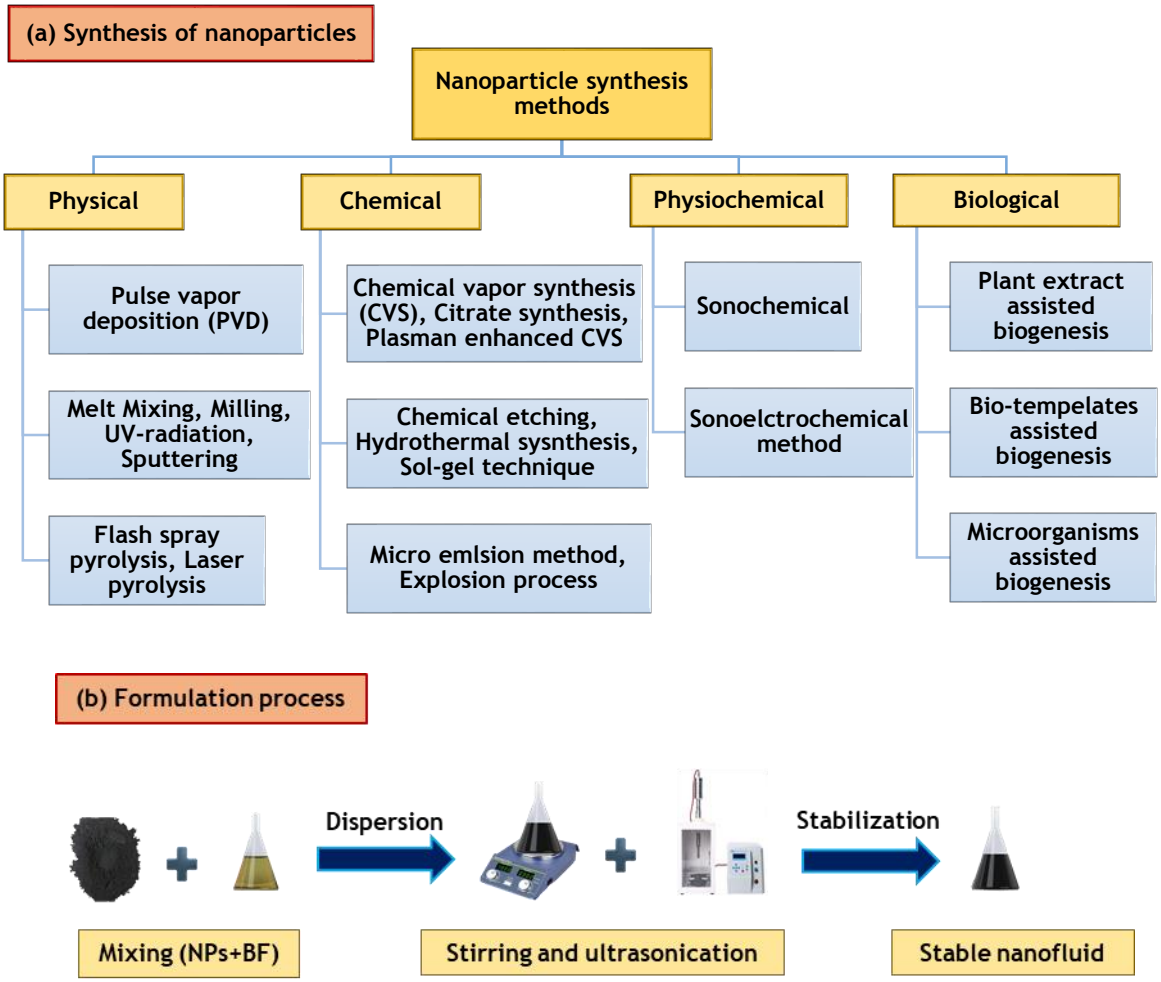

Fig. 6. Formulation of nanofluid in two-step method (a) Synthesis techniques of nanoparticles, (b) dispersion and stabilization of nanomaterials into base fluid.

2.2.2. Single-step technique

The single-step (also familiar as one-step or bottom-up) synthesis technique uses wet-chemistry procedures wherein fabrication of nanomaterials and dispersion into base fluid are performed concurrently to formulate NFs. Several chemical vapor decomposition methods such as plasma arc [31], spraying or sputtering [32], laser ablation [33] and electric explosion [34] techniques are employed to formulate stable nanofluid in this method. These methods eliminate the clustering issues encountered by the two-step process and produce stable suspension of NPs into base fluid. Lo, et al. [35] synthesized CuO/water NF in a single step using Cu wire as the electrode. They revealed that the technique is capable of producing a stable and uniformly distributed suspension without agglomeration of particles. Zhu, et al. [36] introduced an efficient single-step synthesis technique to formulate Cu/ethylene glycol NFs by reducing copper sulfate pentahydrate with sodium hypophosphite solution under microwave radiation. They found this method to be useful for preparing well-dispersed suspensions, and

the reaction rate is stated to be significantly higher when using microwave radiation than conventional heating. Mohammadpoor, et al. [28] developed Cu-based NFs using both single-step and two-step methods and investigated the fluids' thermal properties and stability. They reported that NFs prepared in a single step method were found to be more stable than samples prepared in a two-step technique, whereas the two-step method produced NFs with better heat transfer properties Nonetheless, large-scale fabrication of NFs is unfeasible using the bottom-up approach due to the procedure's complexity and extremely high production cost. Additionally, a few critical parameters, such as particle size and concentration, are difficult to monitor in this fabrication process, as it is based on batch production with limited control over the conditions. The formulation of NFs in single and two-step methods, as well as the stabilization techniques and stability indicator used, are outlined in **Table. 1**.

286 **Table. 1.** Summary of recent studies on NF formulation using standard single step and two-step method along with deployed stabilization
287 techniques.

Nanofluid(s)	**Particle size and concentration (Φ)**	**Surfactants/ Stabilization techniques**	**Formulation method**	**Stability indicator(s)**	**Reference**
Metallic nanofluid					
DI water/Al /Cu	Al (80 nm), Cu (40 nm) Φ = 0.3 vol.%	Sodium dodecyl sulphate (SDS)/ ultrasonication, magnetic stirring.	Two-step	ζ = -41.2 and -38.4 mV respectively	Akash, et al. [11]
DI water/Cu /Fe /Ag	Cu, Fe and Ag (30-50 nm) Φ = 0.1 wt.%	--/Sonication	Single step	7,2 and 5 days, respectively.	Khoshvaght-Aliabadi, et al. [37]
Metal-oxide nanofluids					
Distilled water/ZnO /TiO_2	ZnO (15-30 nm) TiO_2 (21 nm) Φ = 0.15 wt.%	No surfactant used/magnetic stirring, ultrasonication.	Two-Step	ζ = 32 mV ζ = 38.1 mV	Zare, et al. [38]
Water/Al_2O_3	45 nm Φ = 1-3 vol.%	Sodium dodecyl benzene sulfonate (SDBS)/ magnetic stirring, ultrasonic processing.	Two-step	ζ = -38.6 mV	Elminshawy, et al. [39]
Water/TiO_2	25 nm Φ = 0.1 wt.%	SDS/ultrasonic bath, ultrasonication.	Two-step	ζ = -47.9 mV	Ghadimi and Metselaar [40]
Carbon nanotube based nanofluids					
Water/SWCNT	Length: 20-50 nm, Height: 0.1 nm Φ = 0.1-20 mg/mL	SDBS/ultrasonication.	Two-step	Two months	Islam, et al. [41]
DI water/MWCNT	Length: 6 µm, Diameter: 5 nm Φ = 0.3 vol.%	SDS/ultrasonication, magnetic stirring.	Two-step	ζ = 42.3 mV	Akash, et al. [11]
Distilled water/MWCNT	MWCNT (10-20 nm) Φ = 0.15 wt.%	Functionalized by -COOH group, magnetic stirring, ultrasonication.	Two-Step	ζ = 41.4 mV	Zare, et al. [38]
Water/CNT	Length: 10-30 µm, Diameter: 10-20 nm Φ = 0.1-1 wt.%	GA, SDS, PVP/magnetic stirring and ultrasonication.	Two-Step	ζ = -63.2 mV	Almanassra, et al. [42]

Two-dimensional nanomaterial based nanofluids					
DI water/rGO-Ag	Crystalline, 325 mesh, 99% purity Φ = 0.0005-0.05 wt.%	SDBS /ultrasonication.	Two-step	> two weeks	Abdelrazik, et al. [43]
Water/Ti_3C_2	Lateral size = 1-10 µm Thickness = 1 nm Φ = 0.0005 to 0.05 wt.%	CTAB, SDBS/magnetic stirring, ultrasonication.	Two-step	ζ = maximum 62.64 and -124.71 for CTAB and SDBS, respectively.	Abdelrazik, et al. [44]
Water/GNPs	Lateral size = 2 µm Thickness = 2 nm Φ = 0.1 wt.%	BS, SDS, CTAB, and GA/water bath, ultrasonication.	Two-step	> two months	Sarsam, et al. [30]
Water-EG (60:40)/ Graphene	Length = 3 µm Thickness = 123-424 nm Φ = 0.1-0.3 wt.%	NPE 400, HCL + NaOH solution/stirring, sonication.	Two-step	Three weeks.	Sarafraz, et al. [45]
Hybrid nanofluids					
Water/MWCNT-CeO_2	1-20 µm × 20 nm and < 30 nm respectively Φ = 0.25-1.5 vol.%	SDBS, SDS, CTAB, DDC, GA and PVP/ultrasonication	Two-step	> one month	Tiwari, et al. [46]
Water/G-BN	Graphite (40 µm), BN (20 µm) Φ = 0.05-5 vol.%	Covalent functionalization of G/BN composite/ultrasonication.	Two-step	Several months ζ = -48 to -31 mV	Zhao, et al. [47]
Water/Cu-Zn-Al LHD	Length = 49 nm, thickness = 9 nm Φ = 40-240 ppm	--/magnetic stirring, sonication.	Single step	ζ = 34.6 to 38.6 mV	Chakraborty, et al. [48]

3. Thermophysical properties of nanofluids

3.1. Thermal conductivity (k)

The thermal conductivity (TC) of NFs is the most critical property for determining their heat transfer performance (HTP) in thermal energy conversion and storage systems. TC of NFs is superior compared to BF due to greater thermal conductivity of solid particles compared to liquids (demonstrated in **Fig. 7**). Numerous studies have shown a significant increase in TC when NPs are added to the typical BF. Several parameters, however, have both positive and negative impact on the enhancement of TC using various groups of nanomaterials and BFs.

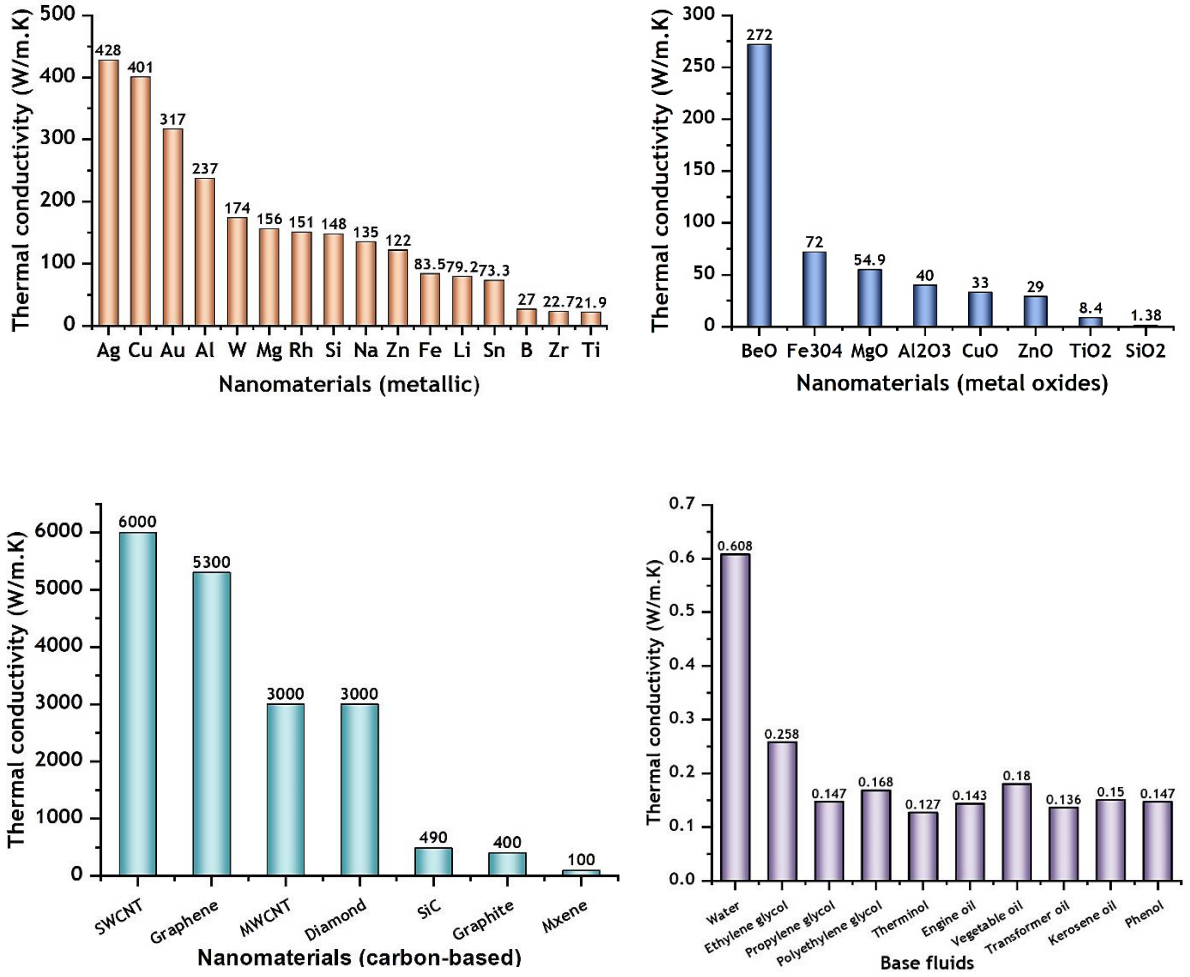

Fig. 7. Thermal conductivity (at 25℃) of frequently used nanomaterials (metallic, metal oxides and carbon-based nanomaterials) and base fluids for synthesis of NFs.

3.1.1. Influential factors effecting TC of NF

TC has been rigorously studied for the last few decades as being one of the key properties of advanced NFs as heat transfer fluids. The studies of NFs show that the presence of solid particles in BF impacts TC significantly. Crucial factors affecting the effective TC and HTP of NFs have been established, such as preparation methods, dispersion stability, concentration (φ), size and shape of NPs, TC of BF, addition of chemical additives, pH of mixture, TC evaluation techniques and operating temperature variation (represented in **Fig. 8**). Gupta, et al. [49] comprehensively reviewed the effect of several parameters on thermophysical properties of NFs including TC, using various types of NPs and dispersed mediums. In addition, several mechanisms related to TC and heat convection using NFs such as: Brownian motion, particle agglomeration, dispersion stability, intermolecular forces between particles and liquid layers of BF were critically investigated by several researchers in the field [50, 51]. Milanese, et al. [52] observed layering phenomena in water/Cu NF as they attempt to find the causes for experimentally evaluated higher TC of water/Cu NF over water/CuO. The numerical MDS study clarified that the formation of double shell-like layers of water molecules on the surface of Cu NP leads to the improved TC of water/Cu NF, while no significant layering is noticed in water/CuO suspension. Iacobazzi, et al. [53] studied the effect of several mechanisms on TC of micrometric and nanometric Al_2O_3 based suspensions using a set of BFs (water, frozen-water, and oil). In comparison to Brownian motion, layering, thermal boundary resistance, clustering, and ballistic phonon motion mechanisms, the effect of mass difference scattering phenomena based on phonon theory was found to be the most efficient in predicting a decrease in the TC of microfluid-nanofluid.

The association of φ and TC of NF is well established as it intensifies for corresponding addition of φ up to an optimum level and subsequently deteriorates due to aggregation of excess particles. In terms of temperature, TC amplification is favorable at elevated temperatures due to the enhanced Brownian motion and kinetic energy of the NPs. These augmentation trends of TC established the effectiveness of NFs in temperature dependent thermal operations e.g., energy storage, solar collectors, heat exchangers and heating/cooling devices [54]. NPs synthesized in different sizes and shapes depending on the used synthesis techniques and structure of the nanomaterials are observed to cause variation in outcomes of TC. Research explored that greater surface to volume ratio of NPs yields more growth in TC, which is exactly why CNT and two-dimensional NP based NFs are generally recognized as more efficient [55]. In addition, formulation of NF at optimized preconditions and stabilization

criteria e.g., sonication time, chemical additives, pH of dispersed mixture, suspension homogeneousness and evaluation approach have substantial impact on TC. TC can be measured using different techniques, e.g., transient hot-wire method, optical measurement method, temperature oscillation method and 3-□ method. The transient-hot-wire (THW) method is the most convenient technique to examine TC of NFs due to its simplicity and good precision. Theoretical correlations developed by researchers are also used to evaluate the TC of various categories of NFs. Numerous experimental and analytical studies on NF have established the linear growth of NFs TC in response to the addition of a wide range of NPs in BF and increasing temperatures. Afrand, et al. [56] investigated TC of water/Fe_3O_4 (20-30 nm) NF at φ of 0.1-0.3 vol.% varying the temperature from 25-55 ℃. The measured TC results using THW-based KD2-pro showed addition of NPs has a dominant impact on improving effective TC (k_{nf}/k_{bf}) relative to escalating temperatures as 90% enhancement is obtained at 3 vol.% and 55℃. The results are consistent with other metal oxides-based NFs e.g., water-based TiO_2, Al_2O_3, CuO, SiO_2, MgO and so on (see **Table. 2**).

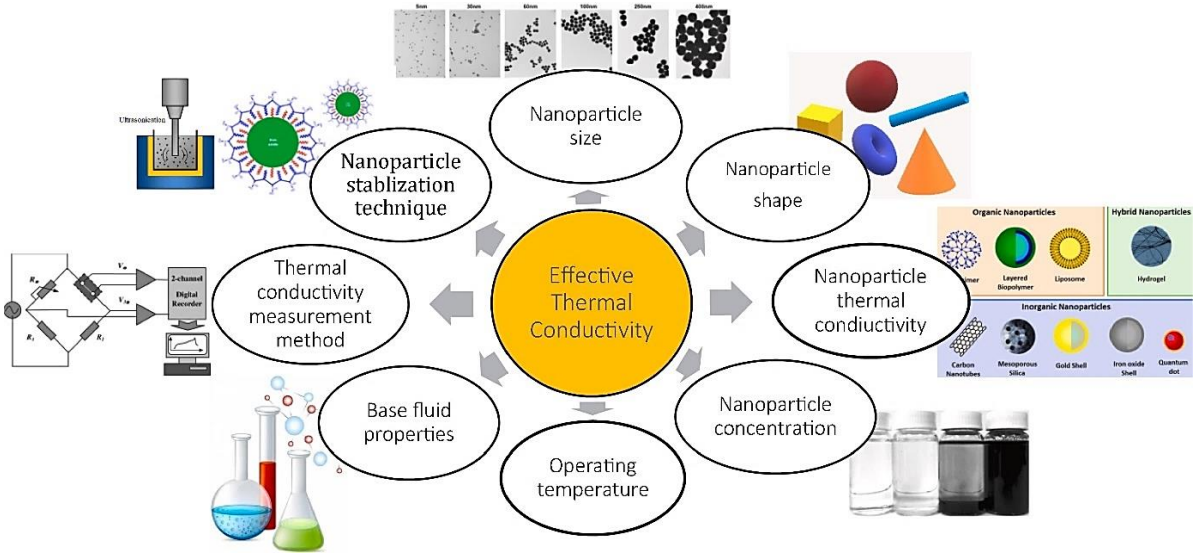

Fig. 8. Influential parameters affecting thermal conductivity of NFs [57].

As mentioned earlier, recent development in manufacturing of carbon-based nanomaterials (e.g., CNT, MWCNT, SWCNT, and two-dimensional Graphene) has received unprecedented attention in nanotechnology due to advanced thermo-physical and electro-chemical properties. Hence, carbon-based nanomaterials are being utilized frequently in traditional liquids to develop innovative NF suspension with advanced TC. Tiwari, et al. [46] studied the effect of solid particles addition and temperature on TC amplification using water/MWCNT-CeO_2 NF. They revealed that the TC ratio increases at rising φ and temperatures. They noticed that TC of the NFs adequately influenced concurrently against temperature and particle loading, the

highest 27.38% augmentation is obtained at 1.5 vol.% and 50℃ (**Fig. 9**). Similar trends in TC augmentation against intensifying φ and temperature using graphene NPs is reported by [58].

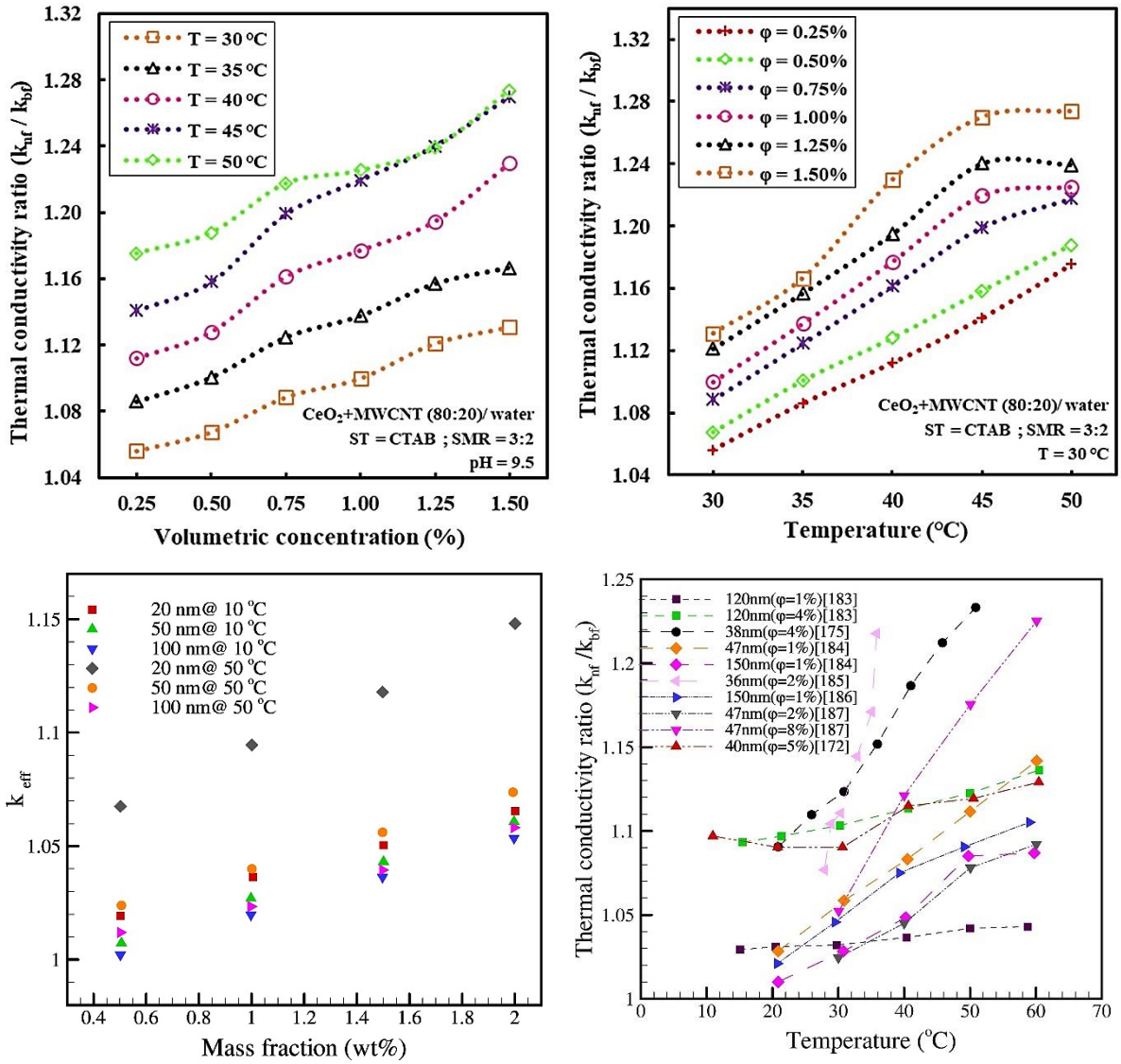

Fig. 9. Effect of particles addition and temperature on thermal conductivity (a, c) variation of TC against increasing particles concentration (b, c, d) TC increment with respect to temperature and particle size variation (for details see [46],[59]).

In an extensive study, Tiwari, et al. [46] investigated effects of sonication time, several surfactants as stabilizers, surfactant to NF ratio (SNF), pH values, φ, and temperature on effective TC ((k_{nf}/k_{bf}) of hybrid water/MWCNT+CeO_2 NF (**Fig. 10**). At optimized conditions (90 min sonication time, CTAB as dispersant, SNF3:2, pH9.5, 1.50 vol.%, and 50°C), the highest increment of 27.38% is obtained. Keklikcioglu Cakmak [60] demonstrated that surfactants have a negative impact on the TC of water/GO NF by examining three separate surfactants (CTAB, SDS, and TX-100) used to stabilize the suspension. Regardless of variation

in φ, NFs elucidated less TC and poor stability relative to BF using the stabilizers. On the contrary, Almanassra, et al. [42] reported that surfactants (GA, SDS and PVP) have no effect on k_{nf}/k_{bf} studying water/CNT (0.1-1wt.%) NF from 20-45℃ at an optimum ratio (particle: surfactant) of 1:0.5.

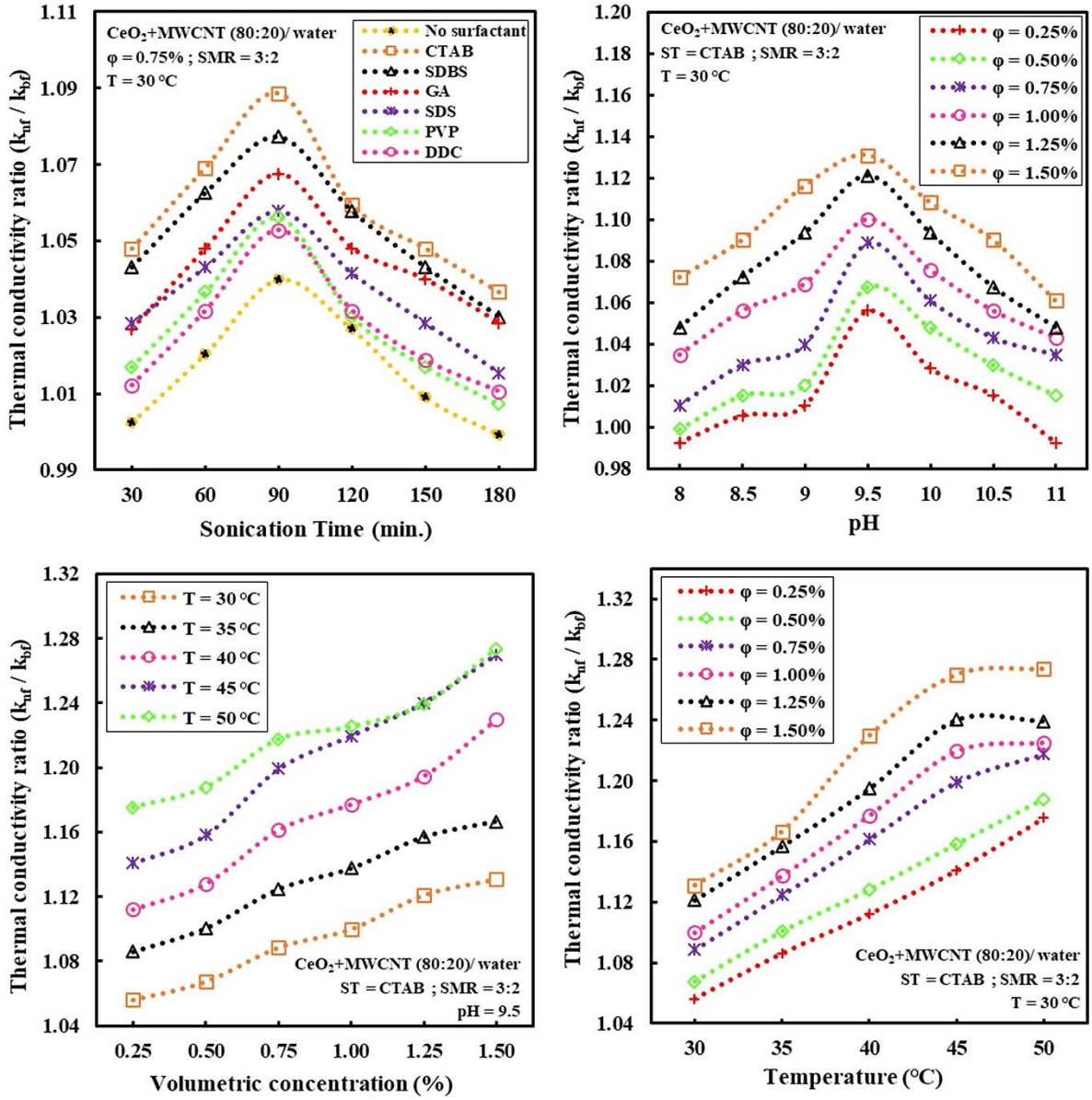

Fig. 10. Effect of different surfactants, sonication time and pH value on TC enhancement of water/MWCNT+CeO_2 nanofluid [46].

Iacobazzi, et al. [61] critically examined the effect of clustering mechanism on TC of water/Al_2O_3 NF. The analysis showed that, within the considered cluster dimension range of 168-20933 nm, the TC ratio deteriorates at smaller clusters (up to 3820 nm), but notably increases at larger dimensions up to 20933 nm. Further assessments on stability and backscattered light revealed that the sedimentation mechanism (i.e., larger clusters) results in

a higher TC ratio due to the convective motion of NPs around the hot wire caused by the gravitational force effect. Teng, et al. [62] observed variation of TC using varying NP size (20, 50 and 100 nm) on water/Al_2O_3 (0.5-2wt.%) at 10-50℃ and concluded that smaller NP sizes can provide a substantial increase in TC than larger particles. Smaller NPs was found to be more temperature sensitive due to higher collision rates relative to larger particles resulting in more augmentation in TC at higher temperatures. Timofeeva, et al. [63] considered different shapes of Al_2O_3 particles at nanoscale range (< 100 nm) to experimentally study shape-effect on TC of water-EG/Al_2O_3 NF at concentration of 1-9 vol.% and 21±0.5℃. As the NP loading increases, k_{nf}/k_{bf} enhances in the order of cylinder > brick > blade > platelet shaped particles. In addition, experimental data confirms that sphericity of less than 0.6 results in deterioration of k_{nf}/k_{bf} as negative interfacial effects dominate. Despite this, researchers concluded that the impact of NP sizes and shapes is subject to major disagreements in the published literature due to a variety of operating conditions, including diverse synthesis/fabrication techniques, TC evaluation methods, a restricted range of NP sizes, temperature, pH value, and NP morphology, and inadequate information on operating conditions and chemicals [57, 64].

Zhang, et al. [65] observed a drastic impact of pH value variation on TC for water/TiO_2 (20nm) NF in the range of 2-12. Their experiment revealed that TC fluctuates severely within an unstable range of pH (5-8) near the isoelectric value of 6.5 whereas smaller (2-4) and higher (9-12) range of pH results. Optimized effective TC (k_{nf}/k_{bf}) is achieved with good suspension stability at pH 10, 0.25 vol.% and 25℃. TC augmentation is attributed to optimum aggregation formed by the NPs and optimized size rather than optimum stability of the particles. In addition, prominent increment is evaluated against raising particle fractions (0.08-2 vol.%) and elevated temperatures (25-60 ℃), the findings are supported by [66].

Garoosi [67] proposed empirical correlations considering key parameters (temperature, particle loading and size) for several combinations of NPs and BFs. The studied model is found to be more reliable than classical models, with a standard deviation of only 4.7%. The correlations are recommended for further analysis of TC in NF-based thermal engineering devices. Cui, et al. [68] performed a MDS study to analyze consequences of NP properties (materials, sizes, shapes and φ) on TC using Cu, Ag, Au and Fe nanomaterials. The proposed model predicts TC of the NFs and concludes that TC improves with raising φ and smaller NP size. Ag NPs had the highest TC of all, while higher fraction of $\varphi > 3vol.\%$ showed a reducing trend for TC. In a recent study established on experimental data by [69], revealed an ANN-based model to predict TC of several metal oxide/water NFs. The model can accurately (uncertainty < 2%)

predict TC data for NP loading of 0.02-2 wt.% at 20-90℃. Zendehboudi, et al. [70] reviewed widely used and effective data-driven numerical approaches to predict TC of a broad range of NFs. Studies on TC of widely utilized water-based mono and hybrid NFs and the mechanism of TC augmentation, impacts of influential parameters along with numerical or molecular dynamics correlations to estimate the TC, are reviewed in **Table. 2**.

418 **Table. 2.** Summary of recent experimental studies on TC of water-based NF with details information and important outcomes.

Reference	**Nanofluids**	**Concentration (Φ)**	**Surfactants/ Dispersants**	**Temperature range**	**Key findings**
Sarsam, et al. [30]	Water/GNPs	2 nm × 2 µm Φ = 0.1 wt.%	DBS, GA, CTAB, and SDS	20-40 °C	● Highest augmentation in TC relative to water, 10.80% with GA surfactant. 60 minutes of ultrasonication time provided the most stable NF and the 2nd highest growth of TC.
Chakraborty, et al. [71]	Water/TiO_2	< 100 nm Φ = 0-100 ppm	Polyvinylpyrrolidone and Tween 20	30-50 °C	● Maximum 8.3% increment is obtained at 40 ppm at 30℃. However, beyond 40 ppm results in a negative outcome due to aggregation.
Das, et al. [72]	Water-[MMIM][DMP]/ MXene	1–10 µm × 1 nm Φ = 0.05-0.2 wt.%	--	25-60 °C	● TC was augmented by 47% at 0.2wt.% using 2D MXene particles and exhibited linear growth with increasing temperature.
Alshayji, et al. [73]	DI water/Diamond	3-10 nm Φ = 0.125-1.25 vol.%	none	20-60 °C	● 25% growth in TC relative to water is observed at 0.125 vol.% and 60°C, attributed to higher conductivity of diamond particles.
Amiri, et al. [74]	Water/GNP-COOH /GNP-SDBS	0.5-3 µm × 0.55-3.74 nm Φ = 0.025-0.1 wt.%	SDBS and solvents (H_2SO_4, HNO_3)	20-80 °C	● Functionalized GNP-COOH NFs attained intensified TC relative to water and better than GNP-SDBS functionalized NFs as well. ● 68% heat transfer enhancement obtained with GNP-COOH NF, which is 33% higher than GNP-SDBS NFs.
Sadri, et al. [75]	Water/GAGNPs	n/a Φ = 0.05 vol.%	--	20-45 °C	● 24.18% TC increment is found by adding acid functionalized GNPs at 45°C and 0.05 vol.%.
Singh, et al. [76]	Water/Al_2O_3 /rGO- Al_2O_3	4-5 nm Φ = 0.01-0.1 vol.%	--	32-45 °C	● While the TC of Al_2O_3 based NF deteriorated above 0.02 vol.%, hybrid NF showed excellent TC, at 45°C and 0.1 vol.%, obtained 2.0766 W/m.K, much higher than 0.608 W/m.K of water .
Sundar, et al. [77]	Water/ND-Co_3O_4 Water-EG/ND-Co_3O_4	ND (4-5 nm), ND-Co_3O_4 (16.95 nm) Φ = 0.05-0.15 wt.%	--	20-60 °C	● Water-based NF outperforms other base fluids in terms of TC improvement. Maximum increments are 15.7, 8.71, and 13.34 % at 0.15 wt.% and 60°C

					for water, EG, and water-EG based hybrid NF, respectively.
Huminic, et al. [78]	Water/Fe-Si	1-20 nm Φ = 0.25-1 wt.%	CMCNa	20-50 °C	● The TC is found to be increasing with temperature and inclusion of hybrid nanocomposite.
Moldoveanu, et al. [79]	Water/Al_2O_3 /SiO_2 /Al_2O_3- SiO_2	43 and 20 nm respectively Φ = 1-3 vol.%	--	20-50 °C	● TC intensifies linearly with inclusion of NPs and increasing temperature. 23.61% higher TC is achieved at 3 vol.% and 50 °C.
Maheshwary, et al. [64]	Water/TiO_2 (spherical, cubic and rod)	16 to 32 nm Φ = 0.5-2.5 wt.%	--	303-353 K	● TC augmented with longer sonication time and reduced particles sizes and it also varies based on shapes of dispersed particles. Contributions of particle concentration, size and shape are 69.43, 24.95 and 5.62% respectively.
Sabiha, et al. [80]	Water/SWCNT	500 nm × 1-2 nm Φ = 0.05-0.25 vol.%	SDS	20-60 °C	● At 0.2 vol.% and 60 °C, TC increased by 36.76%.TC is less at lower temperatures due to less Brownian motion.
Kumar and Sonawane [81]	Water/CuO /TiO_2	26 and 9 nm respectively Φ = 0.02-0.06 vol.%	--	30-50 °C	● CuO NP exhibited higher TC increment for the NFs in comparison with TiO_2 particles, augmentation is 25 and 16% respectively.
Hussein, et al. [82]	Water/CF-MWCNT + CF-GNP + h-BN	5 µm × 15 nm and 2 µm respectively Φ = 0.05-0.1 wt.%	Tween-80	20-60 °C	● 64% intensified TC is achieved for the hybrid NF at 60 °C and 0.1 wt.%. Advance properties of the functionalized particles are attributed as reasoning aspects of TC enhancement.
Hemmat Esfe and Saedodin [83]	Water/MgO	20 to 60 nm Φ = 0.5-2 vol.%	--	--	● The effect of particle concentration and size is examined. The highest vol.% and smallest size of NP are observed to be the best combination for TC enhancement.
Sundar, et al. [84]	Water/Nano-diamond	10-15 nm Φ = 0.2-1 vol.%	H_2SO_4 and HNO_3	293-333 K	● A 22.86% increment is obtained due to effective micro-convection at higher temperature and φ of NPs in base fluid.
Chen, et al. [85]	Saline water/SiC	30 nm Φ = 0.04-1 vol.%	Polyvinylpyrrolidone and NaOH	10-50 °C	● TC of saline-water based NF was improved by 5.2% with respect to BF, SiC has a good impact to

					increase above 6% relative to water at 0.4 vol.% loading.
Zhang, et al. [86]	Water/CRGO	Thickness (~4.3 nm) Φ = 0.2-1 mg/ml	--	20-60 °C	● TC improvement is 32.19% at 60°C for 1 mg/ml CRGO particles. TC advancement is attributed to ultrathin layered structure and extra-large surface area of graphene nanomaterial.
Shalkevich, et al. [87]	Water/Au	2-45 nm Φ = 0.00025-1 vol.%	EGMUDE	25-40 °C	● A highest of 1.4% TC augmentation was recorded for H_2O/Au NF dispersing 40 nm gold particles at 0.11 vol.% and 37 °C.
Srinivas, et al. [88]	Carboxylated water/MWCNT	1-25 µm × 20-40 nm Φ = 0.025-1 wt.%	Sebacic Acid and 2-ethylexanoic Acid	30-50 °C	● 17.85% growth in TC is achieved at 1 wt.% and 50°C for CNTs dispersed in functionalized carboxylate water.
Wu, et al. [89]	Water/SWCNT /MWCNT	1-2 and 8 nm respectively, length < 30 µm Φ = 0.0962-0.3846 vol.%	Humic acid	30-80 °C	● SWCNT-based exhibited superior TC than MWCNT-based suspension. The maximum augmentation found is 40.5% at 0.3846 vol.% of SWCNT nanomaterials.
Wusiman, et al. [90]	Water/MWCNT	5 µm × 5-20 nm Φ = 0.1-1 wt.%	SDBS and SDS	20-45 °C	● TC dropped with increasing φ of surfactants. However, SDBS performed better than SDS as surfactant.
Wang, et al. [66]	Water/Cu /Al_2O_3	25 nm Φ = 0.02-0.8 Wt.%	SDBS	25 °C	● Maximum 15 and 18% increments are attained at 0.8 wt.% for Cu and Al_2O_3 based NFs, respectively. pH and φ of SDBS had a substantial effect on TC of the NFs.
Sahooli, et al. [91]	Water/CuO	4 nm Φ = 1-6 vol.%	Polyvinylpyrrolidone	10-50 °C	● 31% TC enhancement is obtained for the NF at 50°C using PVP as surfactant. pH 8 and PVP φ of 0.095 wt.% caused optimized TC.
Ghadimi and Metselaar [40]	Water/TiO_2	25 nm Φ = 0.1 wt.%	SDS	25 °C	● Variation in sonication time and surfactant φ leads to improvement in TC. 3 h sonication and 0.1wt.% of SDS showed improved TC of the studied NFs.

Song, et al. [92]	Water/stainless steel	70 nm Φ = 0.017 wt.%	SDBS	25 °C	● TC improved 8.3% at pH 11 with 0.017 wt.% of the steel particles. In addition, sonication time of 60 min was observed to be optimum for the NF.
Shahsavar, et al. [93]	Water/CNT-Fe_3O_4	10 µm × 10-30 nm and 13 nm respectively Φ = 0.9 to 2.25 vol.%	Gum Arabic and Ttetramethylammonium hydroxide	25-35 °C	● At a field strength of 470 mT, the highest augmentation of TC observed was 151.31% for 0.9% FF+1.35% CNT.However, temperature had a negative effect on TC due to the presence of the magnetic field.
Garg, et al. [94]	Water/MWCNT	0.5-40 µm × 10-20 nm Φ = 1 wt.%	Gum Arabic	15-35 °C	● TC increased by 20% at 1 wt.% and an optimum ultrasonication period of 40 minutes. The heat transfer coefficient was also augmented by 32% relative to water.
Xing, et al. [95]	Water/SWCNT	5-30 µm × 1-2 nm Φ = 0.1-1 wt.%	CTAB	10-60 °C	● 16.1% improved TC is attained by dispersing 1wt.% of SWCNT nanomaterials and CTAB dispersant at 60 °C.
Taherialekouhi, et al. [96]	Water/Graphene oxide-Al_2O_3	3.4-7 and 20 nm respectively Φ = 0.1-1 vol.%	--	25-50 °C	● TC intensified 33.9% at 1 vol.% and 50°C with the dominant effect of temperature relative to solid concentrations.
Mousavi, et al. [97]	Water/MgO-TiO_2	25-45 and 18-23 nm respectively Φ = 0.1-0.5 vol%	SDS	15-60 °C	● The highest enhancement of TC was obtained to be 21.8% for MgO-TiO_2 (80:20) at 60°C.
Okonkwo, et al. [98]	Water/Al_2O_3-Fe	29 and 46 nm Φ = 0.05-0.2 vol.%	--	25-65 °C	● The hybrid NF showed a 14% enhancement in TC at 0.2 vol.% while it was 7.5% for mono water/ Al_2O_3 NF.
Hussein, et al. [99]	Water/CF-GNPs	2 µm Φ = 0.02-0.1 wt.%	SDS, CTAB, Tween-80 and TX-100	20-60 ºC	● TC augmented 29.2% at 0.1 wt.% of CF-GNPs using an optimum sonication time of 60 minutes. Covalent functionalization of particles leads to higher effective TC.

Table. 3. Summary of proposed empirical correlations to estimate thermal conductivity of water-based NFs.

Reference	**Nanofluids**	**Correlation**	**Applicability**	**Accuracy**

Water-based nanofluids				
Tiwari, et al. [46]	Water/MWCNT-CeO_2	$\frac{k_{nf}}{k_{bf}} = 1 + 0.580453 \times \left(\frac{T}{T_0}\right)^{1.54358} \times \varphi^{0.356853}$	$0.25 \leq \varphi \leq 1.5\ vol.\%$ T = 30-50 °C	Max. error = 0.881%
Garoosi [67]	Water/Ag, Cu, Al_2O_3, TiO_2, CuO, SiO_2, ZnO, MgO, Fe, Fe_3O_4, Al, AlN, $CaCO_3$	$\frac{k_{nf}}{k_{bf}} = \frac{k_p + 2k_{bf} + 2(k_p - k_{bf})\varphi}{k_p + 2k_{bf} - (k_p - k_{bf})\omega\varphi}$ $+3.762 \times \left(\frac{T}{T_0}\right)^{8.661} \left(\frac{d_p}{d_{bf}}\right)^{8.661} \left(\frac{k_p}{k_{bf}}\right)^{8.661} \varphi^{0.64} e^{(-5.742\varphi)}$	$0 \leq \varphi \leq 12\ vol.\%$ $10\ nm \leq d_p \leq 12\ \mu m$	Standard deviation = 4.7%
Alawi, et al. [100]	Water/Al_2O_3 /CuO /SiO_2 /ZnO	$\frac{k_{nf}}{k_{bf}} = \left[\frac{k_p + 2k_{bf} - 2\varphi(k_{bf} - k_p)}{k_s + 2k_{bf} - \varphi(k_{bf} - k_s)}\right] + 5 \times 10^4 \beta\varphi\rho_f C_p \sqrt{\frac{k_B T}{d_p \rho_p} f(T, \varphi)}$	Φ = 1-5 vol.% d_p = 20-100 nm T = 300-320 K	n/a
Hemmat Esfe, et al. [101]	Water-EG/SWCNT-ZnO	$\frac{k_{nf}}{k_{bf}} = 0.8707 + 0.179\varphi^{0.179} e^{0.09642\varphi^2} + \varphi T \times 8.883 \times 10^{-4} + \varphi^{0.252} T \times 4.435 \times 10^{-3}$	Φ = 0.15 to 1.92 vol.% T = 25-50 °C	R^2 =0.9918
Rostamian, et al. [102]	Water-EG/SWCNT-CuO	$\frac{k_{nf}}{k_{bf}} = 1 + (0.04056 \times \varphi T) - 0.003252 \times (\varphi T)^2 + 0.0001181 \times (\varphi T)^3 - 0.000001431 \times (\varphi T)^4$	Φ = 0.02 to 0.75 vol.% T = 20-50 °C	Max. error < 4%
Timofeeva, et al. [63]	Water-EG/Al_2O_3	$\frac{k_{nf}}{k_{bf}} = 1 + (C_k^{shape} + C_k^{surface})\varphi$ $where, C_k^{surface} = -f.l_k$	Φ = 5 vol.% Shapes = platelets (9 nm), blades (60×10 nm), cylinders (80×10 nm), and bricks (40 nm)	n/a

Pare and Ghosh [69]	Water/Al_2O_3 /CuO /ZnO	$\frac{k_{nf}}{k_{bf}} = a + bT + c\varphi + dT^2 + e\varphi^2 + fT\varphi$	Φ = 0.02-2 wt.% T = 20-90 °C d_p = 40 nm	Max. error < 2%
Beck, et al. [103]	Water/Al_2O_3	$k_{nf} = [4.4134\varphi\ (1 - e^{-0.025d_p})]k_{bf} + k_{bf}$	$2 \leq \varphi \leq 4\ vol.\%$ $8\ \leq d_p \leq 282\ nm$ T = 298 K	n/a
Sun, et al. [104]	Water/SiO_2	$\frac{k_e - k_0}{k_\infty - k_0} = 1 - \exp\left[\frac{-6.3\left(\frac{r - r_0}{r_0}\right)^{1.4}}{\varphi^{-0.3}\left(\frac{d_p}{G_p}\right)^{-0.2}}\right]$	$1.96 \leq \varphi \leq 12.85\ vol.\%$ d_p = 10-60 nm	Max. error = ± 20%
Hemmat Esfe, et al. [105]	Water/Fe	$\frac{k_{nf}}{k_{bf}} = 1 + \left(0.26876 \times \varphi^{0.99288} \times {d_p}^{-0.35106}\right)$	$0.000313 \leq \varphi \leq 0.01\ vol.\%$ d_p = 37, 71, 98 nm	R^2 =0.9988
Hemmat Esfe, et al. [106]	Water/CNT- Al_2O_3	$\frac{k_{nf}}{k_{bf}} = \frac{A + T}{B + C\varphi} + \frac{D}{T}$	Φ = 0-1 vol.% T = 303 to 332 K	Max. error = 2%

421

3.2. Specific heat capacity (c_p)

Specific heat (c_p) is one of the most essential thermo-physical properties to characterize thermal heat storage merit of various advanced thermo-fluids. Although TC of NF is generally enhanced by the addition of NPs, c_p may either increase or decrease with the presence of scattered solid particles relative to the fluid. This trend of c_p depends on nanomaterial type, φ, base fluid and temperature. Working fluids must have sufficient heat capacity to provide adequate energy efficiency when used in a thermal heat transfer or storage device. Hence, it is essential to establish an explicit concept of interaction between cp and the influential factors to characterize potential NFs. Generally, various types of thermal DSC devices are employed to experimentally measure c_p of NFs due to its convenience and technical simplicity [107-109].

Wole-Osho, et al. [110] experimentally studied c_p of water-based mono (Al_2O_3 and ZnO) and hybrid (Al_2O_3- ZnO) NFs at 0.33-1.67vol.% and 25-65℃. The presence of solid particles resulted in a linear decrement of up to 30.12%. Starace, et al. [111] evaluated c_p of 13 different NFs considering various BFs (including water and oils), NPs, surfactant, φ, particle size and temperature. They concluded no notable augmentation is caused by the addition of NPs as $\frac{c_{p_{nf}}}{c_{p_{bf}}}$ is found to be below 1 for the majority of the samples. Moldoveanu and Minea [112] analyzed c_p of regular and hybrid NFs using metal oxides (Al_2O_3, SiO_2 and TiO_2). The obtained data indicate that the relative c_p of the NFs is below one for all samples, indicating a decrease in heat capacity due to the addition of solid NPs (0-3vol.%). The authors proposed the following correlation based on the observed data (applicable for the reported NFs at φ of 0-5vol.% and ambient temperature with an uncertainty of 11%).

$$\left(C_p\right)_{nf} = \left(\frac{\rho_p}{\rho_{bf}}\right)^{0.2} \left(1 + \frac{d_p}{50}\right)^{0.4167} \left(1 - \frac{\varphi}{100}\right)^{2.272} \left(C_p\right)_{bf} \qquad (1)$$

In contrast, some published works claim opposite characteristics of heat capacity by analyzing different NFs using various NPs (particularly carbon-based nanomaterials), BFs and experimental conditions. According to the findings of those studies, the formation of a semi-solid layer on the surface of NPs increases TC, allowing NFs to store energy faster than BF. Almanassra, et al. [42] measured c_p of water/CNT (0.1-1wt.%) NF using a DSC and they understood that c_p increases for the NF adding particles marginally at low temperature (15-35℃) while the effect is more dominant at elevated temperature (35-75℃). The highest 65% enhanced c_p is noted at 0.1wt.% and 75℃while they also identified no prominent consequences to c_p adding stabilizers (GA, SDS and PVP) against temperature variation but little increment

of 3% is attained when NP: surfactant ration is varied from 1:0.5 to 1:1, consistent with [113]. Tiwari, et al. [109] compared the c_p of three distinct hybrid water-based NFs containing nanocomposites that were experimentally formulated (comprising MWCNT with CuO, MgO and SiO_2 separately). Variation in c_p is observed against increasing φ (0.25-1.5vol.%), altering particle diameter (20-50 nm) and temperature (25-50℃). The obtained results imply that the c_p deteriorates raising φ and the degradation appears further using larger particles while it improves with temperature. The maximum drop is 12.84% at 25℃ using an average size of 20 nm for CuO-MWCNT (1.5vol.%) composite and the decrement is lessened using 50 nm particles at promoted temperature (**Fig. 11**). Analogous trends are noticed for the other two NFs as well. More experimental studies on c_p of water-based NFs are reviewed in **Table. 4**.

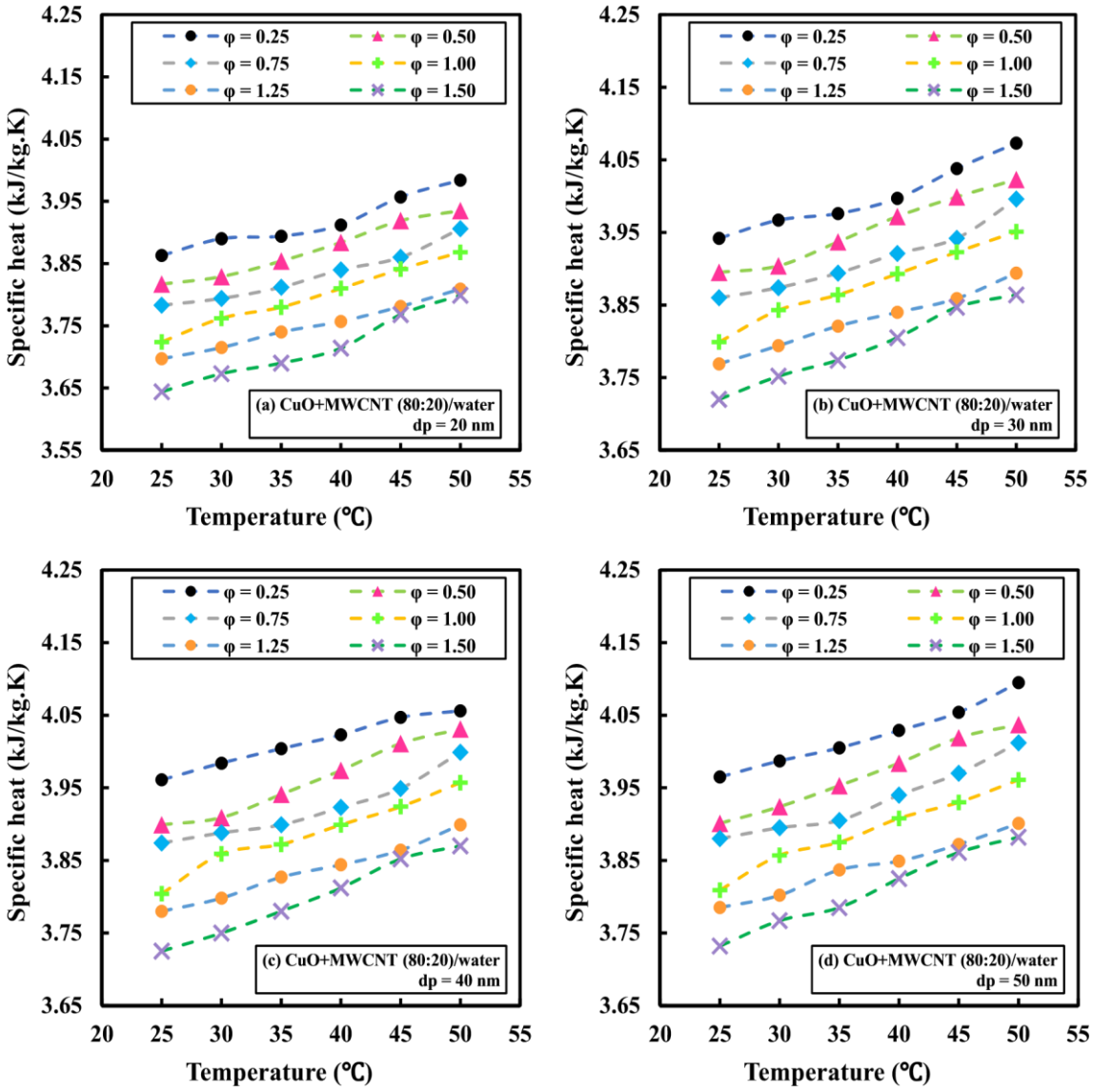

Fig. 11. Variation of c_p with increasing φ, NP diameter and temperature using water/MWCNT-CuO NF , studied by [109].

Theoretical models along with experimental correlations are useful to estimate c_p of a wide range of NFs that has been proposed in literature over the years. The first model presented by Pak and Cho [114] is known as mixture theory to predict c_p of solid-liquid mixture at nonorange scale.

$$C_{p_{nf}} = \varphi C_{p_{np}} + (1-\varphi) C_{p_{bf}} \quad (2)$$

Although this model is commonly used to predict the c_p of NFs, anomalies have been identified due to the model's significant deviation from experimental results.

Xuan and Roetzel [115] proposed a thermal equilibrium model for various NFs based on reviewed experimental results.

$$\rho_{nf} C_{p_{nf}} = \rho_{np} C_{p_{np}} \varphi + (1-\varphi) \rho_{bf} C_{p_{bf}} \quad (3)$$

$$where,\ \rho_{nf} = (1-\varphi)\rho_{bf} + \varphi \rho_{np}$$

This model performs better than mixture theory at predicting data. However, inconsistencies up to a certain range are reported [116, 117].

Fakoor Pakdaman, et al. [118] investigated c_p of NF using MWCNT and developed a correlation to predict c_p.

$$\frac{C_{p_{bf}} - C_{p_{nf}}}{C_{p_{bf}}} = (0.0128 \times T + 1.83282) \times \varphi^{0.4779} \quad (4)$$

The equation is applicable for φ of 0-0.004wt.% and temperature range of 313-343K. Tiwari, et al. [109] formed a correlation for several hybrid NFs considering experimental data (φ, particle size d_{np} and temperature). Valid for $0.25 \leq \varphi \leq 1.5\ vol.\%$, $d_{np} = 20 - 50\ nm$ and $T = 20 - 50$℃, with maximum error of is 2.93%.

$$C_{p_{nf}} = C_{p_{bf}} \left[-10.6364 \times \left(\frac{T}{T_0}\right)^{-0.771} \times \varphi^{0.448} \times \left(\frac{d_{np}}{d_0}\right)^{-0.474} \times \left(\frac{C_{p_{np}}}{C_{p_{bf}}}\right)^{1.027} \times \left(\frac{\rho_{nf}}{\rho_{bf}}\right)^{-2.742} \right] \quad (5)$$

Sekhar and Sharma [119] collected data from 81 different experiments studying c_p of NFs using Al_2O_3, CuO, SiO_2 and TiO_2 to develop which can predict data with a deviation of +10% and -8%.

$$\frac{C_{p_{nf}}}{C_{p_{bf}}} = 0.8429 \left(1 + \frac{T_{nf}}{50}\right)^{-0.3037} \left(1 + \frac{d_{np}}{50}\right)^{0.4167} \left(1 + \frac{\varphi}{100}\right)^{2.272} \quad (6)$$

This correlation is applicable for $0.01 \leq \varphi \leq 4.0\ vol.\%$, $d_{np} = 15 - 50\ nm$ and $T = 20 - 50$℃.

494 **Table. 4.** Summary of recent experimental studies on specific heat capacity (c_p) of water-based with details information and important outcomes.

Reference	**Nanofluids**	**Particle dimension and concentration**	**Surfactants/ Dispersants**	**Temperature range**	**Key findings**
Sadri, et al. [75]	Water/GNPs /GAGNPs	200 nm Φ = 0.05 vol.%	Gallic acid	20-50 °C	● c_p of the NF is reduced with the inclusion of GNPs and enhanced slightly at raising temperature.
Sabiha, et al. [80]	Water/SWCNT	500 nm × 1-2 nm Φ = 0.05-0.25 vol.%	SDS	20-60 °C	● The addition of SWNCT nanomaterial resulted in a decreasing trend of c_p for the NF, while an increasing temperature resulted in the opposite trend.
Hussein, et al. [82]	Water/CF-MWCNT + CF-GNP + h-BN	5 µm × 15 nm and 2 µm respectively Φ = 0.05-0.1 wt.%	Tween-80	20-60 °C	● 11% higher c_p is achieved at 0.1 wt.% and 60°C due to advanced surface energy and greater surface of the dispersed particles.
Wole-Osho, et al. [110]	Water/Al_2O_3 /ZnO /Al_2O_3-ZnO	29 and 70 nm respectively Φ = 0.33-1.67 vol.%	--	25-65 °C	● c_p dropped by 30.12% at 25°C and 1.67 vol.% loading, but it increased at higher temperatures. However, Al_2O_3 NF have a lower c_p compared to ZnO NF at the same temperature.
Tiwari, et al. [109]	Water/CuO-MWCNT /MgO-MWCNT /SnO_2-MWCNT	20-50 nm (CuO, MgO and SnO2) 1-20 µm × 20 nm (MWCNT) Φ =0.25-1.5 vol.%	CTAB	20-50 °C	● The highest φ of MgO-MWCNT composite reduced c_p about 15.09% relative to water at 25°C. When the particle diameter of CuO and MgO nanoparticles is increased from 20 to 50 nm, the deterioration rate decreases.
Wang, et al. [120]	Water-EG/TiO_2 /Aminopropyl-TiO_2 /CD- TiO_2	15 nm Φ = 0.2-0.1 vol.%	(3-aminopropyl) triethoxysilane	30-85 °C	● c_p decreases when particles are added. However, average c_p of water/CD-TiO_2 NF is 3.186 J/g °C which is quite good for heat transfer applications. c_p of the nanofluids reduced at the increasing cooling rate.
Fesenko, et al. [121]	Water/Graphene /Graphene-gold	150-200 nm Φ = 0.002 wt.%	--	30-60 °C	● c_p decreased when the nano-filters were added, but it increased marginally when the temperature was raised.
Moldoveanu and Minea [112]	Water/Al_2O_3 /SiO_2 /TiO_2 /Al_2O_3 + SiO_2	45, 20 and 30 nm respectively Φ = 1 to 3 vol.%	--	--	● c_p dropped substantially for both mono and hybrid NFs at higher φ. Experimental data of the fluids depicted larger deviation from the correlation at higher φ of the dispersed particles.
Selvam, et al. [122]	Water-EG/Graphene	15 µm × 5-10 nm Φ = 0.001 to 0.45 vol.%	Sodium Deoxycholate	30 °C	● c_p decreased by 8% than BF and was observed to be lower than the predicted values from the mixture rule

					to calculate c_p of homogenous NFs. More deviation is noticed when φ is above 0.15 vol.%.
Murshed [117]	Water/TiO_2	15 nm Φ = 1-5 vol.%	--	--	● A c_p reduction of 18% is measured for the NF as 5 vol.% of particles are added to the BF due to much lower c_p of solid material relative to water.
O'Hanley, et al. [123]	Water/Alumina /Silica /CuO	50, 32 and 30 nm respectively Φ = 0-0.3 vol.%	--	35-55 °C	● The c_p data is compared to two widely used correlations. The results indicate that the calculated c_p of formulated NFs agrees very well with the thermal equilibrium-based model rather than the direct mixture model.
Singh, et al. [124]	Water/MWCNT	30 nm Φ = 0.05-0.5 wt.%	Arabic Gum	25-300 °C	● c_p enhanced as φ increased, the highest augmentation is noted 3.1% relative to water. The improvement is attributed to semi-solid layer formed on the surface of the nanomaterial.
Gao, et al. [125]	Water/ Al_2O_3-Graphene oxide	layer number <10 for Graphene oxide, Al_2O_3 (30±5 nm) Φ = 0.05-0.15 wt.%	SDS	20-70 °C	● At lower temperatures, the decrease in c_p for the NFs is much greater (7%) and lessens as c_p increases at higher temperatures.
Devarajan, et al. [126]	Water/CNT /CNT-Al_2O_3	20-30 and 25-40 nm respectively Φ = 0.05-0.1 vol.%	--	0-100 °C	● The c_p is found dominant to BF as it increased notably with the addition of φ. The increment is attributed to stability and absorptivity of the NFs.
Mousavi, et al. [97]	Water/MgO-TiO_2	25-45 and 18-23 nm respectively Φ = 0.1-0.5 vol%	SDS	15-60 °C	● The maximum 1.17% decrease of c_p is measured at 0.5 vol% and 30 °C. It also dropped with inclusion of nanomaterials.

495

4. Colloidal stability of NF

Stability is the most crucial hinder towards persistent application of the NFs for industrial purposes. The ability of NF to resist permanent distortion, i.e., the product of attraction and repulsion forces (between particle-particle and particle-fluid interface) over a given period, is known as its stability. The suspension stability of NPs distributed in BF greatly influences the performance of nanofluids. NPs are prone to instability and aggregation due to a variety of forces, including Van der Waals attraction, magnetic attraction, electrostatic attraction, bouncy and gravitational forces. These forces act against the stability of colloidal suspension and cause formation of large clusters, leading to deterioration of nanofluid performance. The proclivity of NPs to cluster results in the destabilization of nanofluid suspensions. The tendency of agglomeration is caused due to higher surface area as well as surface activity of original fluid with addition of NPs. Therefore, the agglomeration must be avoided to prepare a stable suspension that maintains stable dispersion of the nanomaterials in the pure fluid. The mechanism of dispersion of colloidal suspension is explained by the DLVO theory of particle dispersion [127]. The DLVO theory is based on the Van der Waals attractive force and electrostatic repulsive force that exist among colloidal particles. The net attraction or repulsion force depends on the distance between particles and the summation of Van der Waals attraction force and electrostatic repulsion force. However, this colloidal theory of nanoparticle dispersion is based on a few key assumptions: However, this colloidal theory of nanoparticle dispersion is based on a few key assumptions: (1) particle dispersion is homogeneous and dilute, (2) Van der Waals force and electrostatic force are the only forces acting on the suspension, (3) buoyancy and gravity forces are negligible, and (4) ion distribution in the suspension is controlled by factors such as Brownian motion, electrostatic force, and entropy influenced dispersion.

$$F_T = F_{VdW} + F_{ES} \qquad (7)$$

Where F_{VdW} and F_{ES} are the attractive and repulsive potential between the particles. If the attractive force is stronger than the repulsive potential, suspension will not be defined as unstable. From **Fig. 12**, it can be understood that when total interaction potential is high (i.e., potential barrier is high), NPs are likely to remain stable preventing clusters due to higher separation distance, whereas low net interaction potential will result in unstable suspension. Nevertheless, if the particles collide beyond the potential barrier being affected by influential factors (e.g., temperature, chemical additives) than attractive potential will dominate (i.e., separation distance is less) and form agglomeration (low zeta potential) to deteriorate

suspension homogeneousness. Hence, the separation distance would be low, and it will cause to emerge secondary minima which leads to further aggregation. Electrostatic repulsive potential must be predominant over the attraction force to formulate stable NF. However, mathematical expressions of Van der Waals attraction force and electrostatic repulsive force vary depending on concentration, size, and shape of the particles.

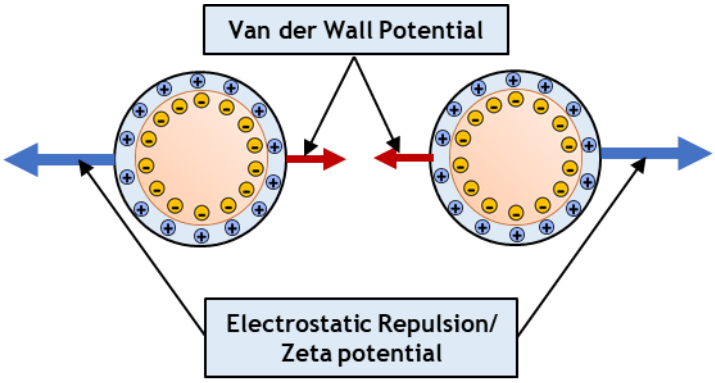

(a)

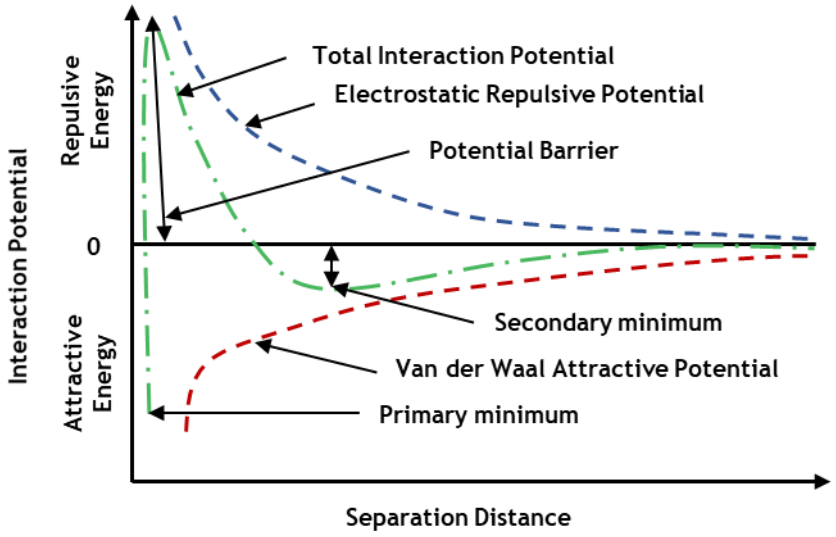

(b)

Fig. 12. (a) Interaction of two NF particles suspended in a BF (b) Schematic representation of the interaction energy of stable NFs as a function of particle separation distance [8].

4.1. Influential parameters effecting stability of NF

Several factors have noteworthy effects on the colloidal stability of NF suspension. The mechanism of some crucial factors influencing the colloidal stability of NF such as dielectric constant (ε) of BFs, φ, pH value, particle shape and size, temperature, Zeta potential (ζ), stabilizing additives/surfactants, and stability evaluation techniques. For instance, various types of BFs are used to formulate NFs based on the potential application of the fluids in low

to high temperature thermal heat transfer systems. The dielectric potential of fluids is an important property as it is directly related to repulsive potential which determines the stability of the fluid. The higher value of the ε for fluid implies higher stability in suspension. Water has a ε of approximately 78.5 at room temperature, which is the maximum among the generally used BF such as oils and glycols [128]. Deterioration of suspension stability of NFs due to addition of NPs is a chemical phenomenon, i.e., more the solid particles in BF, less the suspension stability [8, 11].

Choi, et al. [129] experimentally examined improved stability of water/MWCNT (0.0005-0.002vol.%) NF using different chemical dispersants (surfactants) e.g., SDBS, CTAB, SDS and TX-100. They revealed that the NFs were stable for over 30 days and exhibited improved absorbance property under the impact of surfactants. Tiwari, et al. [130] studied stability of four separate BF (water, EG, therminol-VP1 and silicon oil) based MWCNT-CeO_2 NFs using six unique surfactants (BAC, ALS, CTAC, Bri-700, PLS and Span-80) and substantial rang of ultrasonication period (30-240 minutes) for stabilization of the suspensions (**Fig. 13**). The obtained data elucidated that BAC was the most efficient stabilizer, as it the stability indicator (ζ) relative to other surfactants. Increased ultrasonication time results in a more homogeneous suspension up to a point where further ultrasonication deteriorates the stability of the dispersion due to the formation of clusters. Using BAC as surfactant, silicon oil-based NF performed best stability in terms of ζ, duration and sonication time (66 mV, 30 days, 60 min) followed by EG (61 mV), water (57 mV) and therminol-VP1 (45 mV) based NFs at identical 0.75 vol.% of MWCNT-CeO_2. The effect of increasing temperature (25-50°C) on stability was negative in this experiment, which could be attributed to the stabilizers' limitations at higher temperatures [131]. Similar positive effect of surfactants are observed using water/Al_2O_3 and oil/Al_2O_3 NFs by [132] and [133] respectively. The effect of low-high temperature using different surfactants can be understood from the experiment done by Choi, et al. [129] using water/MWCNT NFs. They stated that stability varies utilizing different dispersants in terms of temperature. In their case, SDBS performed well for low (10℃) and high (85℃) temperature whereas, CTAB and TX-100 showed well stability factor only at high temperature.

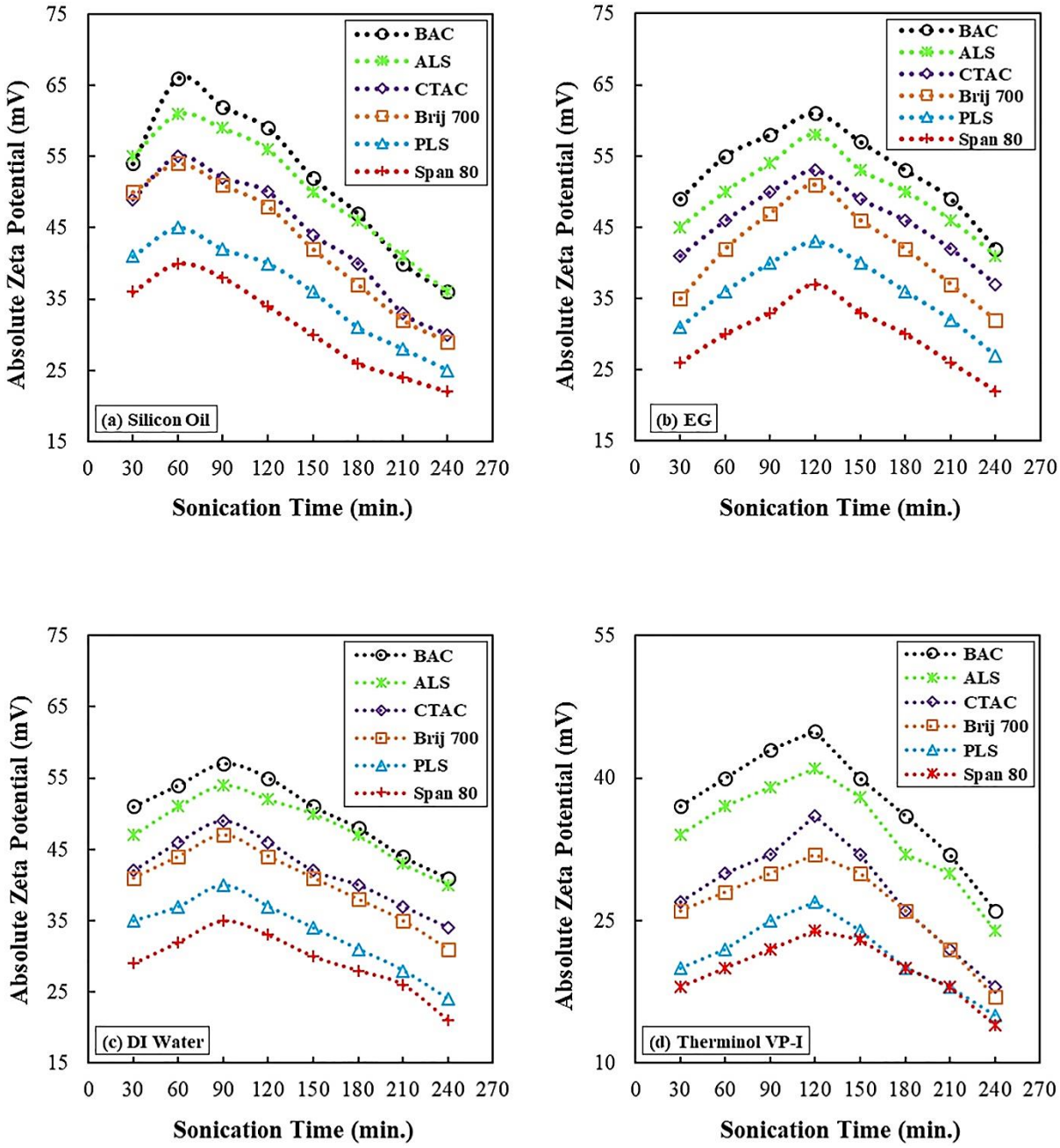

574

575 **Fig. 13.** The impacts of several BFs, surfactants and sonication period on suspension stability
576 of hybrid NFs using MWCNT-CeO_2 nanocomposite and different BFs, investigated by [130].

577 Almanassra, et al. [42] found excellent stability of water/CNT (0.1-1wt.%) NF adding GA,
578 PVP and SDS as stabilizers using an optimum ration of 1:0.5 (NP: surfactant). The stability of
579 GA and PVP-containing samples has been confirmed to exceed six and three months,
580 respectively. Xian, et al. [58] experimentally evaluated the influence of various surfactants e.g.,
581 anionic (SDS, SDC and SDBS), cationic (CTAB) and non-ionic (PVP and Triton X-100) along
582 with the effect of sonication time on water-EG based mono and hybrid NFs using
583 functionalized graphene (COOH-GnP) and graphene (COOH-GnP)-TiO_2 NPs at 0.025-

0.1wt.%. Cationic CTAB and anionic SDBS stabilizers are found to be superior options for homogenizing the suspension using a 90-minute sonication time. The obtained ζ data confirmed robust stability of single particle-based NF (-52 to -60 mV) rather than hybrid (-42 to -46 mV) at all NP loadings. Keklikcioglu Cakmak [60] demonstrated the opposite effect of surfactants, as the stability and absorbance of water/GO NF decreased when CTAB, SDS, and TX-100 were added regardless of φ.

Zhang, et al. [65] investigated the effect of pH variation on the suspension stability of water/TiO_2 NF through sedimentation, TEM photos, DLS analysis, Brownian and settling velocity ratios. NF sample with pH of 12 is observed to remain well dispersed for long time (> 30 days) with a ζ value of -45.06 mV and smallest particle size of approximately 81.19 nm while samples having pH values (4.5-8.5) around IEP 6.5 indicated lowest stability demonstrated in **Fig. 14**.

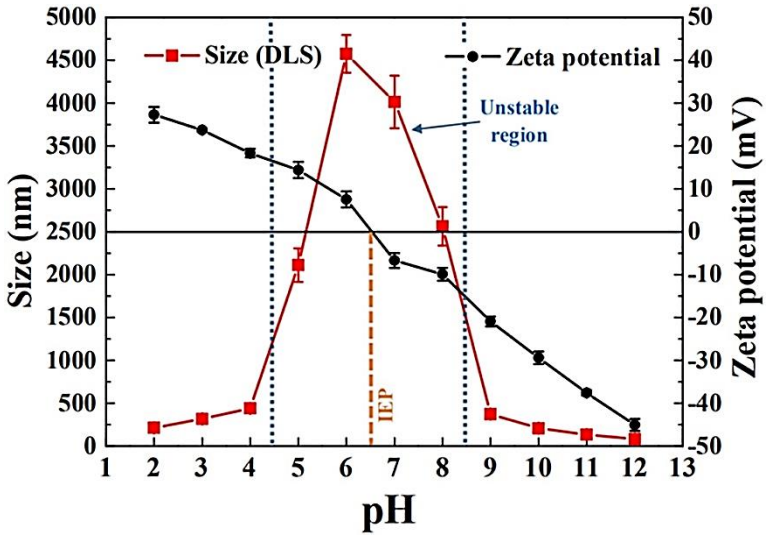

Fig. 14. Influence of pH values on Zeta potential and particle sizes of water/TiO_2 (20 nm, 0.025vol.%) NFs at 25℃[65].

Wang, et al. [66] observed variation in pH (3-11) and surfactant concentration (0-0.15wt.%) noticeably alters suspension agglomeration of water/Cu and water/Al_2O_3 NFs and optimum combination of the parameters can deliver optimized particle distribution, stability, and effective TC. At optimized pH condition (8.0 and 9.5 for alumina and Cu NFs respectively), improved stability indicator value is achieved $\zeta_{\frac{w}{alumina}} = 40.1$ and $\zeta_{\frac{w}{Cu}} = 43.8$ mV. **Table. 5** represents a summary of reviewed experimental works on stability of various NFs with detailed specifications on the operating conditions. Details on stability evaluation methods and stabilization techniques are covered in **Section 4.2 and Section 4.3**, respectively.

4.2. Stability assessment techniques

Different techniques are employed in investigations for assessment of nanofluids suspension stability, i.e., sedimentation and centrifugation, Zeta potential measurement, transmission electron microscopy, spectral absorbance, and transmittance measurement, 3-ω method and dynamic light scattering technique (presented in **Fig. 15**). In the following sections, stability measurement methods of NFs will be discussed briefly.

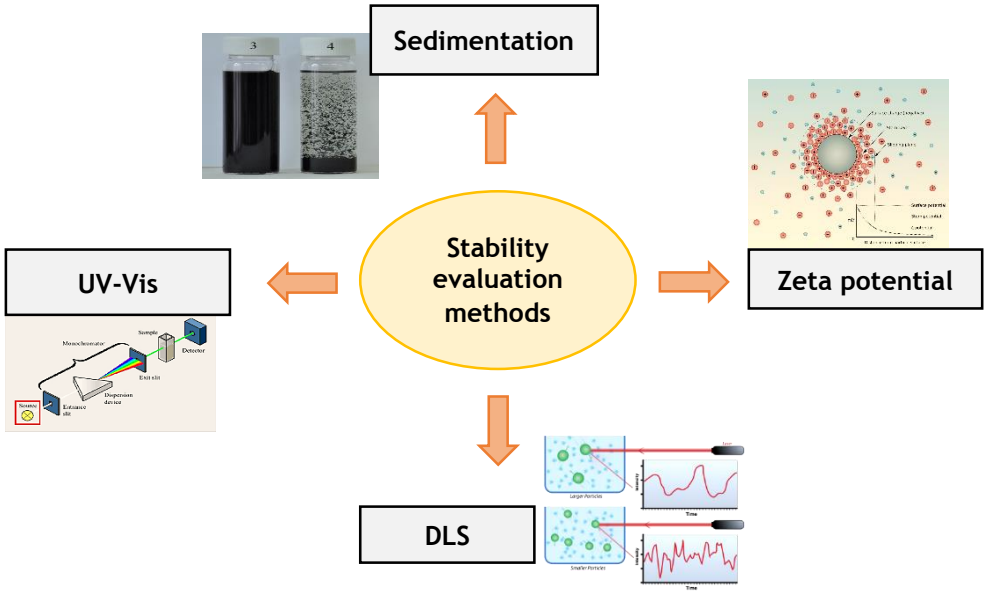

Fig. 15. Effective stability evaluation techniques for nanofluids.

4.2.1. Sedimentation

Sedimentation of NFs is important since it is directly related to their suspension stability. This approach uses static nanofluid images to test the settling activity of NFs due to gravitational force and the internal solid-liquid interaction between scattered particles and BF. Stability is determined using this technique by the time required for the NF sample to precipitate. Stokes law can be used to calculate the gravitational settling of spherical shaped particles:

$$V_t = \frac{2r^2(\rho_p - \rho_b)g}{9\mu} \qquad (8)$$

where V_t, r, ρ_p, ρ_b, g and μ represent terminal velocity of spherical particles, radius of the particles, density of solid particles, density of base fluid, gravity, and dynamic viscosity of the base fluid, respectively. According to the equation, smaller particles have a lower terminal velocity and a higher sedimentation rate than larger nanoparticles distributed in BF. Additionally, it demonstrates that the dynamic viscosity of BF and the density of nanoparticles

are critical parameters for the formation of stable nanofluids. Stability can also be determined using this technique by comparing the height of the sedimented layer to the duration.

Several studies on the stability characterization of NFs have been conducted using the sedimentation technique [134-136]. This approach is advantageous and cost-effective in comparison to other approaches for determining stability, such as zeta potential, UV-vis, and electron microscopy. Rehman, et al. [137] used the sedimentation approach to examine the stability of MWCNT/Jatropha oil nanofluids. For up to three weeks, the nanofluids exhibited no visible sedimentation and exhibited excellent stability over a one-month period. Ilyas, et al. [138] studied stability of Al_2O_3/thermal NFs at natural and functionalized conditions. They revealed that functionalized NFs exhibit suspension stability of more than 4 weeks whereas, natural samples aggregation within a few hours from the formulation of NFs. However, due to significant limitations, this approach is not widely reliable. Due to the impossibility of detecting internal dynamic solid-liquid interactions with the naked eye or by examining images, this method of determining suspension stability may not be predictable. Additionally, it is very difficult to detect sedimentation in dark nanomaterials solely by visualizing the NF samples.

4.2.2. Zeta potential (ζ)

As NPs are distributed in BF, the fluid surrounding the particles forms layers (i.e., stern and diffuse) that combine to form an electrical double layer (EDL). EDL produces a potential difference, referred to as the Zeta potential (ζ), which implies electrostatic attraction between scattered particles. Suspensions having a ζ value of more than ± 30 mV are considered electrostatically stable and above ± 60 mV indicate very good stability. Suspensions having ζ value in the range of ± 15 mV are considered unstable [139]. At a particular pH value of nanosuspension, ζ becomes zero and it is called isoelectric point (IEP). At the IEP, dispersed particles maintain an electrophoretic immobility. The possible electrostatically stable suspension can be obtained by adjusting the pH value in relation to the IEP value for electrostatically stabilized suspensions.

The ζ indicate the potential difference between the stationary layer (stern layer) of mobile particles and the layer of dispersant (diffuse layer) around the particles at the slipping plane. The Stern layer is tightly bound to the surface of the particles by oppositely charged ions, while the diffuse layer is weakly bonded and consists of both neutrally distributed positive and negative ions (demonstrated in **Fig. 16**). The ZP can be calculated using following equations:

$$\mu_e = \frac{V}{E} \qquad (9)$$

where V = particle velocity (μm/s), E = electric field strength (Volt/cm). The ζ can be calculated from the obtained μ_e by the Henry's equation.

$$\mu_e = \frac{2\varepsilon_r \varepsilon_0 \zeta f(ka)}{3\eta} \qquad (10)$$

where ε_r = relative permittivity/dielectric constant, ε_0 = permittivity of vacuum, $f(ka)$ = Henry's function and η = viscosity at experimental temperature. The ζ value significantly effects the colloidal stability of nanofluids [140]. A higher absolute value of ζ indicates more stable suspension, whereas low ζ depicts unstable nanoparticles distribution into the pure fluid [132]. A stable nanofluid possesses higher repulsive force among the dispersed particles because of higher absolute potential difference. According to the most widely accepted DLVO theory, colloid stability depends on the sum of Van der Waals attractive forces and electrostatic repulsive forces due to the EDL. However, the limitations of this theory are stated by Bhattacharjee [141] as it does not provide details on Van der Waals interactions among the dispersed particles. In addition, it should be noted that, in contrast to common practice regarding stability of NFs, ζ value should not be taken as the ultimate indicator of suspension stability of NFs unless the NFs are stabilized by electrostatic repulsion between the particles.

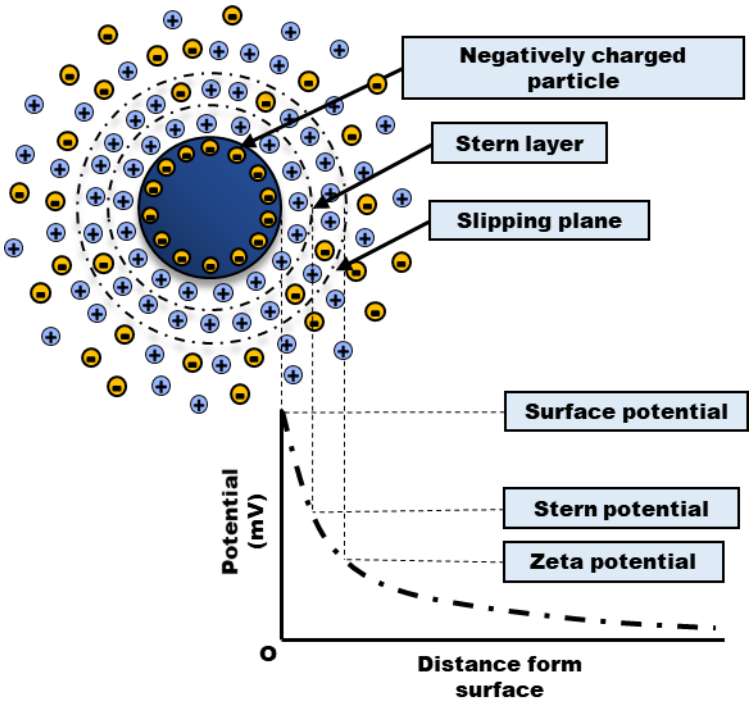

Fig. 16. Charged layers of nanoparticle dispersed in bulk base fluid.

4.2.3. Dynamic light scattering (DLS)

The DLS technique can be utilized to determine particle size distributing of any colloidal solution transmitting a monochromatic beam of light across suspension containing NPs. Light

diffuses in all directions depending on the size and shape of dispersed particles. The intensity of scattered light fluctuates due to Brownian motion of the particles and is then investigated by a photon detector to evaluate the particle size distribution by analyzing the diffusion coefficient (D_τ) which is a function of critical parameters such as particle hydrodynamic size, temperature, and absolute viscosity of the NF. and can be calculated using the Stokes-Einstein equation [141]:

$$D_\tau = \frac{k_B T}{6\pi\mu R_h} \qquad (11)$$

where k_B, T, μ and R_h are the Boltzmann constant, temperature, viscosity hydrodynamic radius of particles. The particle size distribution of a suspension shows the stability of the dispersion by determining the cluster size of the scattered particle over time intervals. Particles with a large cluster size indicate that the suspension is unstable, resulting in sedimentation and agglomeration of scattered particles. Investigations with nanofluids, DLS technique is being used to successfully determine the particle distribution in order to define suspension stability. Anushree and Philip [142] observed the hydrodynamic size of α-Al_2O_3 and TiO_2 NFs decreases significantly with time, implying significant sedimentation and unstable dispersion of the nanofluids. Navarrete, et al. [143] experimentally measured particle size distribution for molten salt-based NFs using a DLS set-up which is designed to perform up to 500ºC. Nevertheless, the DLS technique may interpret inconsistent results when particle concentration is high, and sizes of dispersed multiple nanomaterials are not identical.

4.2.4. Spectral absorbance measurement

The stability of NFs can be determined by measuring the spectral absorbance over a specific band of wavelengths. UV-Vis spectral analysis is often used to determine stability by estimating spectral absorption between 190 and 1100 nm [144]. Stability is evaluated using this technique by analyzing the absorption profiles of NF samples with varying solid concentrations over a specified period. An UV–Vis spectrophotometer uses the fact that the light intensity turns out to be different by absorption and scattering of light passing through a fluid. Stability is determined by assessing the variation in absorption peak characteristics for the fluid against time. Lower value of absorbance after a certain period indicates instability of NF suspension. Absorbance (A_λ) can be estimated using the following equation:

$$A_\lambda = \log_{10}(I_0/I) = \alpha \times l \times c \qquad (12)$$

Absorbance (A_λ) is proportional to particles concentration (c), absorptivity (α) distance traveled by the light source. I_0 and I are the intensity of light beam before and after passing

through the fluid sample. The reduction of solid concentration in the suspension over time is reflected in decreased absorbance due to agglomeration in the suspension. This approach has been shown to be useful in determining the stability of NF in several studies [145, 146]. However, the technique is ineffective for samples with high NF concentrations or dark suspensions because it is difficult to distinguish sediment visibility at high solid concentrations [147].

4.3. Nanofluids stabilization techniques

A thorough understanding of colloidal dispersion mechanisms is needed to clarify the suspension stability of NFs. The dispersion or suspension stability of NF is directly associated to inter-particle interaction and active microscopic forces acting on dispersed nanoparticles in the base fluid. NFs are inherently unstable due to the gravitational force acting on each NP which causes sedimentation of the particles. However, random thermal motion, i.e., Brownian motion of NPs can counterbalance the sedimentation and stabilize the suspension. Along with force action on single NP, interaction forces between the particles in the suspension play a dominant role in the dispersion characteristics of NF [26]. During inter-molecular interaction among adjacent particles, NPs tend to form aggregation due to ubiquitous Van der Waals attraction forces (F_{VdW}). The magnitude of F_{VdW} depends on different factors such as; dielectric constant of the solvent, interfacial interaction between the NP and dispersion medium [148]. In contrary, the electrostatic potential between adjacent particles stabilizes the colloidal suspension through repulsive intermolecular interaction. The resultant potential of these inter-molecular forces is a function of a few key parameters as discussed in **Section 4**. Different effective stabilization techniques for improved stability of NF are summarized and classification of the techniques is shown in **Fig. 17**. In the following sections, these stabilization techniques are enlightened.

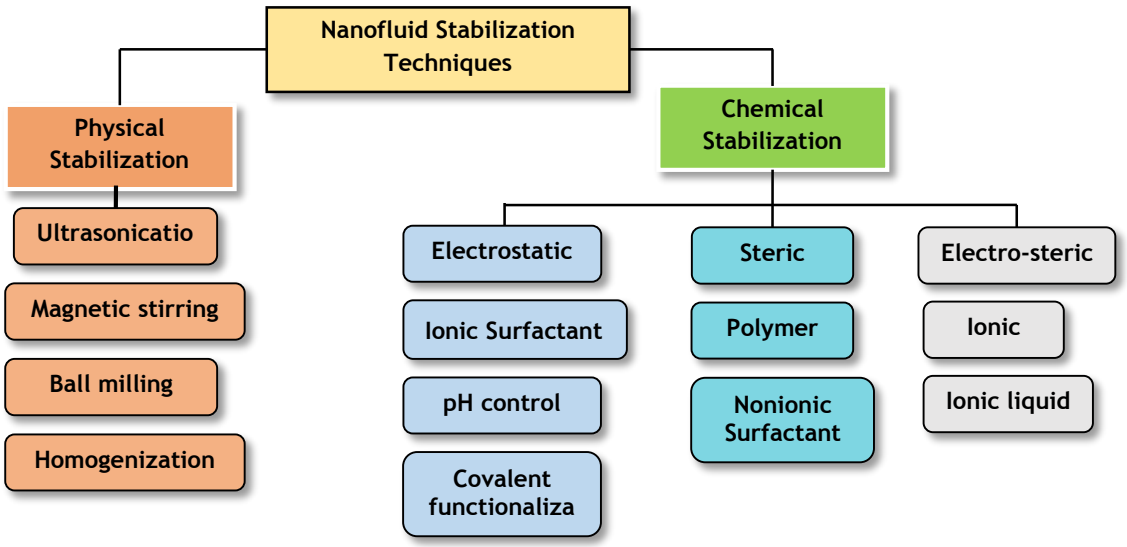

Fig. 17. Stability enhancement techniques for nanofluids.

4.3.1. Physical stabilization

Different physical techniques are often used to stabilize NF suspensions. Mechanical methods such as ultrasonic vibration, magnetic stirring, and homogenization are often used to disperse colloidal mixtures homogeneously.

Ultrasonication is an important mechanical dispersion technique for achieving a homogeneous mixture of NPs and base fluid. Ultrasonication methods, both direct (ultrasonic bath) and indirect (probe sonication), can be used to stabilize colloidal suspensions by dissolving particle clusters and reducing the average particle size distribution. The indirect ultrasonication approach using high frequency probe sonication exhibits superior output in various studies involving NF dispersion. Ultrasonication of colloidal suspensions results in a more homogeneous distribution of NPs within the mixture, resulting in a smaller average cluster size, which has a significant effect on the NP's heat transfer properties [149]. Asadi, et al. [150] reviewed the remarkable effect of ultrasonication on the colloidal dispersion and heat transfer characteristics of NF, highlighting the significant effect of ultrasonication time and power variation on the effective dispersion of NPs into BF. In another article, Asadi, et al. [151] revealed that the optimal time for sonication is 60 minutes for MWCNT/water NFs with the highest thermal conductivity. However, beyond a certain amount of ultrasonication, dispersion characteristics and thermophysical behavior deteriorate noticeably, and this stage is considered the optimal time for stabilization [152].

Magnetic stirring is a fundamental technique for achieving homogeneous dispersion of NPs in a base liquid solvent. A spinning magnetic bead rotates at varying speeds in this process, using

an external magnetic field to break up clusters and disperse the NPs. Studies has shown that effective stirring technique depends on two crucial parameters such as stirring speed and stirring time. Usually, high speed of stirring and longer time of stirring yield better performance dispersing NP clusters. At elevated speed and longer stirring time more NPs can come into contact to the magnetic bead and break apart into smaller particles. Kamalgharibi, et al. [153] reported better stabilization of CuO/water-EG NFs at higher stirring speed. At 700 rpm, they observed the lowest height of sedimentation while lower rpm showed a rise in sedimentation and instability of the suspension. Chen, et al. [154] investigated dispersion stabilization of Al_2O_3/liquid paraffin NF at different stirring periods. They observed that stirring for a longer period increases stability by using stirring in two stages of the stabilization process. They noted that increasing stirring time by 30 to 40 minutes yields 3.14% more thermal conductivity for the studied NFs. In addition, stirring is found to be more effective at elevated temperatures and lower concentration of NPs. To formulate stable NFs, few other effective stabilization methods, for instance; high-pressure homogenization and ball milling are employed in various studies and found prominent improvement of dispersion characteristics [155-157]. However, the stability of NFs remains a challenging issue since the physical maintenance techniques often fall short of providing suspensions that are stable for the long term.

4.3.2 Chemical stabilization

Chemical techniques for stabilization i.e., electrostatic, steric, or electro-steric strategies include surface functionalization, surfactants inclusion, pH control, acid treatment and so on. The sections that follow provide a thorough understanding of these stabilization techniques.

4.3.2.1. Electrostatic stabilization

Electrostatic stabilization of NFs can be obtained when attractive Van der Waals force is stabilized by reciprocal repulsive potential between the identically (positive or negative) charged particles demonstrated in **Fig. 18**. The surface charges of the NPs can be induced by several approaches such as: (a) ionization of surface groups, (b) adsorption of ions from ionic surfactants, (c) substitute of ions, (d) dissociate surface charged parts, (e) physically adsorbed ions, and (f) accumulation or depletion of electrons at surfaces. In liquid suspension, charged NPs are surrounded by opposite charges to sustain charge neutrality of the dispersion and to form the electric double layer (EDL) with a strongly bonded stern layer and diffuse layer. The stern layer contains opposite ions whereas, diffuse layer consists of weakly attached both positive and negatively charged ions due to electrostatic force of the particles. The electric

potential is maximum at the surface of the particles and drops steadily away from the surface to EDL. The electric potential at the outer layer of EDL is defined as Zeta potential, which value is used to estimate the dispersion stability of NF suspension. The objective of electrostatic stabilization is to increase the electric potential between the particles to minimize the attraction force so that particles cannot form agglomeration and disperse homogenously in the liquid medium. The higher the potential, the higher the electrostatic stability of the NFs.

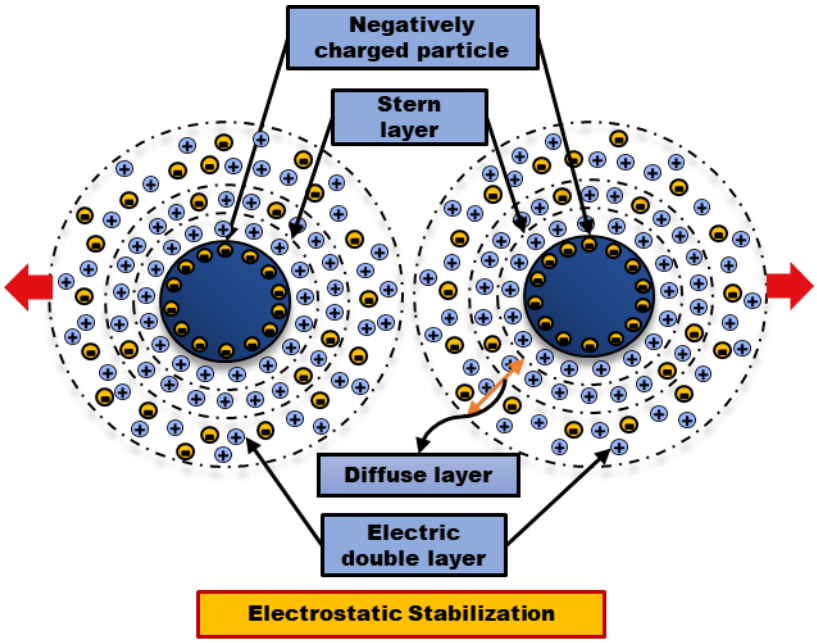

Fig. 18. Electrostatic stabilization technique for nanofluid suspension.

Electrostatic stabilization includes the addition of ionic surfactants to the NF. Several categories such as cationic, anionic, non-ionic, and amphoteric surfactants are employed in BF [158-161]. Amphoteric surfactants, also known as zwitterionic, are surfactants containing both cationic and anionic hydrophilic functional groups in their chemical structure. This class of surfactants can produce cations and anions depending on the acidity (pH) of the suspension. These surfactants exhibit low toxicity, good anti-bacterial characteristics, resistance to the hardness of water and are well-suited with other forms of surfactants. Amiri, et al. [161] reviewed stable liquid-phase exfoliation of two-dimensional graphene using several classes of ionic and non-ionic surfactant stabilizers such as pluronic P-123, Triton X-100, Polyvinylpyrrolidone (PVP), n-Dodecyl β-D-maltoside, Polysodium4-Styrenesulfonate (PSS), Sodium deoxycholate (DOC), Sodium taurodeoxycholate hydrate and so on. Furthermore, pyrene derivative dispersion stabilizers are also used for effective suspension stabilization. Parviz, et al. [162] investigated different pyrene-based stabilizers such as 1-Pyrenesulfonic acid sodium salts (Py-1SO_3), 1-Pyrenesulfonic acid hydrate (Py-SAH), 1,3,6,8-Pyrenetetrasulfonic

acid (Py-4SO_3) and 1-Pyrenecaboxylic acid (PCA) with high concentration of graphene nanosheets. They concluded that pyrene derivatives attached with sulfonyl groups yield the most stable dispersion of NPs over a wide range of pH. Aromatic stabilizers are generally utilized for homogenous dispersion of carbon-based NPs in different BFs [163, 164].

Pyrene derived stabilizers are also considered as anionic surfactant and used as non-covalent functionalization method of NF stabilization. Ionic and non-ionic surfactants are used to obtain electrostatic and steric stabilization of NF dispersion. Non-covalent functionalization can be accomplished by various way such as anionic and cationic surfactant, non-ionic surfactant, polymer, and aromatic surfactant. For carbon-based NFs, the main shortcoming of non-covalent functionalization is the formation of foam inside thermal apparatus leading to lessening in effective heat transfer performance [165, 166]. In contrary, covalent functionalization of carbon-based NF can overcome these shortcomings [74, 167]. The most frequently utilized stabilizers for covalent functionalization of carbon-based NPs are Sodium Dodecyl Sulfate (SDS), Sodium Dodecyl Benzene Sulphonate (SDBS), Gum Arabic (GA) and Triton X-100. Among them, SDBS offers finest dispersion stability of carbon-based NP in water due to strong π-π interaction between the carbon particles [168].

Stability of NFs can also be obtained by substituting the functional groups on the surface of NPs using acid or alkali solution and employing plasma treatment as well. Several functional groups for instance; hydroxyl ($-\mathrm{OH}$), carboxylic ($-\mathrm{COOH}$), carbonyl ($\mathrm{C}=\mathrm{O}$), sulphate (SO_4^{2-}) and amine ($N-H$) leads to advance suspension stability in the polar solvents. Such form of functionalization is identified as the covalent functionalization [161, 169]. Amiri, et al. [167] investigated effect of covalent and non-covalent functionalization of CNT NPs using Gum Arabic and Cysteine respectively. Amiri, et al. [170] reported improvement of dispersion stability of graphene (doped with nitrogen)/ethylene glycol-water NF using cyanamide as stabilizer. Ettefaghi, et al. [171] prepared environment friendly stable graphene-water NF without using citric acid as precursor. They reported NFs were stable for six months at low-cost to formulate the ecofriendly NFs.

pH of NF suspension plays an essential role in terms of stability of the dispersion therefore, pH adjustment of NF mixture leads to attain considerable homogenous dispersion characteristics of the mixture. To obtain good suspension stability pH should be controlled either at higher value or lower value with respect to pH value of isoelectric point (IEP) for the suspension. At IEP, zeta potential for any suspension is zero which implies absence of repulsive force in the mixture hence, the mixture is at unstable state in terms of homogenous dispersion. Lee, et al. [172] showed colloidal mixture performs better suspension stability and thermal performance

at pH value far from the value of IEP using CuO NF. They concluded surface charge as a basic key parameter towards improved thermal performance of NFs. Investigations on effect of pH control on dispersion stability of NF are performed to evaluate optimum pH value for NF under which it performs better suspension stability [66, 173-175].

Several oxidizing agents such as; HNO_3, $K_2S_2O_8$, H_2SO_4, $KMnO_4$ and so on are utilized to improve dispersion stability of colloidal mixture [176, 177]. Ghozatloo, et al. [178] used $K_2S_2O_8$ and KOH solution as oxidizer and pH control agent respectively for alkaline functionalization of hydrophobic graphene nanosheets into hydrophilic structure. The results exhibited improvement in dispersion as well as in thermal conductivity due to the inclusion of $-OH$, $-COOH$, $-COOK$ functional groups in the formulated NF.

However, electrostatic stabilization has some restrictions regarding the applicability of this dispersion technique in different medium as follows; (a) this technique is applicable for non-aqueous colloidal suspension, (b) limited to dilute nanoparticle dispersion, (c) not suitable for systems containing metal ions and saline medium and (d) stable dispersion of the agglomerated particles is not possible in this method of stabilization.

4.3.2.2. Steric stabilization

The steric or polymeric technique of colloidal suspension stabilization is characterized as the addition of polymeric chains to the particle surface in order to generate repulsive forces between the dispersed particles and thus improve suspension stability. The polymer molecules use steric hinders to counteract the attraction force between the NPs (see **Fig. 19**). Non-ionic surfactants and polymers can be used to stabilize NFs sterically [161, 168, 179, 180]. Steric stabilization enables the stabilization of NFs at higher particle loadings than electrostatic stabilization.

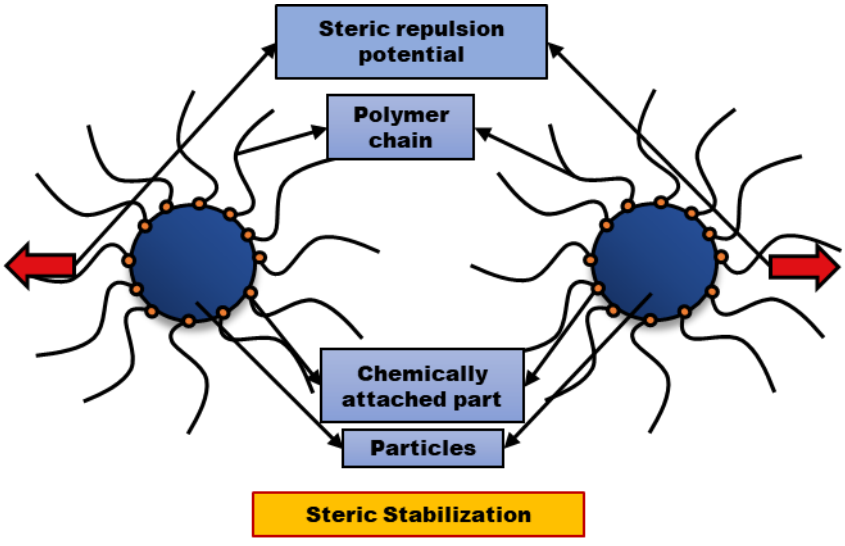

Fig. 19. Steric stabilization technique for nanofluids stabilization.

By grafting polymers or macromolecules onto the surface of NPs, a steric barrier is formed between the dispersed particles, significantly lowering the intermolecular Van der Waals potential [26, 181]. Via chemical or physical adsorption, the polymers become weakly bound to the NP surface. When polymers are grafted onto the surface of particles, they restrict particle movement in the base fluid, creating a barrier that prevents particle aggregation [182]. Compatibility of polymeric additives with BF is critical for successful stabilization. Steric stabilization performance is highly dependent on the absorption properties and length of polymeric chains. For example, increased polymer absorption on the NP surface results in a larger grafted surface, which can result in an improved steric effect in the dispersion. The length of polymeric chains is critical since short polymers exhibit poor absorption properties. Thus, a longer polymeric chain and strong bonding to the NP surface are needed for effective steric stabilization.

Steric stabilization polymers are either homopolymers containing the same monomer or copolymers containing two dissimilar monomers in the same polymeric chain. Co-polymers are classified into three groups based on their monomer structure, namely random, block, and graft co-polymers. If random co-polymers are composed of several groups of monomers randomly assembled, block co-polymers are composed of two monomer blocks of repeating units. In contrast to random and block copolymers, graft copolymers have a main structure composed of one monomer and another monomer on the side chain. For possible steric stabilization, grafted and amphiphilic block polymers are optimal. The criteria for selecting co-polymers for steric technique are that one component should be attracted to the particle surface and the other component should be compatible with the BF medium. Gum Arabic, Oleylamine, Triton-X-100, Tween 20, Span 80, PVP, and oleic acid are all polymers that are often used for steric stabilization of NFs [91, 183, 184].

4.3.2.3. Electro-steric stabilization

Electro-steric stabilization is the combination of electrostatic and steric stabilization Ionic polymers are absorbed by the charged particle surface in this technique, resulting in the formation of a steric barrier and electrostatic barriers that prevent the agglomeration of dispersed NPs. Apart from steric repulsion, the electrostatic double layer developed in this process enhances NF dispersion much further. Electro-steric stabilization is typically accomplished using ionic polymers that incorporate a charged anchor segment and an ionic

polymeric chain to simultaneously provide electrostatic and steric stabilization (illustrated in **Fig. 20**).

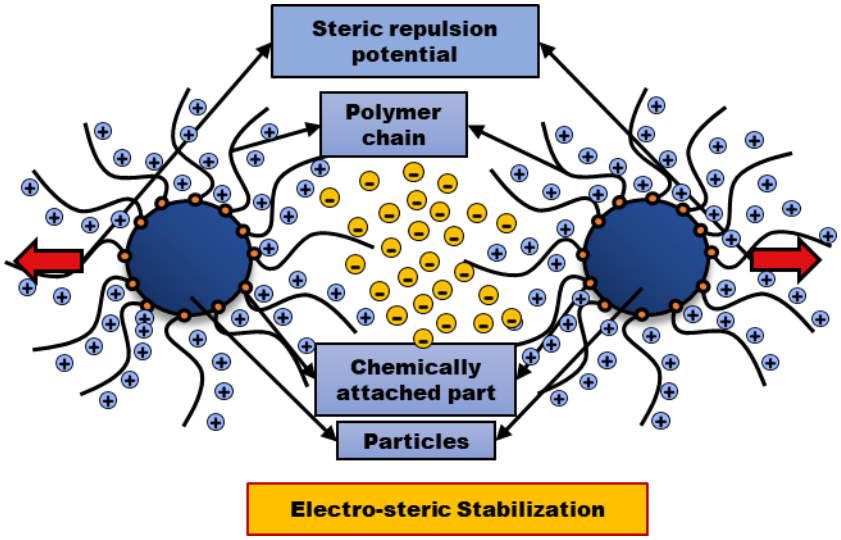

Fig. 20. Electro-steric stabilization for nanofluid suspension.

The polymer used in this method is identified as polyelectrolyte which is an amalgamation of repeating polymer units attached with at least one ionized functional group (such as; carboxylic, sulfonic acid group and so on) and different molecular structure [185]. The most used polyelectrolytes for the electro-steric stabilization of NPs in suspension are poly(styrene sulfonic acid) (PSS), polyacrylic acid (PAA) and poly(1-vinylpyrrolidone-co-acrylic acid) (PVcA) as anionic block co-polymers, poly(vinyl sulfonic acid) (PVSA), and polyethyleneimine (PEI) as cationic polyelectrolyte [185, 186]. The ionized function groups attached to the polymers dissociated into the base fluid to form EDL between the approaching particles. To achieve successful stabilization, the ionic polyelectrolytes and NP should be charged in the opposite direction. Polyampholyte can also be used for electro-steric stabilization because it contains both anionic and cationic functional groups. Owing to their high charge density and heavy chemisorption on the NP surface, ionic liquids are used to stabilize NFs by providing electrostatic repulsion and steric stabilization, respectively [187]. Kong, et al. [188] stabilized cement and deionized water suspensions using melamine formaldehyde sulfonate (MFS) as a solid anionic polyelectrolyte.

921 **Table. 5.** A summary of experimental studies on stability of nanofluids with detailed operating conditions and deployed stabilization techniques.

Reference	**Examined nanofluids**	**Particle size and concentration (φ)**	**Surfactant or chemical additives**	**Stability or Zeta potential (ζ)**	**Stabilization techniques**
Bandyopadhyaya, et al. [189]	Water/SWCNT	30-50 nm Φ = 0.05 wt.%	GA, SDS and CTAC	3 months	Steric and electrostatic stabilization mild sonication
Abdelrazik, et al. [43]	DI water/rGo-Ag	n/a Φ = 0.0005-0.05 wt.%	SDBS	> two weeks	Electrostatic stabilization ultrasonication.
Akash, et al. [11]	DI water/MWCNT DI water/Al DI water/Cu	MWCNT (length = 6 µm, diameter = 5 nm) Al (80 nm), Cu (40 nm) Φ = 0.3 vol.%	SDS	ζ = -42.3, -41.2 and -38.4 mV, respectively.	Electrostatic stabilization mechanical stirring, ultrasonication.
Zhao, et al. [47]	Water/G-BN	Graphite (40 µm), BN (20 µm) Φ = 0.05-5 vol.%	1M Hcl(aq) solution is used for covalent functionalization.	Several months, ζ = -48 to -31 mV	Steric stabilization, ultrasonication Covalent functionalization, ultrasonication pH control.
Das, et al. [72]	Water-[MMIM][DMP]/ MXene	1-10 µm × 1 nm Φ = 0.05 and 0.2 wt.%	--	ζ = -17.88 to -39.54 mV	Physical stabilization: magnetic stirring and ultrasonication.
Zare, et al. [38]	Distilled water/ZnO /TiO_2 /MWCNT	ZnO (15-30 nm) TiO_2 (21 nm) MWCNT (10-20 nm) Φ = 0.15 wt.%	MWCNTs were functionalized with -COOH group.	ζ = 32, 38.1 and 42.3 mV, respectively.	Chemical functionalization: -COOH group. Physical stabilization: magnetic stirring and ultrasonication.
Elminshawy, et al. [39]	Water/Al_2O_3	Φ = 1-3 vol.%	SDBS	ζ = -38.6 mV	Electrostatic stabilization magnetic stirring, ultrasonication.
Islam, et al. [41]	Water/SWCNT	L = 20-50 nm Φ = ≤ 1.0 mg/mL	SDBS, SDS and TX-100	3 months	Electrostatic stabilization Ultrasonication
Amiri, et al. [74]	Water/GNP-COOH /GNP-SDBS	0.5-3 µm × 0.55-3.74 nm Φ = 0.025-0.1 wt.%	SDBS	n/a	Electrostatic stabilization
Chakraborty, et al. [190]	Water/Cu-Zn-Al LHD	49 nm × 9 nm Φ = 200-800 ppm	SDS, Tween 20	ζ = -52.7 mV	Steric and electrostatic stabilization magnetic stirring, ultrasonication.
Sarsam, et al. [30]	Water/GNPs	2 µm × 2 nm Φ = 0.1 wt.%	BS, SDS, CTAB, and GA	> two months	Electrostatic and steric stabilization. water bath, ultrasonication.

Sadri, et al. [75]	Water/GAGNPs	n/a Φ = 0.05 vol.%	--	> 63 days	None Ultrasonication, centrifugation
Zhang, et al. [86]	Water/CRGO	Thickness (~4.3 nm) Φ = 0.2 to 1 mg/ml	--	ζ = -44.68 to -54.52 mV, 45 days	Physical stabilization Ultrasonic probe
Srinivas, et al. [88]	Carboxylated water/MWCNT	1-25 µm × 20-40 nm Φ = 0.025-1 wt.%	Sebacic Acid and 2-ethylexanoic Acid	ζ = 18.88 to 30.11 mV	Electrostatic Ultrasonication
Wu, et al. [89]	Water/SWCNT /MWCNT	1-2 and 8 nm, length < 30 µm Φ = 0.0962-0.3846 vol.%	Humic acid	10 days	Electrostatic stabilization Ultrasonication
Yu, et al. [191]	Water/MWCNT	10-20 nm × 5-10 nm Φ = 0.01-0.4 wt.%	SDS	3 months	Electrostatic stabilization Sonication
Wusiman, et al. [90]	Water/MWCNT	5 µm × 5-20 nm Φ = 0.1-1 wt.%	SDBS and SDS	1 month	Electrostatic stabilization Ultrasonication, stirring
Wang, et al. [66]	Water/Cu /Al_2O_3	25 nm Φ = 0.02-0.8 Wt.%	SDBS	ζ = -43.8 mV	Electrostatic stabilization Ultrasonication, pH control
Sahooli, et al. [91]	Water/CuO	4 nm Φ = 1-6 vol.%	Polyvinylpyrrolidone	7 days ζ = 32.3 mV	Steric stabilization Magnetic stirring, ultrasonication
Fedele, et al. [192]	Water/SWCNH /TiO2 /CuO	100, 21 and 30-50 nm respectively Φ = 0.01-1 wt.%	SDS, hydrochloric acid and PEG	15 days	Electrostatic stabilization Homogenization, sonication, and mechanical shaking
Li, et al. [193]	Water/Cu	25 nm Φ = 0.05-0.1 wt.%	Triton X-100, CTAB and SDBS	7 days ζ = -43.8 to 28.1 mV	Steric and electrostatic stabilization Ultrasonic vibration, pH control
Iqbal, et al. [194]	Saline water/Fe_3O_4	< 100 nm Φ = 0.1 mg/ml	Poly (AMPS-co-AA)	1 month ζ = -53.6 mV	Electrostatic stabilization Sonication,
Ghadimi and Metselaar [40]	Water/TiO_2	25 nm Φ = 0.1 wt.%	SDS	7 days ζ = -33.3 to -55 mV	Electrostatic stabilization Ultrasonication
Song, et al. [92]	Water/stainless steel	70 nm Φ = 0.017 wt.%	SDBS	10 days ζ = -70 mV	Electrostatic stabilization Ultrasonication, pH control
Mousavi, et al. [97]	Water/MgO-TiO_2	25-45 and 18-23 nm respectively Φ = 0.1-0.5 vol%	SDS	ζ = 30.02-40.87 mV	Electrostatic stabilization Ultrasonication, magnetic stirring

922

5. Rheological behaviour of NFs

Rheology is the study of how fluids flow when subjected to applied tensions. The relationship between shear stress and corresponding shear rate is used to assess rheological behavior, where shear stress is defined as the applied force per unit area and shear rate can be calculated by measuring the rate of change in strain. The ratio of these two parameters is defined as viscosity (μ) and it is one of the key parameters for rheological characteristics of fluids.

5.1 Viscosity (μ), Newtonian and non-Newtonian behaviour

The resistance force which causes deformation of fluids against the flow direction is defined as dynamic viscosity (μ). It is one of the key properties of NFs which has significant effect in convective heat transfer performance during implementation on thermal energy conversion systems due to its direct association to pressure drop and pumping power. Rheometers and different viscometers are commonly utilized to experimentally evaluate μ of NFs [195-197]. Rheometers are used to characterize the flow behavior of fluids over a broad range of shear rates and temperatures, while viscometers are used to measure the of fluids.

Considering the relationship between shear stress and shear rate, rheological behavior of fluids can be categorized into Newtonian and non-Newtonian nature. It is established that Newtonian fluids follow linear variation in shear stress against corresponding shear rate or the ratio of shear stress and shear rate i.e., μ of Newtonian fluids remain unchanged with variation of shear rate. Whereas the non-linear relationship of shear stress and shear rate i.e.., variation of μ against corresponding shear rate results in non-Newtonian behavior of fluids. Rheological properties along with μ of NFs is affected by several vital parameters depicted in **Fig. 21**. Numerous experimental and theoretical investigations are performed to scrutinize and estimate rheological characteristics and μ of various NFs. Studies enlighten that the μ of NFs generally increases with the inclusion of solid particles, however the flow characteristics i.e., rheology depends on several parameters and operating conditions, for instance, NFs tends to behave as Newtonian fluid at low particles concentration, high shear-rates and without surfactants or stabilizers while thy act as non-Newtonian fluids at higher dispersed particles, low shear-rates, and addition of surfactants [198-200].

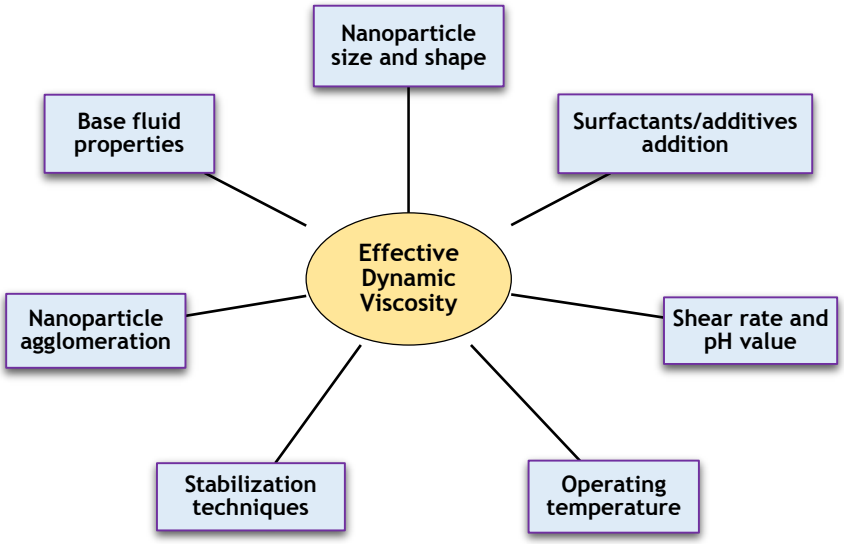

Fig. 21. Key parameters effecting dynamic viscosity of nanofluid.

Nguyen, et al. [201] investigated impact of temperature and NP size on viscosity of water-based metal oxide NF using different size of Al_2O_3 (36 and 47 nm) and CuO (29 nm) from 22 to 75℃. At 4 vol.% or less, effect of particle size is unlikely while at higher loadings (>4vol.%) 47 nm Al_2O_3 based NF exhibited greater viscosity than 36 nm Al_2O_3 particles. CuO NP showed more viscous property than the former. In addition, results showed the presence of a critical temperature beyond which NFs viscous property can alter radically. Barai, et al. [202] studied rheological properties of water dispersed graphene oxide and Fe_3O_4 (10-20 nm) NF for 0.01-0.2 vol.% over a wide range of shear rate (0-10000 s^{-1}). Findings showed 41% augmentation in μ_{nf} and predominant shear thinning property at low shear rates while it altered and remain almost unchanged against higher shear rates and temperatures.

In a systematic experimental approach Minakov, et al. [203] studied several NFs based on three different base fluids (water, glycol and oil) dispersing seven different nanomaterials (Al_2O_3,TiO_2, ZrO_2, CuO, Fe_2O_3, Fe_3O_4 and diamond NPs). The NFs are formulated using two-step method dispersing the NPs at concentration of 0.25-8 vol.% and the size of the nanomaterials differs from 5-150 nm. Considerable augmentation is reported for all the samples when NPs are dispersed in all three liquid mediums. In case of impact of NP size, the results revealed that smaller the NPs higher the μ_{nf} while influence of materials type found to be evident on viscosity as at the same particle size (150 nm). Water-TiO_2 NF exhibited substantially higher viscosity than water-Al_2O_3, also supported by related studies using molecular dynamic method [204, 205]. Effect of BFs also performed and detected that greater viscosity of pure fluids yields overall higher viscosity of NFs e.g., since water has a very low

μ in comparison with others traditional fluids, water adopted NFs are suitable in multifarious thermal applications. Furthermore, rheological assessment of the NFs elucidated that using smaller NPs and higher loading of particles can alter Newtonian behaviour to non-Newtonian while, using identical size of NPs of different class of nanomaterials can also show substantial divergence in rheological behaviour. Although the temperature relationship demonstrated a clear decreasing trend at elevated temperatures, the fascinating fact is that excess dispersed particles can result in hysteresis loss during heating and cooling operations [206], and viscosity of NF is demonstrated in terms of base liquid, φ and size using $\mu_{nf}(T) = \mu_{bf}(T)f(\emptyset, D)$ [207]. Addition of stabilizing surfactants from 0-100 mg/l in water-TiO_2 (150 nm, 2 vol.%) NF shifted Newtonian behaviour to shear thinning property in shear rate of 0-120 s^{-1} and intensified the μ_{nf} by 18% and adding 40 mg/l of polyacrylamide and nearly twice by xanthan surfactant. Jarahnejad, et al. [208] studied the influence of several factors (temperature, NP concentration, size, and surfactant) on effective viscosity of water-Al_2O_3 and water-TiO_2 NFs for 20-50℃ at NP concentration of 3-14.3 wt.%. Different surfactants (octyl-silane, polycarboxylate and trioxadecane acid) were added to formulate the NFs dispersing various sizes of Al_2O_3 (200, 250 and 300 nm) and TiO_2 (140, 200 and 90 nm) NPs. The results confirmed that the rise in μ_{nf} with 200 nm is lower than the NF with 250 and 300 nm particle sizes at 2.4 vol% loading for water-Al_2O_3, although a general trend was not mentioned explicitly. Impact of surfactants resulted an increase in the μ_{nf}, TiO_2 NF using polycarboxylate surfactant had greater μ than the TiO_2 NF using trioxadecane acid. However, association of μ dependency between surfactant and NP size was not clarified. Hence, it cannot be stated that the viscosity increment of nanofluids is completely reliant on the type of stabilizer. Koca, et al. [209] reviewed impact of NP sizes on μ of NFs based on the data from the literatures. They concluded inconsistencies among the studied investigations regarding different particles sizes at similar concentration and altering the NP size can results either increase or decrease of μ by 40%. Timofeeva, et al. [63] experimentally studied effect of four different NP shapes (platelets, blades, cylinders, and bricks) and solution pH for alumina/EG-water. They revealed that with addition of NPs at 1-7 vol.%, platelet-like particles exhibited largest μ_{nf} followed by cylindrical, bricklike, and bladelike particles. NFs using identical NP concentration, platelet-like and blade shaped particles showed Newtonian property while cylindrical and bricklike NP contained NF signifies shear-thinning characteristic above loading of 3 vol.%. Maximizing the pH value resulted substantial 31% reduction in μ_{nf}.

Carbon-based nanomaterials that have been extensively studied exhibit both Newtonian and non-Newtonian behavior in suspension, depending on the particle concentration, distributed medium, size, and shear rate. Sadri, et al. [210] revealed that water-MWCNT NF at 0.5 wt.% shows non-Newtonian shear thinning behavior as μ_{nf} decreases against applied shear-rate up to 140 s^{-1}. In addition, they found that μ_{nf} enhances due to dispersion of NPs and surfactant which can be reduced by optimum sonication of the samples. In a recent 3S research, Tiwari, et al. [130] evaluated impacts of several surfactants, base fluids (water, EG, therminol-VP1 and silicon oil) and sonication time on viscosity of hybrid MWCNT-CeO_2 nanocomposite based NFs. Measurements revealed that increasing ultrasonication time for the samples decreases $\frac{\mu_{nf}}{\mu_{bf}}$ up to an optimum period and further ultrasonication offers opposite consequences due to formation of clusters at longer sonication periods while, addition of nanocomposite (0.25-1.50 vol.%) and surfactants reasonably rises the ratio. Water is found to be most efficient as BF in terms of viscosity and lowest sonication time relative to other fluids although water/MWCNT-CeO_2 NFs exhibited non-Newtonian rheological property under applied shear rates (0-174 s^{-1}) with 0.025-2 vol.% at 25 and 80℃. Phuoc, et al. [211] experimentally studied the rheological property of aqueous MWCNT (0.5-3wt.%) NF using cationic chitosan (0.1-0.2 wt.%) as stabilizer and found both Newtonian and non-Newtonian behavior. The measurement showed that NF exhibit Newtonian behavior up to 200 s^{-1} shear-rate at lowest concentration of nanomaterial and surfactant whereas, shear thinning property is found to be dominant at higher loadings of CNT and chitosan. Zhang, et al. [65] studied pH effect on μ_{nf} of water/TiO_2 at three different points (2,7 and 12) for 0.08-2 vol.% and 25-60 ℃. Results revealed that higher pH value contributed to lower μ_{nf} for a certain temperature which contradict with [130] and particle loading whereas μ_{nf} near IEP-6.5 is reasonably higher due to aggregation.

Parallel to theoretical developments in NF's rheology, numerical simulations and molecular dynamics approaches have also aided in this field's advancements. Wu, et al. [212] performed numerical study on rheology of graphene-PAO NF using nonequilibrium molecular dynamics analysis utilizing statistical data from previous experimental and numerical works. The model was validated, and the results confirmed an improvement in μ_{nf} at higher temperature and shear thinning property is identified for NF samples. Azmi, et al. [213] recommended a μ model obtained by analyzing different experimental data of several water-based metal oxide (Al_2O_3, CuO, SiO_2, ZnO, and TiO_2) NFs using a non-linear regression method for particle sizes varying from 20-170 nm and loading of below 4 vol.%. The model was integrated with various parameters (φ, temperature, and NP size) of the NFs.

Nevertheless, studies on rheology of NF somewhat inconsistent and disorganized in terms of key influential parameters and characteristics of various category of NFs. **Table. 6** represents summary of reviewed works on rheology and viscosity of water-based NFs using wide range of NPs and **Table. 7** and **Table. 8** demonstrate summary of empirical and classical correlations obtained from available studies on this topic.

1044 **Table. 6.** Summary of reviewed experimental studies on viscosity and rheological behavior of various water-based nanofluids.

Reference	**Nanofluids**	**Size and concentration (φ)**	**Temperature range**	**Surfactants**	**Rheological behavior and shear rate (1/s)**	**Key findings**
Minakov, et al. [214]	Water/SiO_2 /Al_2O_3 /TiO_2 /ZrO_2 /C	10-100, 50-150, 71-150, 44-105 and 5 nm respectively Φ = 0.25-2 vol.%	25 °C	--	Non-Newtonian 0-120	● NFs showed degree of shear thinning property even at lowest loading of NPs and non-Newtonian behaviour keep dominating at raising φ as well.
Singh, et al. [76]	Water/rGO-Al_2O_3	4-5 nm Φ = 0.01-0.52 vol.%	25 °C	--	Non-Newtonian 0-2000	● The major pseudoplastic non-Newtonian property of the NF is observed up to 1500 s^{-1} and then achieved the highest shear ordering of the molecules.
Sarsam, et al. [30]	Water/GNPs	2 nm × 2 µm Φ = 0.1 wt.%	25-55 °C	DBS, GA, CTAB, and SDS	Newtonian 20-200	● CTAB based NF exhibited non-Newtonian for certain range of share rate whereas, other surfactant-based NFs showed almost Newtonian behaviour.
Chakraborty, et al. [71]	Water/TiO_2	< 100 nm Φ = 0-100 ppm	30-50 °C	Polyvinylpyrrolidone and Tween 20	Non-Newtonian 0.1-100	● μ_{nf} increases with addition of TiO_2 however, it dropped adding one of the surfactants (Tween 20) into water.
Das, et al. [72]	Water-[MMIM][DMP]/ MXene	1–10 µm × 1 nm Φ = 0.05-0.2 wt.%	20-50 °C	--	Newtonian 30-100	● μ_{nf} found to be higher for NF samples while rise in temperature reduces it substantially.
Alshayji, et al. [73]	DI water/Diamond	3-10 nm Φ = 0.125-1.25 vol.%	20-60 °C	--	Newtonian n/a	● The experiment showed that the μ_{nf} decreased notably with temperature while it increased by 36% at maximum φ.
Amiri, et al. [74]	Water/GNP-COOH /GNP-SDBS	0.5-3 µm × 0.55-3.74 nm Φ = 0.025-0.1 wt.%	20-80 °C	SDBS	n/a 300	● Non-covalent NFs found to be more viscous than covalent NFs. Highest 136.4% growth of μ_{nf} is observed with GNP-SDBS particles at 0.1 wt.% while, GNP-COOH exhibited 29.4% increment.

Singh, et al. [76]	Water/rGO- Al_2O_3	4-5 nm Φ = 0.1 vol.%	25 °C	--	Non-Newtonian 0 to 2000	● Rheology of the nanocomposite exhibited non-Newtonian (0-1500 S^{-1}) behaviour although at higher shear rates μ_{nf} tends to remain constant.
Sabiha, et al. [80]	Water/SWCNT	500 nm × 1-2 nm Φ = 0.05-0.25 vol.%	20-60 °C	SDS	Non-Newtonian 24.46-293.5	● NF showed significantly low μ_{nf} at high temperature and reduced nonlinearly with increasing shear-rate which implies shear thinning fluid flow behaviour.
Hussein, et al. [82]	Water/CF-MWCNT + CF-GNP + h-BN	5 µm × 15 nm and 2 µm respectively Φ = 0.05-0.1 wt.%	20-60 °C	Tween-80	Non-Newtonian 50-200	● NF performed non-Newtonian shear-thickening behaviour as μ_{nf} rises with corresponding growth of shear-rates.
Zhang, et al. [86]	Water/CRGO	Thickness (~4.3 nm) Φ = 0.2-1 mg/ml	10-60 °C	--	Newtonian 0-140	● μ_{nf} linearly decreased at elevated temperature and all the NFs behaved as Newtonian fluid at higher shear-rate (60 to 140 s^{-1}).
Shahsavar, et al. [93]	Water/CNT-Fe_3O_4	10 µm × 10-30 nm and 13 nm respectively Φ = 0.9-2.25 vol.%	25-35 °C	Gum Arabic and Ttetramethylammonium hydroxide	Newtonian 1-100	● μ_{nf} of CNT- Fe_3O_4 increased when strength of magnetic field raised, whereas it decreased at elevated temperature. Furthermore, shear thinning behaviour is observed at low shear-rates.
Garg, et al. [94]	Water/MWCNT	0.5-40 µm × 10-20 nm Φ = 1 wt.%	15-35 °C	Gum Arabic	Non-Newtonian 10-80	● Shear thinning and thickening was noticed for 10-60 and 60-75 s^{-1} shear-rate, respectively.
Phuoc, et al. [211]	Water/MWCNT	10-30 µm × 20-30 nm Φ = 0.5-3 wt.%	25 °C	Chitosan	Non-Newtonian 20-200	● Addition of dispersant and nanomaterials enhance the μ_{nf} notably and lead to non-Newtonian characteristic.
Wang, et al. [215]	Water/MWCNT	5-30 µm × 20-30 nm Φ = 0.05-1.27 vol.%	20-50 °C	TritonX-100 and SDBS	Newtonian to non-Newtonian 1-120	● Shear-thinning behaviour is observed for high φ. Addition of dispersants yielded better NF stability but increased μ_{nf}.
Mondragon, et al. [216]	Water/SiO_2	12 nm Φ = 0.002-0.132 vol.%	n/a	--	Newtonian to non-Newtonian 0.1-1000	● The NF depicted Newtonian behaviour at below 0.069% vol.%, while shear-thinning behaviour is detected at higher φ.

Aladag, et al. [217]	Water/Al_2O_3 /CNT	30 nm and 200 µm × 9 µm respectively Φ = 1 wt.%	2-10 ºC	--	Newtonian and non-Newtonian 0.1 to 5000	● NF comprising CNTs shows approximately Newtonian behaviour at > $100s^{-1}$ and exhibits a non-Newtonian behaviour at low shear rates. Al_2O_3 NF exhibits shear-thickening behaviour. Both NFs are thixotropic.
Abdelhalim, et al. [218]	Water/Au	10-50 nm Φ = 0.01 vol.%	37-42 ºC	--	Newtonian 200 to 2000	● NF containing NPs of 50 nm performed higher viscosity than NF using 10 and 20 nm size of particles. As the temperature grows, the μ_{nf} drops.
Jeong, et al. [219]	Water/ZnO	90-210 nm (Rectangular) and 20-40 nm (Spherical) Φ = 0.05-5 vol.%	22 ºC	Ammonium polymethacrylate	--	● Rectangular shaped NPs exhibited more μ_{nf} relative to spherical, maximum increment at 5 vol% is found 19.8 and 16% respectively.
Eshgarf and Afrand [220]	Water-EG/SiO_2-MWCNT	20-30 nm and 50 µm 5-15 nm respectively Φ = 0.0625-2 vol.%	27.5-50 ºC	--	Non-Newtonian 0.612-122.3	● NF revealed pseudoplastic behaviour for φ. NF follows power-law model and shear-thinning behaviour is dominant for the studied range of shear-rate.
Yang, et al. [221]	Aqueous CTAC-NaSal/Cu	50 nm Φ = 0.05-2.5 vol.%	298.15-318.15 K	Cetyltrimethylammonium chloride/sodium salicylate	Non-Newtonian 0-1000	● The μ_{nf} of the measured NF is marginally higher than its BF and it raises with the φ and decreases with the escalating temperature.
Bahrami, et al. [222]	Water-EG/Fe-CuO	35-45 and 25-55 nm respectively Φ = 0.05-1.5 vol.%	25-50 ºC	--	Non-Newtonian to Newtonian 3.669-122.3	● The measurements revealed that the NF has Newtonian behaviour at low φ and non-Newtonian behaviour at high φ.
Omrani, et al. [223]	Water/MWCNT	0.5-30 µm × < 50 nm Φ = 0.05 vol.%	10-45 ºC	SDBS and Triton X-100	Newtonian 100-1000	● Linear relationship between shear stress and shear-rate indicates Newtonian behaviour of nanofluids. μ_{nf} declined with increasing aspect ratio of CNTs.
Barai, et al. [202]	Water/rGO-Fe_3O_4	10-20 nm Φ = 0.01-0.2 vol.%	18-45 ºC	--	Non-Newtonian 0-10000	● μ_{nf} exponentially dropped with raising shear-rates i.e., shear thinning flow behaviour whereas, at high shear-rates (6000-$10000s^{-1}$) it remained almost unchanged.

1046 **Table. 7.** A summary of reviewed correlations proposed based on experimental data to estimate the viscosity of nanofluids.

Reference	**Nanofluid**	**Correlation**	**Applicability**	**Accuracy**
Garoosi [67]	Water/Ag, Cu, Al_2O_3, TiO_2, CuO, SiO_2, ZnO, MgO, Fe, Fe_3O_4, Al, AlN, $CaCO_3$	$\frac{\mu_{nf}}{\mu_{bf}} = 1 + 49.6 \times \left(\frac{d_p}{d_f}\right)^{-0.414} \varphi^{0.908} e^{10.8\varphi}$ $where,$ $d_f = 0.1\left(\frac{6M}{N\pi\rho_f}\right)^{1/3}$	$0 \le \varphi \le 12\ vol.\%$ $10\ nm \le d_p \le 12\ \mu m$	Standard deviation = 2.88%
Tiwari, et al. [130]	Water/MWCNT-CeO_2	$\frac{\mu_{nf}}{\mu_{bf}} = 1 + 5.01795 \times \left(\frac{T}{T_a}\right)^{0.321298} \times \varphi^{0.153641}$	$0 \le \varphi \le 1.50\ vol.\%$ $55 \le \varphi \le 80$ ℃	Average deviation = 2.39%
Azmi, et al. [213]	Water/Al_2O_3 /ZnO /TiO_2	$\mu_{nf} = \mu_{bf}\left(1 + \frac{\varphi}{100}\right)^{11.3}\left(1 + \frac{T_{nf}}{70}\right)^{-0.038}\left(1 + \frac{d_p}{170}\right)^{-0.061}$	Φ < 4 vol.% T = 0-100 °C	Max. error = 3.5%
Khanafer and Vafai [224]	Water/Al_2O_3	$\mu_{eff} = -0.4491 + \frac{28.837}{T} + 0.574\varphi_p - 0.1634{\varphi_p}^2 + 23.053\frac{{\varphi_p}^2}{T^2} + 0.0132{\varphi_p}^3 - 2354.735\frac{\varphi_p}{T^3} + 23.498\frac{{\varphi_p}^2}{d_p^2} - 3.0185\frac{{\varphi_p}^3}{d_p^2}$	$1 \le \Phi \le 9$ vol.% T = 20-70 °C $13 \le d_p \le 131$ nm	$R^2 = 0.99$
Corcione [225]	Water/Al_2O_3 /TiO_2 /SiO_2 /Cu	$\mu_{nf} = \frac{\mu_{bf}}{1 - 34.87\left(\frac{d_p}{d_f}\right)^{-0.3}\varphi^{1.03}}$ $where, d_f = 0.1\left(\frac{6M}{N\pi\rho_f}\right)^{1/3}$	Φ = 0.1-7.1 vol.% T = 293-333 K $25 \le d_p \le 200$ nm	Standard deviation = 1.84%
Sekhar and Sharma [119]	Water/Al_2O_3	$\frac{\mu_{nf}}{\mu_{bf}} = 0.935\left(1 + \frac{T_{nf}}{70}\right)^{0.5602}\left(1 + \frac{d_p}{80}\right)^{-0.05915}\left(1 + \frac{\varphi}{100}\right)^{10.51}$	$0.01 \le \Phi \le 5$ vol.% T = 20-70 °C $13 \le d_p \le 100$ nm	Standard deviation = 15%

Syam Sundar, et al. [226]	Water/Fe_3O_4	$\mu_{nf} = \mu_{bf}\left(1 + \frac{\varphi}{12.5}\right)^{6.356}$	Φ = 0-2 vol.% T = 20-60 °C	Standard deviation = 7.62%
Hemmat Esfe, et al. [227]	Water-EG/MWCNT-TiO_2	$\mu_{nf} = 6.35 + 2.56\varphi - 0.24T - 0.068\varphi T + 0.905\varphi^2 + 0.0027T^2$	Φ = 0.05-0.85 vol.% T = 10-50 °C	R^2 = 0.9913

Table. 8. Summary of classical models of viscosity estimation for NFs.

Reference	**Model**	**Applicability**
Einstein [228]	$\mu_{eff} = \mu_{bf}(1 + 2.5\varphi)$	Dilute suspension of spherical particle with low solid concentration of < 1 vol.%
Brinkman [229]	$\mu_{eff} = \mu_{bf}(1 - \varphi)^{-2.5}$	Extended form of the Einstein model, applicable for even less dilute suspensions.
Roscoe [230]	$\mu_{eff} = \mu_{bf}\left(1 - \frac{\varphi}{\varphi_m}\right)^{-2.5}$	This model is appropriate for suspensions of equal sized rigid sphere particles at low to high concentrations.
Krieger and Dougherty [231]	$\mu_{eff} = \mu_{bf}\left(1 - \frac{\varphi}{\varphi_m}\right)^{-[\mu]\varphi_m}$	Power law-based semi-empirical to predict viscosity containing any volumetric concentration of particles.
Brenner and Condiff [232]	$\mu_{eff} = \mu_{bf}(1 + \eta\varphi)$	Suitable for rod-shaped particles suspensions at higher shear rate. Applicable for up to $1/r^2$ volume concentration.
Jeffrey and Acrivos [233]	$\mu_{eff} = \mu_{bf}\left[3 + \frac{4}{3}\left(\frac{\varphi r^2}{\ln(\frac{\pi}{\varphi})}\right)\right]$	To predict the viscosity of non-dilute suspension rod-shaped in extensional flow.
Batchelor [234]	$\mu_{eff} = \mu_{bf}(1 + 2.5\varphi + 6.2\varphi^2)$	Brownian motion is considered in this model to predict the viscosity of dilute suspensions.
Graham [235]	$\mu_{eff} = \mu_{bf}[(1 + 2.5\varphi) + \frac{2.25}{\left(1 + \frac{h}{2a}\right)} \times \left[\frac{1}{\frac{h}{a}} - \frac{1}{\left(1 + \frac{h}{a}\right)} - \frac{1}{\left(1 + \frac{h}{a}\right)^2}\right]$	This model is applicable for spherical particles. Intermolecular spacing and particle radius is considered to predict viscosity by this formula.

6. Application of water-based NFs on non-concentrating solar collectors

Solar collectors (SCs) are advanced types of heat exchangers capable of spontaneously absorbing and converting solar irradiation into usable thermal energy in the case of thermal collectors, or into thermal and electrical energy utilizing photovoltaic/thermal hybrid SCs. Solar energy incident on the surface of the SC is converted to heat through a working fluid flowing through integrated copper tubes in the SCs [236]. SC is one of the most simple, sustainable, environmentally friendly, and efficient renewable thermal energy conversion systems available. It can be used in a wide variety of applications, including but not limited to domestic and industrial heating processes. SCs are primarily known as thermal or hybrid collectors (a combination of photovoltaic panel and thermal collector). Alternatively, thermal collectors are classified as non-concentrating or concentrating based on the concentration of incident solar radiation on the collector's specific surface area. Several forms of SCs are classified and illustrated in **Fig. 22**.

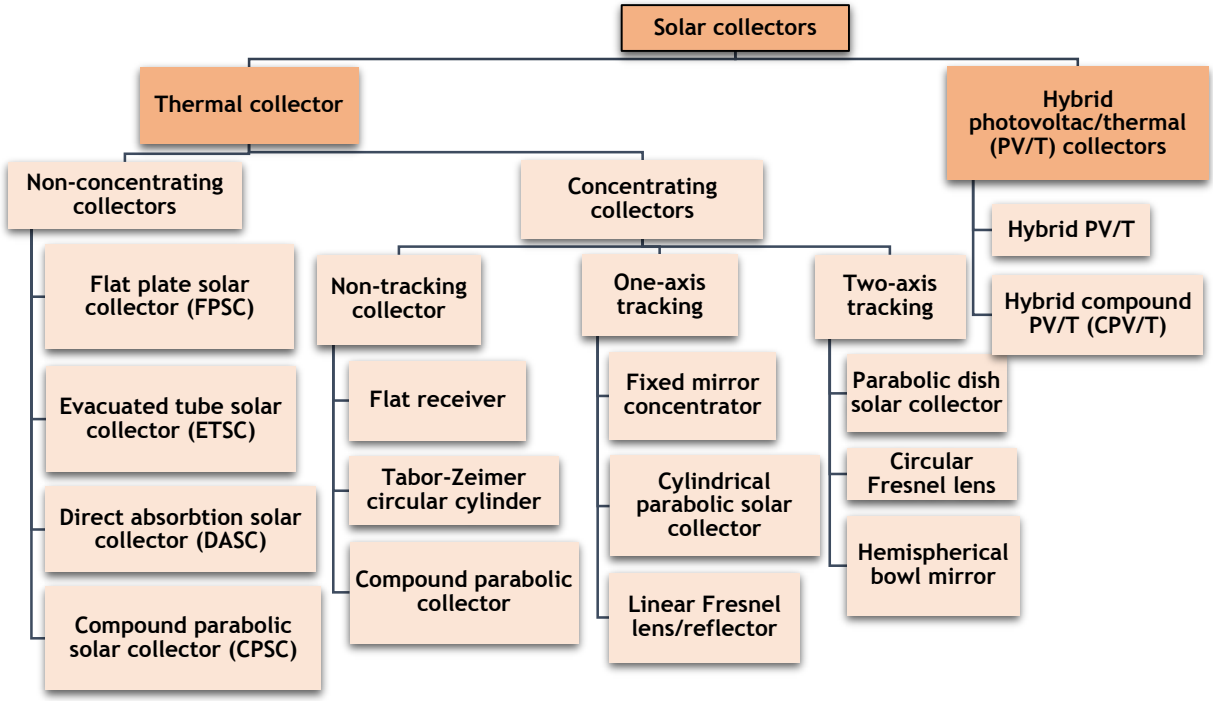

Fig. 22. Classification of solar thermal collectors.

The performance of solar collectors is determined by a variety of factors, including the collector's configuration and, most significantly, the amount of energy absorbed by the working fluid from intercepted solar irradiation on the receiver surface. However, the thermal energy efficiency of SCs is heavily influenced by the heat transfer properties of the working fluids. For the last decade or so, extensive research has been conducted on the use of numerous

NFs in place of traditional heating or cooling fluids in SC technology [237]. In recent years, the use of advanced nanomaterials and BFs to develop and implement superior working fluids on SCs has been extensively investigated. The aim of this review is to examine the potency and effect of advanced water-based NFs as working fluids in low temperature SC systems. In general, water-based NFs are frequently utilized in non-concentrating i.e., low-temperature solar thermal collectors like FPSC, ETSC, DASC, CPSC and hybrid PV/T due to their superior thermal and optical behavior. The following sections explain various types of NF-based solar collectors that use water as the BF, and **Table. 9** summarizes previous research with main findings.

6.1. Flat plate solar collector (FPSC)

FPSC is the simplest, most primitive, cost-effective, and most commonly used SC in a variety of domestic and industrial heating applications. Solar irradiation is absorbed on the absorber plate and transferred and stored in the SC's working fluid through the tubes. FPSC consists of five important components (see **Fig. 23**) such as (i) transparent glass surface (glazing) to capture incident irradiations and inhibit heat loss by radiation and convection to the environment (ii) absorber plate (made from copper, aluminum or other metal coating) to absorb solar energy (iii) header and raiser tubes to exchange the heat energy to circulating working fluid passing through the tubes (iv) insulation materials to minimize the heat loss (v) an overall encapsulation or casing to protect the collector from external hinders and hold all the integrated components together.

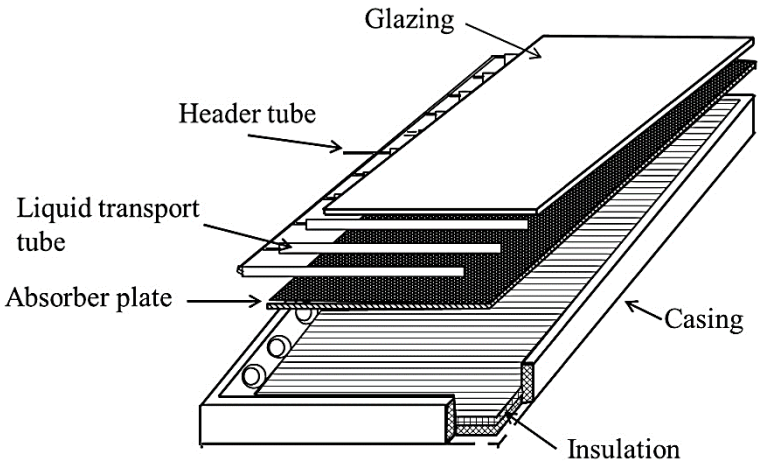

Fig. 23. Structure of a typical flat-plate solar collector [238].

To improve the performance of a FPSC, research is being conducted in structural design, heat loss reduction due to convection heat transfer, and the use of advanced working fluids such as

nanofluid [239]. Generally, water, oils and ethylene glycol are employed as working fluid. However, poor heat transport properties of these fluids restrict the performance of the SCs. Researchers and engineers in recent studies on solar collectors have strongly suggested that emerging nanomaterial-based NFs can be implemented on SC systems for performance enhancement [240]. Yousefi, et al. [241] experimentally studied effect of Al_2O_3-water NF on a FPSC. Their results revealed that the inclusion of Al_2O_3 NPs into water led the instantaneous energy efficiency of the thermal collector to 28.3% higher relative to conventional water driven FPSC. Fraction (weight or volume) of dispersed NPs, type of nanomaterials, mass flow rate and intensity of solar irradiations are the important parameters that governs the effectiveness of a FPSC. Verma, et al. [242] investigated the effect of metal oxide (MgO and CuO) and MWCNT-based NFs on FPSC as a high-performance working fluid. They examined the effect of collector efficiency and entropy production on two metal oxide, one carbon nanotube, and two hybrid NFs, as illustrated in **Fig. 24**. They revealed that increasing the particle loading in the base fluid initially increases efficiency before it reaches an optimal level, at which point efficiency degrades due to agglomeration and clustering. For both sole and hybrid NFs, a similar pattern is observed with varying mass flow rates. Colangelo and Milanese [243] numerically evaluated the impact of concentration (1-3 vol.%) of Al_2O_3 nanoparticles on FPSC using water-based NF. The investigation was performed considering practical weather conditions for summer and winter solstices, with inlet temperatures ranging from 30 to 65°C and a steady flow rate of 0.02 kg/s. Using 3 vol.% of Al_2O_3 NPs, a maximum 7.54% augmented efficiency was achieved, while efficiencies were much lower at lower concentrations (1-2 vol.%). The obtained results, however, are based on the assumption of uniform particle dispersion in the BF.

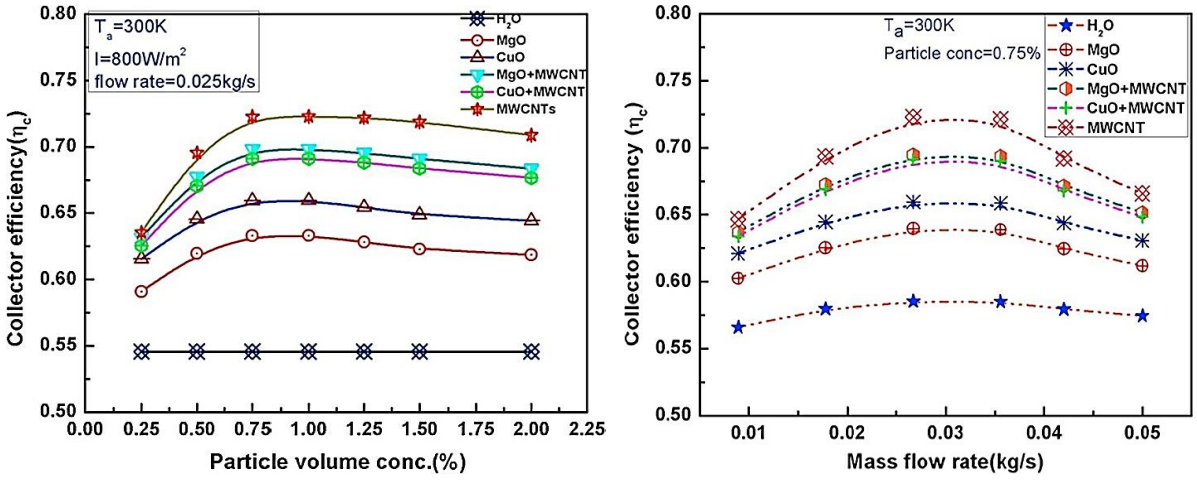

(a) **(b)**

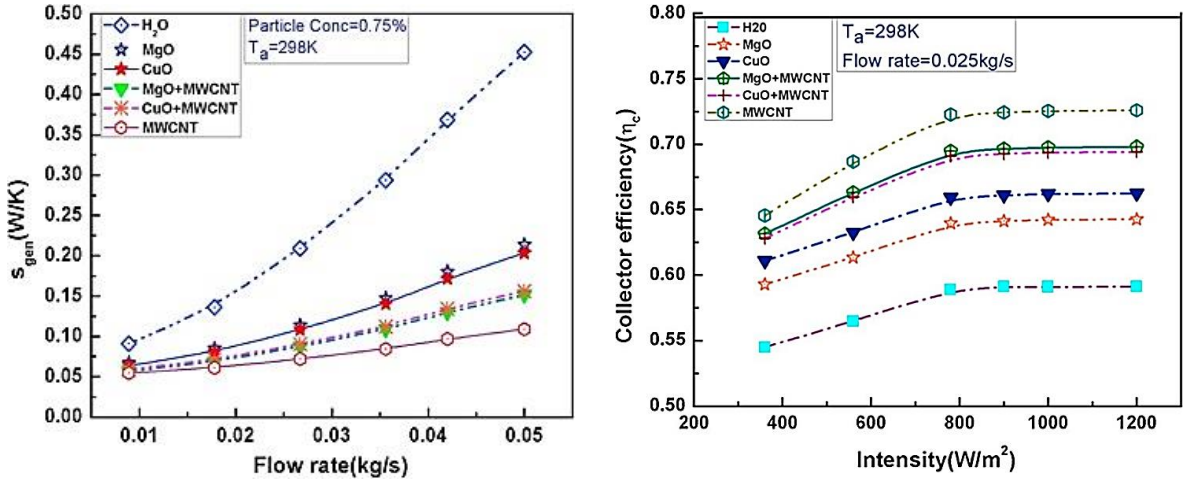

Fig. 24. Influence of important parameters on efficiency of FPSC [242] (a) variation of collector efficiency with raising concentration of nanomaterials (a) variation of collector efficiency at various mass flow rates (c) entropy generation at various flow rate (d) variation of efficiency at elevating solar intensity.

Akram, et al. [244] experimentally investigated the performance of FPSC using water NFs incorporated with metal oxides (SiO_2 and ZnO) carbon-based (GNP) materials. The results show that carbon material has a greater impact than metal oxides, with the highest enhancements of 17.45, 13.05, and 12.36% obtained using the particles, respectively. In a recent comparative investigation between ETSC and FPSC, Eltaweel, et al. [245] reported that FPSC showed superior performance than ETSC in terms of overall heat loss coefficient, heat removal factor, thermal and exergy efficiency using MWCNT NF. Furthermore, increasing the heat flux rate improves the heat removal factor, which reduces total heat loss and increases the collector's performance. The use of NF on the collectors often results in a decrease in the size of the SCs. **Table. 9** summarizes recent experimental findings on NF-based FPSC.

6.2. Evacuated tube solar collector (ETSC)

ETSC is the more efficient form of solar energy conversion system which can provide more thermal energy relative to conventional FPSC due to low heat dissipation because of the existence of its vacuum insulation system. A vacuum separation between the glass tube and absorber surface integrated with pipe (thermosyphon, U-pipe or heat pipe) demotes heat losses caused by conduction and convection. Absorber plate and incorporated pipe are placed inside the innertube and generally made of copper or aluminum materials. The working fluid circulates through the heat pipes in a closed loop and absorbs the energy from solar radiation,

condenses in the manifold and returns to heat pipes for the next cycle (a typical ETSC is demonstrated in **Fig. 25**).

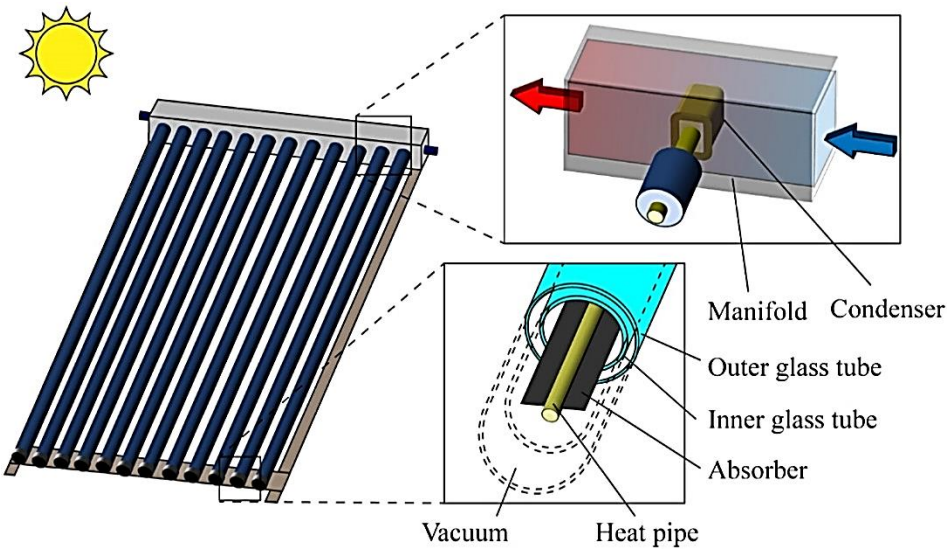

Fig. 25. Main components evacuated tube solar collector system [237].

Ghaderian, et al. [246] evaluated the efficiency of ETSC experimentally using water/CuO NF. The ETSC was equipped with a thermosyphon, and circulating NF as the absorption medium at a concentration of 0.03-0.06 vol.% of CuO nanomaterials and a mass flow rate of 20-60 L/h. The attained results showed that ETSC delivers highest 14% improved thermal efficiency at 0.03vol.% and 20 L/h relative to water. Investigation impact of water/WO_3 NF on ETSC, Sharafeldin and Gróf [247] revealed heat gain and output temperature has intensified by 23 and 21% respectively when WO_3 NPs (0.014-0.042vol.%) were added at 900 W/m^2. In addition, 19.3% supplemented thermal-optical efficiency is achieved over conventional collector. Sabiha, et al. [248] measured output of ETSC comprised with heat pipe by employing water/SWCNT (0.05-0.2vol.%). They observed thermal efficiency of ETSC enhances with increasing flow rate (0.0008-0.0.025kg/s) and φ. A maximum 93.43% augmentation is achieved at 0.2vol.%, which is 39.06% beyond the water based ETSC at 0.025kg/s. Furthermore, the NF based was collector found to be 4.5% more effective even on cloudy days than water based ETSC on sunny days.

Kim, et al. [249] assessed impacts of several parameters (e.g., solar irradiation, φ, NP size and flow rate) on effectiveness of an evacuated U-tube solar collector substituting water with water/ Al_2O_3 (20-10 nm, 0.5-1.5vol.%) NF at 0.033-0.047 kg/s flow rate (see **Fig. 26**). Average outlet temperature is improved by 1.2% although effect was minimal at low solar radiations. The elevated efficiency of the ETSC is observed at optimum φ of 1.5vol.%, smallest diameter of NPs (20 nm) and highest flow rate of 0.047 kg/s. 72.4% elevated output is measured at

optimized conditions which is considerably superior to water as working fluid. Natividade, et al. [250] reported notable intensification in efficiency of ETSC integrated with parabolic concentrator and multi-layered graphene/water as operating fluid. Combined effect of concentrator and NF caused 298% enhanced efficiency than water as working fluid without concentrator.

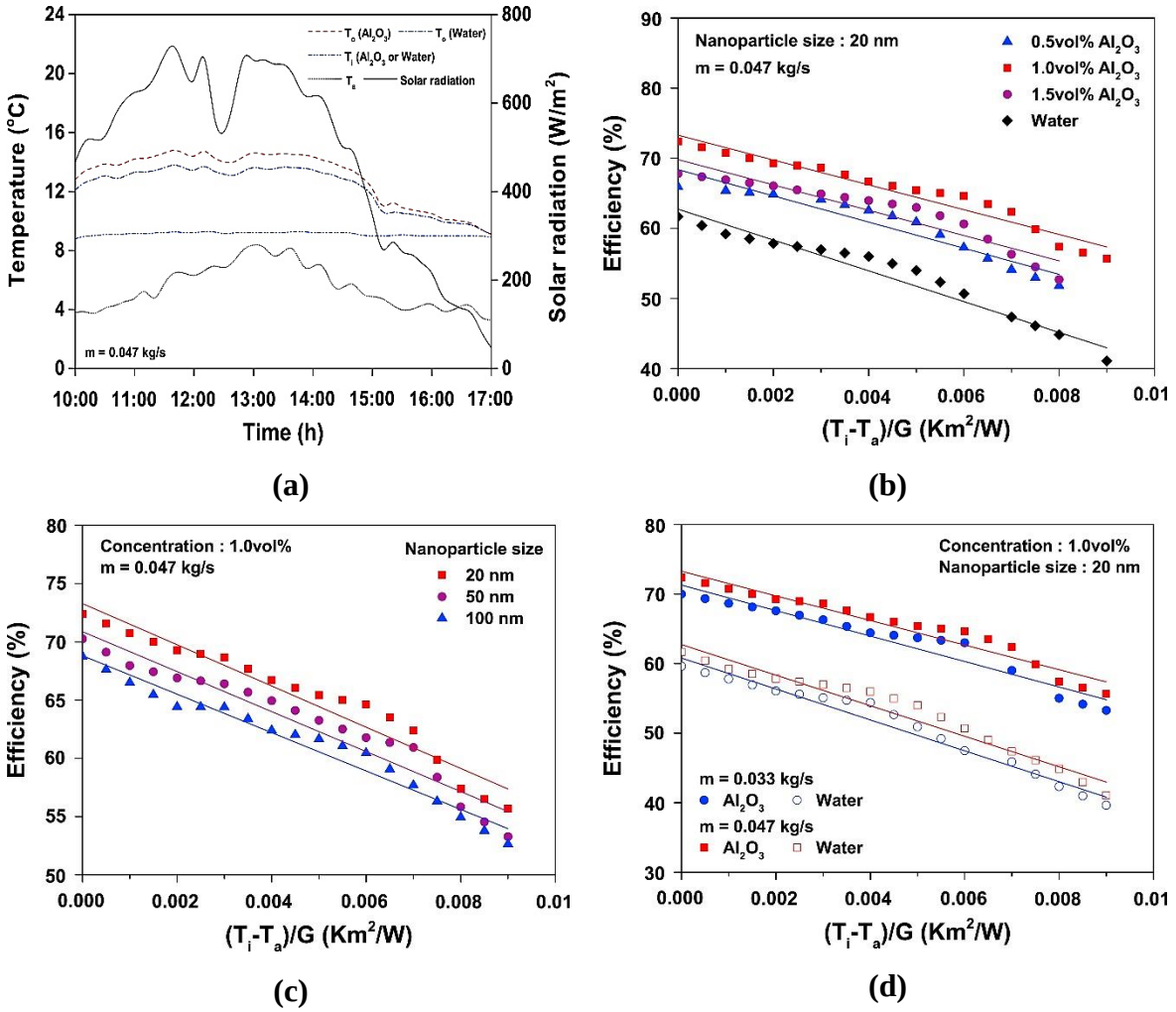

Fig. 26. Effect of various parameters on efficiency of evacuated U-tube solar system; variation of (a) outlet temperatures against corresponding time and solar irradiations (b) efficiency using different vol.% of particles (c) efficiency for different sizes of Al_2O_3 particles (d) efficiency boosting mas flow rate [249].

6.3. Photovoltaic thermal (PV/T) collector

Photovoltaic (PV) thermal hybrid systems can concurrently produce thermal and electrical energy by capturing and converting the renewable solar irradiations to useable forms. Traditional PV modules are adversely affected at high temperature as excessive heat reduces the overall efficiency of the panel. Hybrid PV/T technology allows extraction of surplus heat

assimilating a cooling unit with improved properties to advance the thermal-electrical output of the PV/T compared to PV module and conventional fluid equipped systems. The thermal unit of the collector absorbs the additional heat generated from the PV module to optimize the effectiveness of the system. A typical hybrid PV/T solar collector is illustrated in **Fig. 27**.

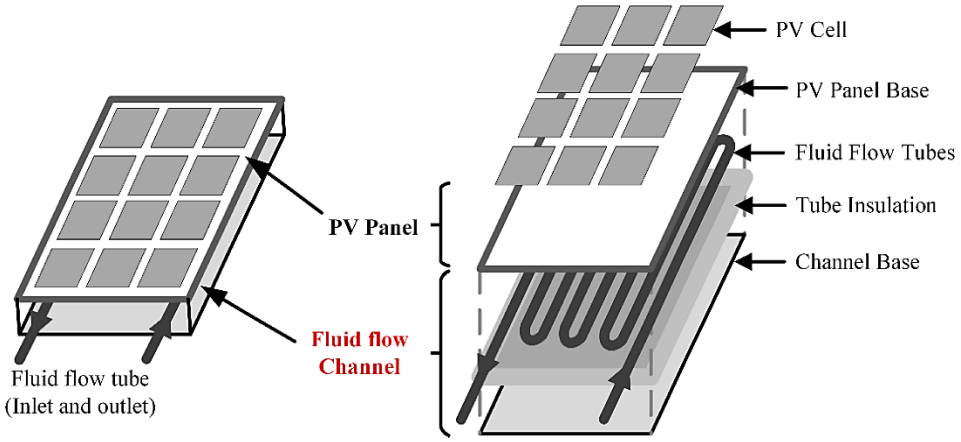

Fig. 27. Schematic of hybrid PV/T collector, PV panel integrated with thermal cooling system using nanofluid [72].

Aberoumand, et al. [251] experimentally examined energy and exergy performance of PV/T collector operating water/Ag NF at 2-4wt.% for laminar-transient-turbulent (0.0085-0.029 kg/s) flow regimes. They noted excellent effect of NF on performance as NF controlled system offers maximum 10 and 30% higher energy and exergy efficiencies at 0.029 kg/s (turbulent) flow rate relative to collector operated by water. In an outdoor experiment using water-based graphene and MWCNT NFs, Alous, et al. [252] revealed that overall (i.e., thermal, electrical and cooling) performance of PV/T enhanced (see **Fig. 28**). The results indicate up to 16℃ temperatures drop of the PV module using MWCNT particles and advanced energetic and energetic efficiencies of 22.1 and 20.6% for the graphene NF compared to the water-cooled system.

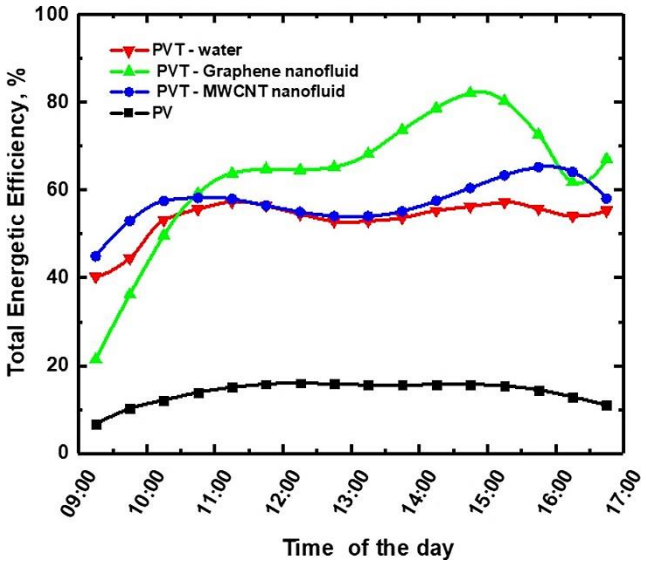

Fig. 28. Variation in efficiency of standalone PV and hybrid PV/T collectors operated with water-based NFs [252].

6.4. Direct absorption solar collector (DASC)

Traditional non-concentrating solar collector technologies employ solid absorber surfaces made of selective materials (e.g., polymer, copper, titanium, still and black carbon-based coatings) and circulate HTFs through tubes enclosed in an encapsulated insulation to exchange solar energy absorbed by the absorber surface. This technique results in low solar collector efficiency since substantial heat is lost from the hot absorber plate to the collector's other components (via conductions) and to the atmosphere (by convection and radiation). The volumetric DASC, on the other hand, is an advanced system where operating fluid is directly exposed to solar radiation that allows to eliminate thermal resistance formed by absorber surface in indirect collectors [253]. **Fig. 29** presents a schematic and thermal resistance diagram of indirect and DASC systems. Nevertheless, the concern with DASCs is that the employed regular HTFs have weak photothermal characteristics including low absorbance capacity for visible range of solar spectrum. Replacing conventional fluids with advance NFs as absorption medium can boost the absorptivity and performance of the DASCs due to supplemented optical effect of dispersed nanoscale particles.

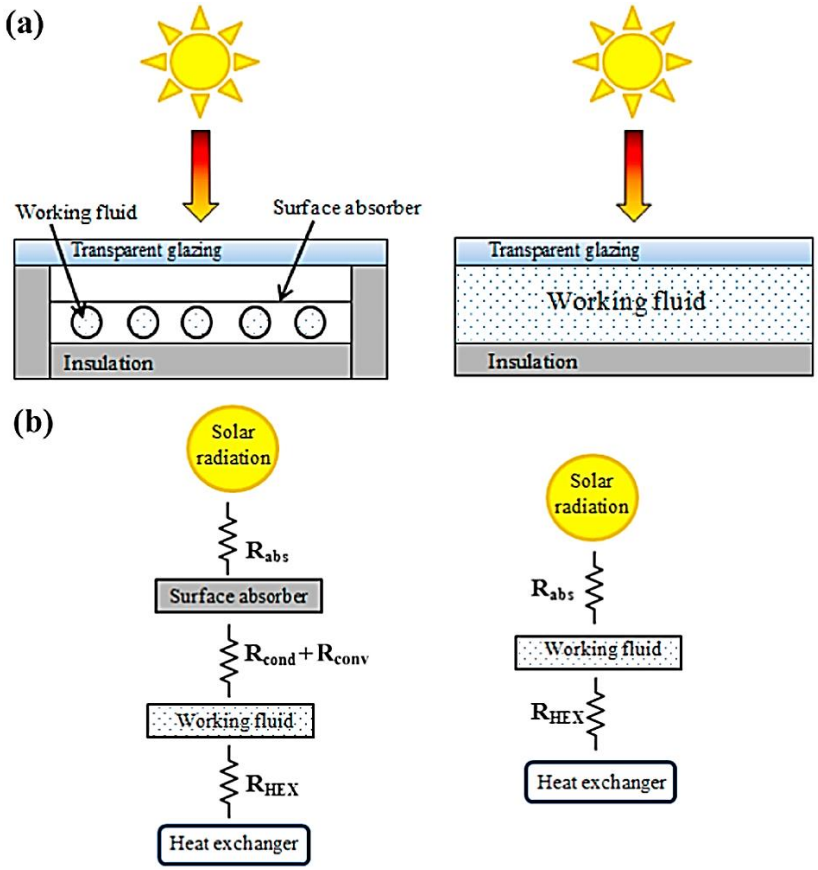

Fig. 29. (a) Schematic illustration of surface absorption based and DASC system (b) thermal resistance networks [25].

Milanese, et al. [254] experimentally assessed the optical merit of several water-based NFs using six different nanomaterials (CuO, CeO_2, TiO_2, Al_2O_3, ZnO and Fe_2O_3) to determine their potential use in DASC. The extinction distance, transmittance and/or absorbance measurements were performed for all the NFs using volumetric concentrations of 0.05-1% for each of the NPs. The measurements were conducted over a limited range of solar irradiation from 200-1300 nm. The results revealed distinct optical characteristics of the NFs depending on nanomaterials and their concentrations. They found that at lower vol.% of NPs, the extinction distance exceeds the typical diameter (1cm) of a collector receiver. CuO and Fe_2O_3 dispersed NFs exhibited better absorbance relative to other NFs, while TiO_2 based NF was reported as the best alternative due to its ability to absorb nearly 100% of solar radiation at a low concentration (0.05 vol.%) within the absorption depth. In their subsequent study [255], they evaluated the optical properties and stability of these NPs (ZnO, CeO_2 and Fe_2O_3) with respect to temperature (25-500℃). The obtained results suggest that there was no substantial shift in the optical properties of the NPs at elevated temperatures, as the absorption coefficient remained nearly constant. Chen, et al. [256] conducted a systematic study of the solar

absorbance of 13 distinct plasmonic nanoparticles and revealed that Cu@SiO_2 NPs with a core-shell structure were the most efficient at a 5:7 ratio. The NPs are proposed as potential energy conversion materials for application in DASC.

Guo, et al. [257] revealed that using 0.005-0.05wt.% of MWCNT (5-30 nm) in water substantially augments photothermal conversion relative to water based DASC. The results exhibited that inclusion of 15 nm MWCNT at 0.01wt.% produced optimum photothermal conversion of 65.4%. Karami [258] revealed 21.7 and 66.4% augmented efficiencies of DASC using hybrid NF dispersing Fe_3O_4 and SiO_2 NPs. They also checked the performance using CuO [259] and MWCNT [260] based NFs at identical conditions in separate articles where it is noticed that CNT nanomaterial outstrip the former one (see **Table. 9**). Li, et al. [261] performed an experimental and numerical comparison study between volumetric and surface absorption based solar collector operated with water (low-temperature) or Therminol-55 (high-temperature) based MWCNT NF. The surface absorber is comprised of a chrome-coated copper tube. Simulation findings indicated that in the 50–250 °C, the global heat deficit in the NF based absorber was approximately twice greater than the coated absorber, because of the glass tube have greater emissivity than surface absorber. They recommended using vacuum installation across the receivers and a low emissive coating on the tubes to improve the volumetric system as it resulted in significantly lessened convective heat loss consequences. On-sun measurements on the two prototypes revealed that the volumetric absorber performed poorly than the surface absorber. At 80°C, the exterior absorber gained 68% efficiency, while the NF-based absorber gained just 54% efficiency. When vacuum packaging is used at 200°C, the outputs were 47 and 26%, respectively. To cope with surface absorbers, it is suggested that NF absorbers require anti-reflective and selective coatings. Wang, et al. [262] investigated the photothermal energy conversion efficiency of two-dimensional multi-layered MXene and graphene NFs in water to optimize DASC performance. They achieved a maximum photothermal efficiency of 63.35 and 60.92%, respectively, when using MXene and graphene-incorporated NFs.

6.5. Parabolic trough solar collector (PTSC)

The PTSC is considered as the future of sustainable renewable energy resources that can be implemented commercially to develop sustainable solar energy conversion systems. PTSC is the one of the concentrating solar system of solar collector technologies comprised with parabolic shaped mirror reflector and cylindrical absorber surrounded by anti-reflecting glass layer to prevent heat loss due to convection and radiation (depicted in **Fig. 30**). Solar energy is

concentrated on the receiver and then transformed to a working fluid that flows through it, converting solar energy to thermal energy. [263]. The performance of PTSCs is determined by the photothermal properties of the working fluid used in the cycle. Water-based NFs are commonly used in PTSC at temperatures below 100°C as they are the most innovative and effective medium for light-to-heat conversion [22]. Although PTSC is capable of operating at higher temperatures, water-based NFs have a small temperature range due to their low boiling point.

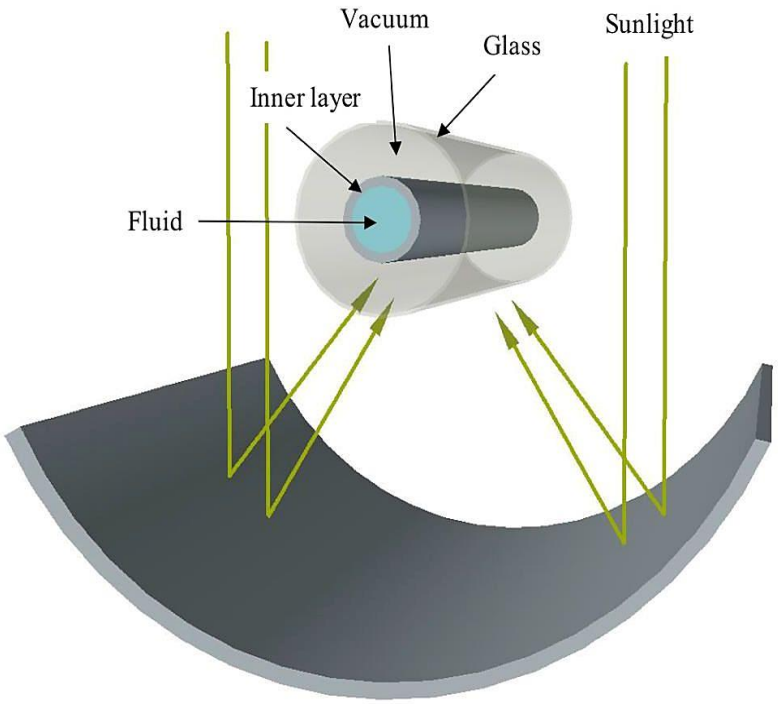

Fig. 30. Schematic diagram of the PTSC system [22].

Menbari, et al. [264] investigated low-temperature direct absorption PTSCs by operating with water/CuO NF at a concentration of 0.002-0.008 vol.% and a flow rate of 10-100 L/h to increase the collector's thermal effectiveness and absorption property. The results demonstrate an increase in thermal efficiency of up to 52% compared to BF at the peak loading of 0.008 vol.%. Hachicha, et al. [265] recently investigated the impact of experimentally formulated water-based NF on the optical and thermo-hydraulic efficiency of PTSC dispersing low-cost industrial-grade MWCNT (0.05-0.3 vol.%) nanomaterial. The numerical application of the fluids is performed at four different locations in UAE and 49.52% thermal efficiency is achieved with 21% increment in Nusselt number. In addition, parametric analysis showed that thermo-hydraulic performance of the system increases at lower flow rates (below 0.2 L/s) and low concentration of NPs while, higher concentrations can be effective for further increase in

flow rate. Okonkwo, et al. [266] evaluated performance of the LS-2 PTSC system employing water/SiO2 and water/TiO2 NFs synthesized from olive leaf and barley husk. Green formulation techniques result in a decrease in thermal losses and an increase in energy and exergy efficiency. The proposed NFs improved heat transfer efficiency by 128 and 138%, respectively. Sekhar, et al. [267] used several NPs (CeO_2, Al_2O_3 and TiO_2) with water at 0.5-3 vol.% to evaluate the output of the PTSC system. In comparison to water as working fluid, the thermal efficiency of the system was augmented by 27, 25 and 23% for the NFs, respectively. Subramani, et al. [268] investigated the heat transfer properties of PTSC under turbulent flow conditions using water/Al_2O_3 NF. They observed up to 8.54% increment in efficiency at a flow rate of 0.05 kg/s and 0.5 vol.% of NP. Nusselt number and overall heat transfer coefficient of the collector are found to be improved as well. In a numerical fluid dynamics investigation, Ghasemi and Ranjbar [269] examined heat transfer and friction factor characteristic of PTSC using water/Al_2O_3 and water/CuO NF. The obtained results showed 28 and 35% enhanced heat transfer coefficient using the NFs, respectively. Moreover, lower friction factor is caused by water/Al_2O_3 than that of water/CuO.

The studies concluded that the PTSC solar collector based on water-NF outperformed the traditional fluid-based system in terms of energy and exegetic efficiency. However, one of the major disadvantages of water-based NFs is that, due to their restricted low boiling point, they are not suitable for use at medium-high temperatures on PTSC. **Table. 9** summarizes recent research on PTSC using water-based NFs, including comprehensive details and key results.

Table. 9. Summary of key findings from recent experimental studies on various water-based NFs in low-temperature application on non-concentrating thermal solar collectors.

Reference	Nanofluids	Particle size and concentration (φ)	Solar collector	Operating temperature	Flow rate	Key findings
Verma, et al. [270]	Water/CuO Al_2O_3 TiO_2 SiO_2 Graphene MWCNT	42, 45, 44, 10, 20 nm, respectively. MWCNT (AR=200, dia 7nm) Φ = 0.25 to 2 vol.%	FPSC	< 80 ºC	0.01-0.05 kg/s	● MWCNT-based NF produced the highest efficiencies, with improved exergy and energy efficiency relative to water of 29.3 and 23.47%, respectively. ● 19.01% reduction in area is observed using MWCNT NF, which is optimum among the studied NFs.
Sarsam, et al. [271]	Water/Ala-MWCNT	< 8 nm and 20-30 nm Φ = 0.025 to 0.1 wt.%	FPSC	< 80 ºC	0.6-1.4 kg/min	● Functionalized MWCNT NPs lifted the output of FPSC up to 9.55% with 0.1 wt.% at 1.4 kg/min. ● MWCNT particles with a smaller diameter (8 nm) performed significantly better than those with a larger diameter (20-30 nm).
Choudhary, et al. [272]	Water/MgO	40 nm Φ = 0.1 to 0.3 vol.%	FPSC	< 80 ºC	0.5-1.5 L/min	● Higher thermal conductivity and c_p of NF at elevated temperature enhanced thermal efficiency which is approximately 70.4% at 3 vol.% on the day NF was prepared. ● Thermal output declined by 13.1% after a 10-day period at 0.3 vol.% while it decreased slightly using 0.1 vol.% loading.
Hussein, et al. [82]	Water/CF-MWCNT+ CF-GNP	Diameter 15 nm, length 5 µm Φ = 0.05-0.1 wt.%	FPSC	< 80 ºC	2-4 L/min	● Hybrid nanocomposite at 0.1 wt.% of MWCNT and GNP, augmented thermal efficiency of the collector by 20% relative to water as working fluid. ● The highest increase for F_R (τα) and F_RU_L were 21.9 and 78.3%.
Gad and Said [273]	Water/Al_2O_3 /TiO_2	25 nm Φ = 2 wt.%	FPSC	< 80 ºC	2-6L/min	● Both metal oxide particles improved effectiveness of the FPSC being maximum 30 and 32% at 2 l/m mass flow rate for Al_2O_3 and TiO_2 NF, respectively.

						● Efficiency decreased as the flow rate of NFs increased as well as the Reynolds number increased from 4500-11000.
Sundar, et al. [274]	Water/Nano-diamond	10 nm Φ = 0.2-1 vol.%	FPSC	< 80 ºC	0.033- 0.083 kg/s	● Inclusion of 1 vol.% of nano-diamond intensified the collector efficiency by 39.62% than water. Solar absorbance also contributed to the rise in efficiency. ● Heat transfer and Nusselt number increased by 52.33 and 32.31%, respectively, at Reynold number 12766.
Moravej, et al. [275]	Water/TiO_2	n/a Φ = 1-5 wt.%	FPSC	< 80 ºC	0.015-0.045 L/s	● Highest 33.54% energy gained using 5 wt.% of water/TiO_2 replacing water as working fluid. ● Efficiency increases from 0.53 to 0.65 with raising solar irradiance from 195 to 888 W.
Alklaibi, et al. [276]	Water/Nano-diamond	100 nm Φ = 0.2-1 vol.%	FPSC	< 80 ºC	0.02 kg/s	● 12.7% higher with addition of optimum 1 vol.% diamond particles. ● Entropy of generation decreased using water/ND nanofluid although frictional entropy increased by 16.59% relative to water as working fluid.
Yousefi, et al. [241]	Water/Al_2O_3	15 nm Φ = 0.2 wt.%	FPSC	< 80 ºC	1-3 L/min	● Al_2O_3 particles enhanced the performance of the collector by 28.3% over the water based FPSC system.
Tong, et al. [277]	Water/MWCNT Al_2O_3 CuO Fe_3O_4	20, 20, 40 and 30 nm Φ = 0.005, 0.1, 0.5 and 0.015 vol.% respectively.	FPSC	< 80 ºC	0.47 kg/s	● Maximum efficiency of the collector is achieved with MWCNT nanofluid which is 25% higher than water based FPSC. ● Efficiency found to be reduced by increasing the size of all the dispersed particles. Highest 7.9% reduction is observed for 500% increase (20-100nm) of Al_2O_3 particles.
Allouhi and Benzakour Amine [278]	Water/CuO Al_2O_3 TiO_2	n/a Φ = 0-3 vol.%	FPSC	< 80 ºC	0.018-0.036 kg/s	● Less cp of NF yielded higher performance increment of the FPSC. CuO exhibited best enhancement in energy and exergy efficiency by 2.7 and 11.1% correspondingly.

						● More energy gained at increasing flow rate of NFs; 2.95% better energy attained with CuO NF at 0.036 kg/s. However, maximum 13.26% for CuO NF.
Choudhary, et al. [279]	Water-EG/Fe_3O_4	n/a Φ = 0.2-1 vol.%	FPSC	< 80 ºC	30-150 L/h	● Highest outlet temperature of the collector is achieved 350.26K, which is 15.98K higher than water-EG. ● Thermal performance was increased by 15.27 % and remained nearly constant for 15 days. Furthermore, 17.05% increment in absorption and 40.17% drop of heat loss at 1 vol.% and 30 L/h.
Verma, et al. [242]	Water/ /MgO /CuO /MWCNT /MgO-MWCNT /CuO-MWCNT	CuO (42 nm) MWCNT (AR=200, dia 7 nm) Φ = 0.25-2 vol.%	FPSC	< 80 ºC	0.5-2 L/min	● Hybrid CuO and MgO with MWCNT exhibited performed better than solo CuO and MgO based NFs although MWCNT alone observed to be most efficient NF among all. ● MgO and CuO-based hybrid NFs exhibit the highest thermal efficiency increments of 20.52 and 18.05%, and exergy efficiency increments of 33.78 and 30.09%, respectively.
Eltaweel, et al. [245]	Water/MWCNT	Length 20 µm, diameter 10-40 nm Φ = 0.005 to 0.05 wt.%	FPSC and ETSC	< 80 ºC	0.0097-0.0338 kg/s m^2 (FPSC) 0.0133-0.0464 kg/s m^2 (ETSC)	● The maximum average energy efficiency obtained using the 0.05 wt.% of Water/MWCNT was 55% and 59%, respectively, and the exergy efficiency was 10% and 11.5% for ETSC and FPSC. ● The inclusion of NF leads to a size reduction in ETSC and FPSC by 29.5% and 26.7%, respectively.
Hosseini and Shafiey Dehaj [280]	Water/TiO_2 (spherical) /TiO_2 (wire-like)	40-60 and 14.2 nm Φ = 1 vol.%	ETSC	20-60 ºC	0.1-0.5 L/min	● Both wire-like and spherical titania particles demonstrated superior efficiency, with the highest values being 21.1 and 12.2%, respectively. The flow rate was also added to the performance index.
Mahbubul, et al. [281]	Water/SWCNT	1-2 nm Φ = 0.05-0.2 vol.%	ETSC	< 80 ºC	0.265 kg/s	● Using NF at 0.2vol.% intensified the efficiency by 10%. Most significant increment is observed at irradiance of 900 W/m^2.
Ozsoy and Corumlu [282]	Water/Ag	60 nm Φ = 20 ppm	ETSC	< 80 ºC	n/a	● Replacing water with NF produced up to 40% increment in the efficiency. It is understood that NP

						layers accumulated on the evaporator surface clearly affect the heat transfer.
Daghigh and Zandi [283]	Water/MWCNT /CuO /TiO_2	n/a Φ = 0.1 vol.%	ETSC	< 80 ºC	n/a	● Output of the ETSC augmented more using carbon based MWCNT dispersed NF (25%) relative to CuO (12%) and TiO_2 (5%) based NFs. ● Fuel consumption was reduced by 67.7% using the designed solar system.
Sharafeldin, et al. [284]	Water/Cu	50 nm Φ = 0.01-0.03 vol.%	ETSC	< 80 ºC	0.6-0.8 L/min	● Using NF, temperature raised by 50% in the outlet and removal factor increased significantly to reach the highest value of 0.97. Maximum efficiency intensified by 51% at 0.03vol.% and 0.8 L/min. ● Positive impact of Cu NPs is observed in CO_2 reduction and economic perspective.
Dehaj and Mohiabadi [285]	Water/MgO	74.5 nm Φ = 0.014-0.032 vol.%	ETSC/HPSC	< 80 ºC	5 to 14 L/min	● Efficiency stands high at higher flow rate; 77% effectiveness is obtained at 14L/m using 0.032 vol.% of MgO along with superior absorption capacity of the NF.
Sadeghi, et al. [286]	Water/Cu_2O	15-20 nm Φ = 0.04-0.08 vol.%	ETSC	< 80 ºC	10-50 L/h	● 28% augmented efficiency is achieved using parabolic concentrator and NF at 0.08 vol.% and 50 L/h replacing water. Furthermore, 3.7% supplemented exergy output.
Al-Waeli, et al. [287]	Water/SiC	40-60 nm Φ = 3 wt.%	Hybrid PV/T	< 80 ºC	-	● Overall effectiveness was strengthened by 88.9 employing NF relative to standalone PV unit.
Alous, et al. [252]	Water/MWCNT /Graphene	8-35 µm×18-28 nm and 1-12 µm×0.55-1.12 nm respectively Φ = 0.5 wt.%	Hybrid PV/T	< 80 ºC	0.5 L/m	● The highest 16°C temperature drop of a PV unit was obtained with MWCNT dispersed NF, while graphene dispersed NF revealed superior efficiencies of 63.1 and 20.6% in terms of energetic and energetic standpoint.
Al-Shamani, et al. [288]	Water/SiO_2 /TiO_2 /SiC	< 100 nm Φ = 0.5-2 wt.%	Hybrid PV/T	< 80 ºC	0.068-0.17 kg/s	● Highest combined efficiency is achieved 81.73% with SiC NF at 0.17 kg/s and 1000 W/m^2 solar irradiance. Overall energy coefficient is 0.93.

Rajendiran, et al. [289]	Water/CuO	27 nm Φ = 0.05-0.2 vol.%	Hybrid PV/T	45-65 ºC	40 L/h	● Higher sonication time provided optimized performance of the PV/T system. 95.8% maximum overall efficiency of the PV/T collector was found for 0.2% CuO/water NF after 4 h of sonication.
Abdelrazik, et al. [43]	DI water/rGo-Ag	Φ = 0.0005-0.05 wt.%	Hybrid PV/T	< 80 ºC	n/a	● NFs produced more thermal and electrical efficiency relative to water-based PV/T collector and standalone PV panel without thermal cooling component.
Wole-Osho, et al. [290]	Water/Al_2O_3-ZnO	29 and 70 nm respectively Φ = 0.01-1 vol.%	Hybrid PV/T	< 80 ºC	0.01-0.1 kg/s	● The hybrid NF had significant influence at optimum conditions of 0.01 vol.%, 0.1 kg/s flow rate and 0.47 mixture ratio (Al_2O_3: ZnO). 34% optimized energetic efficiency is remarked.
Das, et al. [72]	Water-[MMIM][DMP]/ MXene	1–10 µm × 1 nm Φ = 0.05-0.2 wt.%	Hybrid PV/T	< 80 ºC	0.01-0.07 kg/s	● 14 and 14.4% higher thermal and electrical efficiency is achieved relative to metallic alumina/water NF. ● PV cell temperature dropped by 12.5 ºC using NF instead of water as cooling fluid.
Elminshawy, et al. [39]	Water/Al_2O_3	Φ = 1-3 vol.%	Low photovoltaic concentrator (LCPV)	< 80 ºC	0.01 kg/s	● Temperature of the collector cooled be=y 16.47 ºC in comparison with uncooled system. ● In addition, daily electrical output was augmented by 13.58% using NF instead of water.
Li, et al. [291]	DI water/MXene	MAX-phase (25 µm) Φ = 10 to 200 ppm	DASC	300-370 K	36 L/h	● Water/MXene NFs exhibited superior photothermal conversion efficiency of the DASC relative to water-based system due to distinct absorption of solar radiation with the NFs. ● Highest intercept efficiency is obtained 77.49% at 100 ppm loading of MXene flakes which is significantly higher than the base fluid.
Esmaeili, et al. [292]	Water/ CuO CuO foam	30 nm Φ = 0.01-0.1 vol.%	DASC	< 80 ºC	0.0075-0.0225 kg/s	● CuO NFs produced better output than metal oxide foam based working fluid. Maximum improvement is achieved 26.8% higher than water and 3% higher than metal oxide foam.

Wang, et al. [293]	Water/ZrC	40 nm Φ = 10-100 ppm	DASC	< 80 ºC	--	● Reverse illumination is recommended for NF-based DASCs. The highest conversion effectiveness is increased up to 51.9%.
Karami, et al. [259]	Water-EG/CuO	40 nm Φ =25-100 ppm	DASC	< 80 ºC	50-90 L/h	● Efficiency of the DASC raised with addition of NPs and speeding up the flow rate and up to 17% supplemented efficiency is achieved during solar water heating.
Delfani, et al. [260]	Water-EG/CuO	40 nm Φ =25-100 ppm	DASC	< 80 ºC	50-90 L/h	● MWCNT dispersed NF produced better output (up to 29%) relative to CuO [259] at identical conditions indicates superior absorption of carbon nanomaterials.
Karami [258]	Water/Fe_3O_4-SiO_2	30 and 15 nm respectively Φ =500-200 ppm	DASC	< 80 ºC	0.0075-0.0225 kg/s	● Energy and exergy efficiencies augmented by 21.7 and 66.4% at maximum φ and flow rate. Entropy generation was reduced using NF and contribution of pressure drop was insignificant.
Hachicha, et al. [265]	Water/MWCNT	30-50 µm × 8-15 nm Φ =0.05-0.3 vol.%	PTSC	35-55 ºC	0.08-1 L/s	● Nusselt number improved against increasing Reynolds number and particle concentration. The Cost is considerably lower than research grade MWCNT.
Minea and El-Maghlany [294]	Water:EG/Ag-MgO, Al_2O_3-Cu, GO-Co_3O_4	< 100 nm Φ =0.05-2 vol.%	PTSC	< 100 ºC	--	● The hybrid NFs performed better when water was used as BF due to low pressure drop relative to EG. 115-125% augmented heat transfer coefficient is obtained using water-EG/GO-Co_3O_4 at 0.15 vol.%.
Ehyaei, et al. [295]	Water/Al_2O_3, /CuO, Therminol VP-1/ Al_2O_3, /CuO	< 100 nm Φ = 1-5 vol.%	PTSC	< 80 ºC	0.08 kg/s	● Water performed better than the oil as BF. CuO NPs showed higher energy and exergy output than Al_2O_3 particles due to higher TC of CuO.
Bretado de los Rios, et al. [296]	Water/Al_2O_3	10 nm Φ =1-3 vol.%	PTSC	< 80 ºC	--	● Replacing water with the NF resulted in 11.6% enhancement in thermal efficiency as well as outlet temperature using 3 vol.% of NPs.
Rehan, et al. [297]	Water/Al_2O_3 /Fe_2O_3	20 and 20-40 nm Φ =0.2-0.3 wt.%	PTSC	< 60 ºC	1-2 L/min	● 13 and 11% elevated thermal efficiency is attainted, respectively. Temperature difference increased dispersing NPs, while it declined raising the flow rate.

1305

7. Challenges with NFs and its application

NFs are the latest promising thermo-fluids which are evolving at considerable pace to establish its place in impending practical applications. Nevertheless, over the last decade, researchers and engineers have identified many critical issues with NF in terms of its advanced characteristics and successful implementation in real-world solar thermal engineering applications. Numerous sophisticated issues posed in numerous studies on NF are summarized in the following points (also depicted in **Fig. 31**).

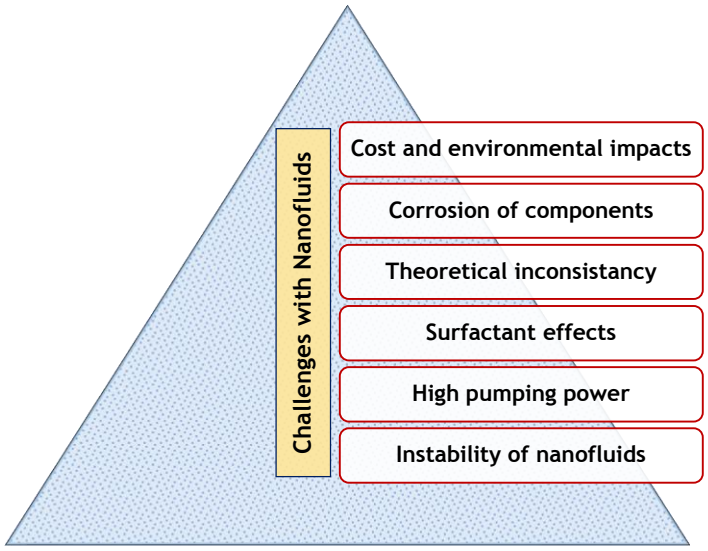

Fig. 31. Identified challenges with nanofluids.

- Inadequate stability of NF suspensions (as stated in **Section 3**) is a fundamental shortcoming as it degrades major properties and dictates essential implementation of the NF in any solar thermal systems. The majority of available techniques for stabilizing NF suspension fall short of providing industrial standard stable NF. Some techniques including surfactant or chemical stabilizers addition and pH modulation are reported to have positive impact on stability within certain conditions. Yet, consequences (i.e., thermal, and optical properties degradation, foam formation, corrosion, and fouling factors) of these methods are responsible for deterioration of the properties at critical operating conditions like high temperature and high particle loading. Conventional NP synthesis and NF formulation procedures should be improved to produce more stable suspension. Furthermore, there are no standard indicator for reporting stability that can indisputably interpret suspension stability characteristic in terms of duration (days or months), hence, rigorous observation approach is essential to report accurate assessments. Zeta potential (ζ) is often proposed as an ideal indicator of NF stability in

literatures; however, it is not appropriate since high ζ value does not necessary implies high suspension stability. Rather, it indicates electrostatic repulsion potential between NPs. In the in case steric stabilization technique, ζ can be low while remaining completely stable [298]. Therefore, reporting of stability is still in an ambiguous state and needs to be construed with generic standard to allow comparisons across a broad range of NFs.

- Dispersion of nanoscale particles results in an increment of BF viscosity (μ) which in turn escalates pressure drop in the NF-operated dynamic systems, i.e., solar collectors. Inevitably, the drop extends further as particle loading and mass flow rate increase. Since a dynamic system's pumping power is directly related to pressure drop and flow rate, an increase in pressure drop implies an increase in pumping power demand [299].
- Surfactants or chemical stabilizing additives are deployed to ameliorate the stability of NFs. However, the stabilizers often result in penalties in terms of thermo-optical properties and performance. Although most of the studies concur regarding positive impact on stabilization, notable limitations (i.e., ineffectiveness above 50-60℃and non-Newtonian flow property) and conflicts among reported studies due to diverse classification of the surfactants make it difficult to select an ideal stabilizer for a particular NF.
- Theoretical unpredictability reflected in literature regarding interactions among thermophysical properties (particularly, TC and c_p) and affecting constraints is another crucial challenge to conquer. Numerical based models and correlations developed for an individual combination of BF and NP i.e., NF under specific conditions could not provide accurate estimation of data for other NFs due to interactions of an extensive number of dependent variables. Therefore, advanced ANN and machine learning models must be developed that incorporate a variety of variables with NF properties and make use of accumulated practical data to strengthen the prediction.
- Several NFs exhibited perceptible corrosivity operating as working fluid in thermal devices which can lead to significant damage to the entire system. Chemical interactions, pH value variation and mechanical stabilization of the fluids are the culpable factors that cause surface degradation [300]. To avoid this sort of inconvenience, additional maintenance is necessary.
- NFs comprised of nanoscale particles may cause toxic environmental and biological effects. Due to the tiny size of NPs, it is reasonable that the particles can get into human

skin and cause respiratory, inflammation and carcinogenic infections [301]. In future research on NF, scientists and engineers should consider green synthesis techniques to develop NFs that are non-toxic, ecologically beneficial, and safe for industrial usage. Besides, the potential challenge of high production costs must be reduced since it hinders application of NF on energy conversion systems, including but not restricted to SCs.

8. Conclusions and recommendations

This study of the thermophysical properties, stability phenomena, and development of water-dependent NFs on low temperature SCs includes causes and effects analyses based on detailed experimental and numerical investigations. Due to their superior potency and influence at low temperatures, this analysis focuses on the most frequently used water-based and hybrid NFs. Several critical areas are examined and discussed, including thermophysical properties, suspension stability and mechanisms, and application to solar collector products. Nevertheless, research needs to progress in right directions for further advancement in the field of NF and its utilization on solar thermal collector devices. Several critical areas are examined and discussed, including thermophysical properties, suspension stability and mechanisms, and application to solar collector products. Nonetheless, research must continue in the right direction to advance the sector. In this regard, the authors have drawn some critical conclusions and recommendations about the current state of research in this field and possible research directions.

On synthesis and formulation of NF:

- The single-step method produces more stable NFs, while the two-step method produces NF with more efficient thermal properties. Given the limitations of both approaches in terms of concurrently formulating stable and thermally optimized NF, a systematic approach should be applied considering critical parameters, operating conditions, and desired performance (described in **Section 2**). Further research is needed to develop a process for producing NF that is sustainable, cost efficient, and scalable. Carrillo-Berdugo, et al. [302] recently revealed a novel interface based three step techniques to formulate stable NF that produced optimized thermo-optical properties.

On thermo-physical characteristics of NF:

- Effective TC of water and water-based NFs amplifies prominently dispersing carbon contained nanomaterials rather than traditional metal and metal-oxides. Nevertheless, numerous works reveal chaotic conflicts with respects to few sophisticated factors

(mentioned in **Section 3**) emerged from the diverse operating conditions. Therefore, a comprehensive systematic approach should be performed considering the wide-ranging finite variable operating conditions to establish fundamental relationship with TC of diverse NFs. While TC intensifies dispersing nanomaterial in BF, c_p drops for most of the NFs due to lower heat capacity of solid particles relative to liquids. Nevertheless, opposite trends are reported in few studies using carbon-based particles. Since higher c_p value has remarkable impact on renewable energy sector, particularly energy storage and SC devices, comprehensive experiments are required to come up with detailed understanding on c_p enhancement of NFs.

- The dynamic viscosity (μ) of water-based NFs enhances with the inclusion of nanoscale materials but it declines noticeably at higher temperatures. Moreover, Newtonian, and non-Newtonian properties are dominant at low to high φ respectively. While hybrid NFs usually elucidate non-Newtonian flow characteristics.
- Existing theoretical and empirical models derived for a specific NF are inaccurate to estimate heat transfer behavior (Nusselt number, pressure drop and performance factor), thermal conductivity, μ, and c_p of other NFs when compared to experimental data. This could be because only a few significant criteria and operating conditions are considered. Analytical studies are needed to build specific models that analyze possible factors to precisely estimate these critical properties.

On suspension stability of NF:

- Stability determines the overall performance of the NF and the thermal system on which it operates, i.e., improved stability results in increased system efficiency. Generally, most the formulated NFs reported in the studies exhibit short-term stability due to agglomeration of dispersed particles caused by various factors. The instability of NFs is identified as a function of multifarious variables, for instance formulation techniques, BF, NPs (φ, size and shape), temperature, and stabilization methods (physical and chemical). However, NFs containing very low φ of carbon nanomaterials in water medium offer prominent suspension stability and effective performance augmentation using in SC based energy conversion application. Further investigations should emphasis on rigorous tracking of stability for longer periods employing techniques associated with stabilizers and functionalization to provide explicit reports about the impacts of stabilizing additives.

- By evaluating related destabilization factors, comparisons between various NF stabilization strategies (e.g., ionic, and non-ionic stabilizers, surface adjustment and functionalization) should be made. Deployment of advance particle functionalization using irreversible polymers grafting can during synthesis of NP may evade limitations and provide robust protection against the undermining factors. Furthermore, there are no clear analytical correlations linking NF stability, operating conditions, and properties that can be addressed in future research.

On implementation and performance evaluation of NF on various solar collector systems:

- The selection of stable NF (i.e., BF and NP) is a critical precondition for their use in solar energy conversion operations. The efficiency of several low flux SCs is significantly enhanced when NFs are used in place of traditional HTFs. Desired properties for SC application of NFs include high heat transport and energy storage capacity (i.e., TC and c_p) alongside low viscosity and Newtonian flow behavior which are observed to have important impacts on the performance.
- Water-based NFs are well suited for low temperature energy systems and SCs due to their low viscosity and high thermo-optical properties. In low flux SCs such as FPSC, ETSC, DASC, and hybrid PV/T, water-based NFs containing carbon nanomaterials perform better.
- Inadequate studies were observed estimating production cost, surface deterioration, safety, and ecological aspects of NFs. Such instructive statistics would provide essential assistance to determine prospective execution of the NFs in industrial sectors.

Acknowledgement

We appreciate financial support from Yayasan Universiti Teknologi Petronas (research grant no. 015LC0-118). Fazlay Rubbi would like to dedicate his efforts in this project to his adoring mother, Rahima Khatun.

References

[1] H. Masuda, A. Ebata, K. Teramae, and N. Hishinuma, "Alteration of thermal conductivity and viscosity of liquid by dispersing ultra-fine particles. dispersion of Al2O3, SiO2 and TiO2 ultra-fine particles," *Netsu Bussei*, vol. 7, no. 4, pp. 227-233, 1993.

[2] S. U. S. Choi and J. A. Eastman, "Enhancing thermal conductivity of fluids with nanoparticles," United States, 1995, Research Org.: Argonne National Lab., IL (United States), Sponsor Org.: USDOE, Washington, DC (United States).

[3] S. Kakaç and A. Pramuanjaroenkij, "Review of convective heat transfer enhancement with nanofluids," *International Journal of Heat and Mass Transfer,* vol. 52, no. 13, pp. 3187-3196, 2009/06/01/ 2009.
[4] L. Qiu *et al.*, "A review of recent advances in thermophysical properties at the nanoscale: From solid state to colloids," *Physics Reports,* vol. 843, pp. 1-81, 2020/02/13/ 2020.
[5] B. Wang, X. Wang, W. Lou, and J. Hao, "Thermal conductivity and rheological properties of graphite/oil nanofluids," *Colloids and Surfaces A: Physicochemical and Engineering Aspects,* vol. 414, pp. 125-131, 2012/11/20/ 2012.
[6] M. E. Nakhchi and J. A. Esfahani, "Cu-water nanofluid flow and heat transfer in a heat exchanger tube equipped with cross-cut twisted tape," *Powder Technology,* vol. 339, pp. 985-994, 2018/11/01/ 2018.
[7] S. Chakraborty, I. Sarkar, A. Ashok, I. Sengupta, S. K. Pal, and S. Chakraborty, "Synthesis of Cu-Al LDH nanofluid and its application in spray cooling heat transfer of a hot steel plate," *Powder Technology,* vol. 335, pp. 285-300, 2018/07/15/ 2018.
[8] S. Chakraborty and P. K. Panigrahi, "Stability of nanofluid: A review," *Applied Thermal Engineering,* vol. 174, p. 115259, 2020/06/25/ 2020.
[9] N. A. Che Sidik, M. Mahmud Jamil, W. M. A. Aziz Japar, and I. Muhammad Adamu, "A review on preparation methods, stability and applications of hybrid nanofluids," *Renewable and Sustainable Energy Reviews,* vol. 80, pp. 1112-1122, 2017/12/01/ 2017.
[10] A. Hajatzadeh Pordanjani, S. Aghakhani, M. Afrand, B. Mahmoudi, O. Mahian, and S. Wongwises, "An updated review on application of nanofluids in heat exchangers for saving energy," *Energy Conversion and Management,* vol. 198, p. 111886, 2019/10/15/ 2019.
[11] A. R. Akash, S. Abraham, A. Pattamatta, and S. K. Das, "Experimental Assessment of the Thermo-Hydraulic Performance of Automobile Radiator with Metallic and Nonmetallic Nanofluids," *Heat Transfer Engineering,* vol. 41, no. 3, pp. 235-251, 2020/02/04 2020.
[12] R. Kumar, V. Deshmukh, and R. S. Bharj, "Performance enhancement of photovoltaic modules by nanofluid cooling: A comprehensive review," *International Journal of Energy Research,* https://doi.org/10.1002/er.5285 vol. 44, no. 8, pp. 6149-6169, 2020/06/25 2020.
[13] D. P. Kulkarni, D. K. Das, and R. S. Vajjha, "Application of nanofluids in heating buildings and reducing pollution," *Applied Energy,* vol. 86, no. 12, pp. 2566-2573, 2009/12/01/ 2009.
[14] S. Soltani, A. Kasaeian, A. Lavajoo, R. Loni, G. Najafi, and O. Mahian, "Exergetic and enviromental assessment of a photovoltaic thermal-thermoelectric system using nanofluids: Indoor experimental tests," *Energy Conversion and Management,* vol. 218, p. 112907, 2020/08/15/ 2020.
[15] A. Bhattad, J. Sarkar, and P. Ghosh, "Improving the performance of refrigeration systems by using nanofluids: A comprehensive review," *Renewable and Sustainable Energy Reviews,* vol. 82, pp. 3656-3669, 2018/02/01/ 2018.
[16] R. A. Rasih, N. A. C. Sidik, and S. Samion, "Recent progress on concentrating direct absorption solar collector using nanofluids," *Journal of Thermal Analysis and Calorimetry,* vol. 137, no. 3, pp. 903-922, 2019/08/01 2019.
[17] A. H. Elsheikh, S. W. Sharshir, M. E. Mostafa, F. A. Essa, and M. K. Ahmed Ali, "Applications of nanofluids in solar energy: A review of recent advances," *Renewable and Sustainable Energy Reviews,* vol. 82, pp. 3483-3502, 2018/02/01/ 2018.

[18] T. R. Shah and H. M. Ali, "Applications of hybrid nanofluids in solar energy, practical limitations and challenges: A critical review," *Solar Energy,* vol. 183, pp. 173-203, 2019/05/01/ 2019.
[19] F. Rubbi, K. Habib, R. Saidur, N. Aslfattahi, S. M. Yahya, and L. Das, "Performance optimization of a hybrid PV/T solar system using Soybean oil/MXene nanofluids as A new class of heat transfer fluids," *Solar Energy,* vol. 208, pp. 124-138, 2020/09/15/ 2020.
[20] N. Goel, R. A. Taylor, and T. Otanicar, "A review of nanofluid-based direct absorption solar collectors: Design considerations and experiments with hybrid PV/Thermal and direct steam generation collectors," *Renewable Energy,* vol. 145, pp. 903-913, 2020/01/01/ 2020.
[21] L. Das *et al.*, "State-of-the-art ionic liquid & ionanofluids incorporated with advanced nanomaterials for solar energy applications," *Journal of Molecular Liquids,* p. 116563, 2021/05/24/ 2021.
[22] H. Olia, M. Torabi, M. Bahiraei, M. H. Ahmadi, M. Goodarzi, and M. R. Safaei, "Application of Nanofluids in Thermal Performance Enhancement of Parabolic Trough Solar Collector: State-of-the-Art," *Applied Sciences,* vol. 9, no. 3, 2019.
[23] O. Mahian *et al.*, "Recent advances in using nanofluids in renewable energy systems and the environmental implications of their uptake," *Nano Energy,* vol. 86, p. 106069, 2021/08/01/ 2021.
[24] S. H. A. Ahmad, R. Saidur, I. M. Mahbubul, and F. A. Al-Sulaiman, "Optical properties of various nanofluids used in solar collector: A review," *Renewable and Sustainable Energy Reviews,* vol. 73, pp. 1014-1030, 2017/06/01/ 2017.
[25] T. B. Gorji and A. A. Ranjbar, "A review on optical properties and application of nanofluids in direct absorption solar collectors (DASCs)," *Renewable and Sustainable Energy Reviews,* vol. 72, pp. 10-32, 2017/05/01/ 2017.
[26] F. Yu *et al.*, "Dispersion stability of thermal nanofluids," *Progress in Natural Science: Materials International,* vol. 27, no. 5, pp. 531-542, 2017/10/01/ 2017.
[27] J. A. Ranga Babu, K. K. Kumar, and S. Srinivasa Rao, "State-of-art review on hybrid nanofluids," *Renewable and Sustainable Energy Reviews,* vol. 77, pp. 551-565, 2017/09/01/ 2017.
[28] M. Mohammadpoor, S. Sabbaghi, M. M. Zerafat, and Z. Manafi, "Investigating heat transfer properties of copper nanofluid in ethylene glycol synthesized through single and two-step routes," *International Journal of Refrigeration,* vol. 99, pp. 243-250, 2019/03/01/ 2019.
[29] Y. Zhang, Y. Chen, P. Westerhoff, K. Hristovski, and J. C. Crittenden, "Stability of commercial metal oxide nanoparticles in water," *Water Research,* vol. 42, no. 8, pp. 2204-2212, 2008/04/01/ 2008.
[30] W. S. Sarsam, A. Amiri, S. N. Kazi, and A. Badarudin, "Stability and thermophysical properties of non-covalently functionalized graphene nanoplatelets nanofluids," *Energy Conversion and Management,* vol. 116, pp. 101-111, 2016/05/15/ 2016.
[31] T.-P. Teng, C.-M. Cheng, and F.-Y. Pai, "Preparation and characterization of carbon nanofluid by a plasma arc nanoparticles synthesis system," *Nanoscale Research Letters,* vol. 6, no. 1, p. 293, 2011/04/05 2011.
[32] Y. Hwang *et al.*, "Production and dispersion stability of nanoparticles in nanofluids," *Powder Technology,* vol. 186, no. 2, pp. 145-153, 2008/08/11/ 2008.
[33] H. J. Kim, I. C. Bang, and J. Onoe, "Characteristic stability of bare Au-water nanofluids fabricated by pulsed laser ablation in liquids," *Optics and Lasers in Engineering,* vol. 47, no. 5, pp. 532-538, 2009/05/01/ 2009.

[34] S. Aberoumand and A. Jafarimoghaddam, "Experimental study on synthesis, stability, thermal conductivity and viscosity of Cu–engine oil nanofluid," *Journal of the Taiwan Institute of Chemical Engineers*, vol. 71, pp. 315-322, 2017/02/01/ 2017.
[35] C.-H. Lo, T.-T. Tsung, L.-C. Chen, C.-H. Su, and H.-M. Lin, "Fabrication of copper oxide nanofluid using submerged arc nanoparticle synthesis system (SANSS)," *Journal of Nanoparticle Research*, vol. 7, no. 2, pp. 313-320, 2005/06/01 2005.
[36] H.-t. Zhu, Y.-s. Lin, and Y.-s. Yin, "A novel one-step chemical method for preparation of copper nanofluids," *Journal of Colloid and Interface Science*, vol. 277, no. 1, pp. 100-103, 2004/09/01/ 2004.
[37] M. Khoshvaght-Aliabadi, M. Nouri, O. Sartipzadeh, and M. Salami, "Performance of agitated serpentine heat exchanger using metallic nanofluids," *Chemical Engineering Research and Design*, vol. 109, pp. 53-64, 2016/05/01/ 2016.
[38] P. Zare, P. Keshavarz, and D. Mowla, "Membrane Absorption Coupling Process for CO2 Capture: Application of Water-Based ZnO, TiO2, and Multi-Walled Carbon Nanotube Nanofluids," *Energy & Fuels*, vol. 33, no. 2, pp. 1392-1403, 2019/02/21 2019.
[39] A. Elminshawy, K. Morad, N. A. S. Elminshawy, and Y. Elhenawy, "Performance enhancement of concentrator photovoltaic systems using nanofluids," *International Journal of Energy Research*, https://doi.org/10.1002/er.5991 vol. n/a, no. n/a, 2020/09/15 2020.
[40] A. Ghadimi and I. H. Metselaar, "The influence of surfactant and ultrasonic processing on improvement of stability, thermal conductivity and viscosity of titania nanofluid," *Experimental Thermal and Fluid Science*, vol. 51, pp. 1-9, 2013/11/01/ 2013.
[41] M. F. Islam, E. Rojas, D. M. Bergey, A. T. Johnson, and A. G. Yodh, "High Weight Fraction Surfactant Solubilization of Single-Wall Carbon Nanotubes in Water," *Nano Letters*, vol. 3, no. 2, pp. 269-273, 2003/02/01 2003.
[42] I. W. Almanassra, A. D. Manasrah, U. A. Al-Mubaiyedh, T. Al-Ansari, Z. O. Malaibari, and M. A. Atieh, "An experimental study on stability and thermal conductivity of water/CNTs nanofluids using different surfactants: A comparison study," *Journal of Molecular Liquids*, vol. 304, p. 111025, 2020/04/15/ 2020.
[43] A. S. Abdelrazik, K. H. Tan, N. Aslfattahi, R. Saidur, and F. A. Al-Sulaiman, "Optical properties and stability of water-based nanofluids mixed with reduced graphene oxide decorated with silver and energy performance investigation in hybrid photovoltaic/thermal solar systems," *International Journal of Energy Research*, https://doi.org/10.1002/er.5770 vol. 44, no. 14, pp. 11487-11508, 2020/11/01 2020.
[44] A. S. Abdelrazik, K. H. Tan, N. Aslfattahi, A. Arifutzzaman, R. Saidur, and F. A. Al-Sulaiman, "Optical, stability and energy performance of water-based MXene nanofluids in hybrid PV/thermal solar systems," *Solar Energy*, vol. 204, pp. 32-47, 2020/07/01/ 2020.
[45] M. M. Sarafraz, M. R. Safaei, Z. Tian, M. Goodarzi, E. P. Bandarra Filho, and M. Arjomandi, "Thermal Assessment of Nano-Particulate Graphene-Water/Ethylene Glycol (WEG 60:40) Nano-Suspension in a Compact Heat Exchanger," *Energies*, vol. 12, no. 10, 2019.
[46] A. K. Tiwari, N. S. Pandya, Z. Said, H. F. Öztop, and N. Abu-Hamdeh, "4S consideration (synthesis, sonication, surfactant, stability) for the thermal conductivity of CeO2 with MWCNT and water based hybrid nanofluid: An experimental assessment," *Colloids and Surfaces A: Physicochemical and Engineering Aspects*, vol. 610, p. 125918, 2021/02/05/ 2021.

[47] H. Zhao *et al.*, "Green Synthesis of Graphene/Boron Nitride Composites for Ultrahigh Thermally Conductive Fluids," *ACS Sustainable Chemistry & Engineering,* vol. 7, no. 16, pp. 14266-14272, 2019/08/19 2019.
[48] S. Chakraborty, I. Sarkar, A. Ashok, I. Sengupta, S. K. Pal, and S. Chakraborty, "Thermo-physical properties of Cu-Zn-Al LDH nanofluid and its application in spray cooling," *Applied Thermal Engineering,* vol. 141, pp. 339-351, 2018/08/01/ 2018.
[49] M. Gupta, V. Singh, R. Kumar, and Z. Said, "A review on thermophysical properties of nanofluids and heat transfer applications," *Renewable and Sustainable Energy Reviews,* vol. 74, pp. 638-670, 2017/07/01/ 2017.
[50] R. V. Pinto and F. A. S. Fiorelli, "Review of the mechanisms responsible for heat transfer enhancement using nanofluids," *Applied Thermal Engineering,* vol. 108, pp. 720-739, 2016/09/05/ 2016.
[51] M. M. Tawfik, "Experimental studies of nanofluid thermal conductivity enhancement and applications: A review," *Renewable and Sustainable Energy Reviews,* vol. 75, pp. 1239-1253, 2017/08/01/ 2017.
[52] M. Milanese, F. Iacobazzi, G. Colangelo, and A. de Risi, "An investigation of layering phenomenon at the liquid–solid interface in Cu and CuO based nanofluids," *International Journal of Heat and Mass Transfer,* vol. 103, pp. 564-571, 2016/12/01/ 2016.
[53] F. Iacobazzi, M. Milanese, G. Colangelo, M. Lomascolo, and A. de Risi, "An explanation of the Al2O3 nanofluid thermal conductivity based on the phonon theory of liquid," *Energy,* vol. 116, pp. 786-794, 2016/12/01/ 2016.
[54] M. U. Sajid and H. M. Ali, "Recent advances in application of nanofluids in heat transfer devices: A critical review," *Renewable and Sustainable Energy Reviews,* vol. 103, pp. 556-592, 2019/04/01/ 2019.
[55] S. M. S. Murshed and C. A. Nieto de Castro, "Superior thermal features of carbon nanotubes-based nanofluids – A review," *Renewable and Sustainable Energy Reviews,* vol. 37, pp. 155-167, 2014/09/01/ 2014.
[56] M. Afrand, D. Toghraie, and N. Sina, "Experimental study on thermal conductivity of water-based Fe3O4 nanofluid: Development of a new correlation and modeled by artificial neural network," *International Communications in Heat and Mass Transfer,* vol. 75, pp. 262-269, 2016/07/01/ 2016.
[57] T. Ambreen and M.-H. Kim, "Influence of particle size on the effective thermal conductivity of nanofluids: A critical review," *Applied Energy,* vol. 264, p. 114684, 2020/04/15/ 2020.
[58] H. W. Xian, N. A. C. Sidik, and R. Saidur, "Impact of different surfactants and ultrasonication time on the stability and thermophysical properties of hybrid nanofluids," *International Communications in Heat and Mass Transfer,* vol. 110, p. 104389, 2020/01/01/ 2020.
[59] L. Yang, W. Ji, J.-n. Huang, and G. Xu, "An updated review on the influential parameters on thermal conductivity of nano-fluids," *Journal of Molecular Liquids,* vol. 296, p. 111780, 2019/12/15/ 2019.
[60] N. Keklikcioglu Cakmak, "The impact of surfactants on the stability and thermal conductivity of graphene oxide de-ionized water nanofluids," *Journal of Thermal Analysis and Calorimetry,* vol. 139, no. 3, pp. 1895-1902, 2020/02/01 2020.
[61] F. Iacobazzi, M. Milanese, G. Colangelo, and A. de Risi, "A critical analysis of clustering phenomenon in Al2O3 nanofluids," *Journal of Thermal Analysis and Calorimetry,* vol. 135, no. 1, pp. 371-377, 2019/01/01 2019.

[62] T.-P. Teng, Y.-H. Hung, T.-C. Teng, H.-E. Mo, and H.-G. Hsu, "The effect of alumina/water nanofluid particle size on thermal conductivity," *Applied Thermal Engineering*, vol. 30, no. 14, pp. 2213-2218, 2010/10/01/ 2010.
[63] E. V. Timofeeva, J. L. Routbort, and D. Singh, "Particle shape effects on thermophysical properties of alumina nanofluids," *Journal of Applied Physics*, vol. 106, no. 1, p. 014304, 2009/07/01 2009.
[64] P. B. Maheshwary, C. C. Handa, and K. R. Nemade, "A comprehensive study of effect of concentration, particle size and particle shape on thermal conductivity of titania/water based nanofluid," *Applied Thermal Engineering*, vol. 119, pp. 79-88, 2017/06/05/ 2017.
[65] H. Zhang, S. Qing, Y. Zhai, X. Zhang, and A. Zhang, "The changes induced by pH in TiO2/water nanofluids: Stability, thermophysical properties and thermal performance," *Powder Technology*, vol. 377, pp. 748-759, 2021/01/02/ 2021.
[66] X.-j. Wang, D.-s. Zhu, and S. yang, "Investigation of pH and SDBS on enhancement of thermal conductivity in nanofluids," *Chemical Physics Letters*, vol. 470, no. 1, pp. 107-111, 2009/02/24/ 2009.
[67] F. Garoosi, "Presenting two new empirical models for calculating the effective dynamic viscosity and thermal conductivity of nanofluids," *Powder Technology*, vol. 366, pp. 788-820, 2020/04/15/ 2020.
[68] W. Cui, Z. Shen, J. Yang, S. Wu, and M. Bai, "Influence of nanoparticle properties on the thermal conductivity of nanofluids by molecular dynamics simulation," *RSC Advances*, 10.1039/C4RA07736A vol. 4, no. 98, pp. 55580-55589, 2014.
[69] A. Pare and S. K. Ghosh, "A unique thermal conductivity model (ANN) for nanofluid based on experimental study," *Powder Technology*, vol. 377, pp. 429-438, 2021/01/02/ 2021.
[70] A. Zendehboudi, R. Saidur, I. M. Mahbubul, and S. H. Hosseini, "Data-driven methods for estimating the effective thermal conductivity of nanofluids: A comprehensive review," *International Journal of Heat and Mass Transfer*, vol. 131, pp. 1211-1231, 2019/03/01/ 2019.
[71] S. Chakraborty, I. Sarkar, D. K. Behera, S. K. Pal, and S. Chakraborty, "Experimental investigation on the effect of dispersant addition on thermal and rheological characteristics of TiO2 nanofluid," *Powder Technology*, vol. 307, pp. 10-24, 2017/02/01/ 2017.
[72] L. Das, K. Habib, R. Saidur, N. Aslfattahi, S. M. Yahya, and F. Rubbi, "Improved Thermophysical Properties and Energy Efficiency of Aqueous Ionic Liquid/MXene Nanofluid in a Hybrid PV/T Solar System," *Nanomaterials*, vol. 10, no. 7, 2020.
[73] A. Alshayji, A. Asadi, and I. M. Alarifi, "On the heat transfer effectiveness and pumping power assessment of a diamond-water nanofluid based on thermophysical properties: An experimental study," *Powder Technology*, vol. 373, pp. 397-410, 2020/08/01/ 2020.
[74] A. Amiri *et al.*, "Performance dependence of thermosyphon on the functionalization approaches: An experimental study on thermo-physical properties of graphene nanoplatelet-based water nanofluids," *Energy Conversion and Management*, vol. 92, pp. 322-330, 2015/03/01/ 2015.
[75] R. Sadri *et al.*, "A novel, eco-friendly technique for covalent functionalization of graphene nanoplatelets and the potential of their nanofluids for heat transfer applications," *Chemical Physics Letters*, vol. 675, pp. 92-97, 2017/05/01/ 2017.
[76] K. Singh, D. P. Barai, S. S. Chawhan, B. A. Bhanvase, and V. K. Saharan, "Synthesis, characterization and heat transfer study of reduced graphene oxide-Al2O3

nanocomposite based nanofluids: Investigation on thermal conductivity and rheology," *Materials Today Communications*, vol. 26, p. 101986, 2021/03/01/ 2021.

[77] L. S. Sundar, G. O. Irurueta, E. Venkata Ramana, M. K. Singh, and A. C. M. Sousa, "Thermal conductivity and viscosity of hybrid nanfluids prepared with magnetic nanodiamond-cobalt oxide (ND-Co3O4) nanocomposite," *Case Studies in Thermal Engineering*, vol. 7, pp. 66-77, 2016/03/01/ 2016.

[78] G. Huminic, A. Huminic, F. Dumitrache, C. Fleacă, and I. Morjan, "Study of the thermal conductivity of hybrid nanofluids: Recent research and experimental study," *Powder Technology*, vol. 367, pp. 347-357, 2020/05/01/ 2020.

[79] G. M. Moldoveanu, G. Huminic, A. A. Minea, and A. Huminic, "Experimental study on thermal conductivity of stabilized Al2O3 and SiO2 nanofluids and their hybrid," *International Journal of Heat and Mass Transfer*, vol. 127, pp. 450-457, 2018/12/01/ 2018.

[80] M. A. Sabiha, R. M. Mostafizur, R. Saidur, and S. Mekhilef, "Experimental investigation on thermo physical properties of single walled carbon nanotube nanofluids," *International Journal of Heat and Mass Transfer*, vol. 93, pp. 862-871, 2016/02/01/ 2016.

[81] N. Kumar and S. S. Sonawane, "Experimental study of thermal conductivity and convective heat transfer enhancement using CuO and TiO2 nanoparticles," *International Communications in Heat and Mass Transfer*, vol. 76, pp. 98-107, 2016/08/01/ 2016.

[82] O. A. Hussein, K. Habib, A. S. Muhsan, R. Saidur, O. A. Alawi, and T. K. Ibrahim, "Thermal performance enhancement of a flat plate solar collector using hybrid nanofluid," *Solar Energy*, vol. 204, pp. 208-222, 2020/07/01/ 2020.

[83] M. Hemmat Esfe and S. Saedodin, "Turbulent forced convection heat transfer and thermophysical properties of Mgo–water nanofluid with consideration of different nanoparticles diameter, an empirical study," *Journal of Thermal Analysis and Calorimetry*, vol. 119, no. 2, pp. 1205-1213, 2015/02/01 2015.

[84] L. S. Sundar, M. J. Hortiguela, M. K. Singh, and A. C. M. Sousa, "Thermal conductivity and viscosity of water based nanodiamond (ND) nanofluids: An experimental study," *International Communications in Heat and Mass Transfer*, vol. 76, pp. 245-255, 2016/08/01/ 2016.

[85] W. Chen, C. Zou, X. Li, and L. Li, "Experimental investigation of SiC nanofluids for solar distillation system: Stability, optical properties and thermal conductivity with saline water-based fluid," *International Journal of Heat and Mass Transfer*, vol. 107, pp. 264-270, 2017/04/01/ 2017.

[86] H. Zhang, S. Wang, Y. Lin, M. Feng, and Q. Wu, "Stability, thermal conductivity, and rheological properties of controlled reduced graphene oxide dispersed nanofluids," *Applied Thermal Engineering*, vol. 119, pp. 132-139, 2017/06/05/ 2017.

[87] N. Shalkevich, W. Escher, T. Bürgi, B. Michel, L. Si-Ahmed, and D. Poulikakos, "On the Thermal Conductivity of Gold Nanoparticle Colloids," *Langmuir*, vol. 26, no. 2, pp. 663-670, 2010/01/19 2010.

[88] V. Srinivas, C. V. K. N. S. N. Moorthy, V. Dedeepya, P. V. Manikanta, and V. Satish, "Nanofluids with CNTs for automotive applications," *Heat and Mass Transfer*, vol. 52, no. 4, pp. 701-712, 2016/04/01 2016.

[89] G. S. Wu, J. K. Yang, S. L. Ge, Y. J. Wang, M. H. Chen, and Y. F. Chen, "Thermal Conductivity Measurement for Carbon-Nanotube Suspensions with 3ω Method," *Advanced Materials Research*, vol. 60-61, pp. 394-398, 2009.

[90] K. Wusiman, H. Jeong, K. Tulugan, H. Afrianto, and H. Chung, "Thermal performance of multi-walled carbon nanotubes (MWCNTs) in aqueous suspensions with surfactants

SDBS and SDS," *International Communications in Heat and Mass Transfer,* vol. 41, pp. 28-33, 2013/02/01/ 2013.

[91] M. Sahooli, S. Sabbaghi, and M. Shariaty Niassar, "Preparation of CuO/Water Nanofluids Using Polyvinylpyrolidone and a Survey on Its Stability and Thermal Conductivity," (in en), *International Journal of Nanoscience and Nanotechnology,* vol. 8, no. 1, pp. 27-34, 2012.

[92] Y. Y. Song, H. K. D. H. Bhadeshia, and D.-W. Suh, "Stability of stainless-steel nanoparticle and water mixtures," *Powder Technology,* vol. 272, pp. 34-44, 2015/03/01/ 2015.

[93] A. Shahsavar, M. R. Salimpour, M. Saghafian, and M. B. Shafii, "Effect of magnetic field on thermal conductivity and viscosity of a magnetic nanofluid loaded with carbon nanotubes," *Journal of Mechanical Science and Technology,* vol. 30, no. 2, pp. 809-815, 2016/02/01 2016.

[94] P. Garg, J. L. Alvarado, C. Marsh, T. A. Carlson, D. A. Kessler, and K. Annamalai, "An experimental study on the effect of ultrasonication on viscosity and heat transfer performance of multi-wall carbon nanotube-based aqueous nanofluids," *International Journal of Heat and Mass Transfer,* vol. 52, no. 21, pp. 5090-5101, 2009/10/01/ 2009.

[95] M. Xing, J. Yu, and R. Wang, "Thermo-physical properties of water-based single-walled carbon nanotube nanofluid as advanced coolant," *Applied Thermal Engineering,* vol. 87, pp. 344-351, 2015/08/05/ 2015.

[96] R. Taherialekouhi, S. Rasouli, and A. Khosravi, "An experimental study on stability and thermal conductivity of water-graphene oxide/aluminum oxide nanoparticles as a cooling hybrid nanofluid," *International Journal of Heat and Mass Transfer,* vol. 145, p. 118751, 2019/12/01/ 2019.

[97] S. M. Mousavi, F. Esmaeilzadeh, and X. P. Wang, "A detailed investigation on the thermo-physical and rheological behavior of MgO/TiO2 aqueous dual hybrid nanofluid," *Journal of Molecular Liquids,* vol. 282, pp. 323-339, 2019/05/15/ 2019.

[98] E. C. Okonkwo, I. Wole-Osho, D. Kavaz, and M. Abid, "Comparison of experimental and theoretical methods of obtaining the thermal properties of alumina/iron mono and hybrid nanofluids," *Journal of Molecular Liquids,* vol. 292, p. 111377, 2019/10/15/ 2019.

[99] O. A. Hussein, K. Habib, R. Saidur, A. S. Muhsan, S. Shahabuddin, and O. A. Alawi, "The influence of covalent and non-covalent functionalization of GNP based nanofluids on its thermophysical, rheological and suspension stability properties," *RSC Advances,* 10.1039/C9RA07811H vol. 9, no. 66, pp. 38576-38589, 2019.

[100] O. A. Alawi, N. A. C. Sidik, H. W. Xian, T. H. Kean, and S. N. Kazi, "Thermal conductivity and viscosity models of metallic oxides nanofluids," *International Journal of Heat and Mass Transfer,* vol. 116, pp. 1314-1325, 2018/01/01/ 2018.

[101] M. Hemmat Esfe, A. A. Abbasian Arani, and M. Firouzi, "Empirical study and model development of thermal conductivity improvement and assessment of cost and sensitivity of EG-water based SWCNT-ZnO (30%:70%) hybrid nanofluid," *Journal of Molecular Liquids,* vol. 244, pp. 252-261, 2017/10/01/ 2017.

[102] S. H. Rostamian, M. Biglari, S. Saedodin, and M. Hemmat Esfe, "An inspection of thermal conductivity of CuO-SWCNTs hybrid nanofluid versus temperature and concentration using experimental data, ANN modeling and new correlation," *Journal of Molecular Liquids,* vol. 231, pp. 364-369, 2017/04/01/ 2017.

[103] M. P. Beck, Y. Yuan, P. Warrier, and A. S. Teja, "The effect of particle size on the thermal conductivity of alumina nanofluids," *Journal of Nanoparticle Research,* vol. 11, no. 5, pp. 1129-1136, 2009/07/01 2009.

[104] C. Sun, B. Bai, W.-Q. Lu, and J. Liu, "Shear-rate dependent effective thermal conductivity of H2O+SiO2 nanofluids," *Physics of Fluids,* vol. 25, no. 5, p. 052002, 2013/05/01 2013.
[105] M. Hemmat Esfe, S. Saedodin, S. Wongwises, and D. Toghraie, "An experimental study on the effect of diameter on thermal conductivity and dynamic viscosity of Fe/water nanofluids," *Journal of Thermal Analysis and Calorimetry,* vol. 119, no. 3, pp. 1817-1824, 2015/03/01 2015.
[106] M. Hemmat Esfe, S. Saedodin, W.-M. Yan, M. Afrand, and N. Sina, "Study on thermal conductivity of water-based nanofluids with hybrid suspensions of CNTs/Al2O3 nanoparticles," *Journal of Thermal Analysis and Calorimetry,* vol. 124, no. 1, pp. 455-460, 2016/04/01 2016.
[107] E. De Robertis *et al.*, "Application of the modulated temperature differential scanning calorimetry technique for the determination of the specific heat of copper nanofluids," *Applied Thermal Engineering,* vol. 41, pp. 10-17, 2012/08/01/ 2012.
[108] S. Sonawane, K. Patankar, A. Fogla, B. Puranik, U. Bhandarkar, and S. Sunil Kumar, "An experimental investigation of thermo-physical properties and heat transfer performance of Al2O3-Aviation Turbine Fuel nanofluids," *Applied Thermal Engineering,* vol. 31, no. 14, pp. 2841-2849, 2011/10/01/ 2011.
[109] A. K. Tiwari, N. S. Pandya, H. Shah, and Z. Said, "Experimental comparison of specific heat capacity of three different metal oxides with MWCNT/ water-based hybrid nanofluids: proposing a new correlation," *Applied Nanoscience,* 2020/10/21 2020.
[110] I. Wole-Osho, E. C. Okonkwo, D. Kavaz, and S. Abbasoglu, "An experimental investigation into the effect of particle mixture ratio on specific heat capacity and dynamic viscosity of Al2O3-ZnO hybrid nanofluids," *Powder Technology,* vol. 363, pp. 699-716, 2020/03/01/ 2020.
[111] A. K. Starace, J. C. Gomez, J. Wang, S. Pradhan, and G. C. Glatzmaier, "Nanofluid heat capacities," *Journal of Applied Physics,* vol. 110, no. 12, p. 124323, 2011/12/15 2011.
[112] G. M. Moldoveanu and A. A. Minea, "Specific heat experimental tests of simple and hybrid oxide-water nanofluids: Proposing new correlation," *Journal of Molecular Liquids,* vol. 279, pp. 299-305, 2019/04/01/ 2019.
[113] V. Kumaresan and R. Velraj, "Experimental investigation of the thermo-physical properties of water–ethylene glycol mixture based CNT nanofluids," *Thermochimica Acta,* vol. 545, pp. 180-186, 2012/10/10/ 2012.
[114] B. C. Pak and Y. I. Cho, "Hydrodynamic and heat transfer study of dispersed fluids with submicron metallic oxide particles," *Experimental Heat Transfer,* vol. 11, no. 2, pp. 151-170, 1998/04/01 1998.
[115] Y. Xuan and W. Roetzel, "Conceptions for heat transfer correlation of nanofluids," *International Journal of Heat and Mass Transfer,* vol. 43, no. 19, pp. 3701-3707, 2000/10/01/ 2000.
[116] H. O'Hanley, J. Buongiorno, T. McKrell, and L.-w. Hu, "Measurement and Model Validation of Nanofluid Specific Heat Capacity with Differential Scanning Calorimetry," *Advances in Mechanical Engineering,* vol. 4, p. 181079, 2012/01/01 2012.
[117] S. M. S. Murshed, "Determination of effective specific heat of nanofluids," *Journal of Experimental Nanoscience,* vol. 6, no. 5, pp. 539-546, 2011/10/01 2011.
[118] M. Fakoor Pakdaman, M. A. Akhavan-Behabadi, and P. Razi, "An experimental investigation on thermo-physical properties and overall performance of MWCNT/heat transfer oil nanofluid flow inside vertical helically coiled tubes," *Experimental Thermal and Fluid Science,* vol. 40, pp. 103-111, 2012/07/01/ 2012.

[119] Y. R. Sekhar and K. V. Sharma, "Study of viscosity and specific heat capacity characteristics of water-based Al2O3 nanofluids at low particle concentrations," *Journal of Experimental Nanoscience,* vol. 10, no. 2, pp. 86-102, 2015/01/22 2015.
[120] Y. Wang, C. Zou, W. Li, Y. Zou, and H. Huang, "Improving stability and thermal properties of TiO2 nanofluids by supramolecular modification: high energy efficiency heat transfer medium for data center cooling system," *International Journal of Heat and Mass Transfer*, vol. 156, p. 119735, 2020/08/01/ 2020.
[121] O. Fesenko, V. Korskanov, A. Yaremkevych, T. Tsebriinko, and V. Dolgoshey, "Thermodynamics of the formation of water dispersions of graphene and water solutions of the nanostructures based on graphene and gold nanoparticles," *Applied Nanoscience,* vol. 10, no. 12, pp. 4609-4616, 2020/12/01 2020.
[122] C. Selvam, D. Mohan Lal, and S. Harish, "Thermal conductivity and specific heat capacity of water–ethylene glycol mixture-based nanofluids with graphene nanoplatelets," *Journal of Thermal Analysis and Calorimetry*, vol. 129, no. 2, pp. 947-955, 2017/08/01 2017.
[123] H. O'Hanley, J. Buongiorno, T. McKrell, and L.-w. Hu, "Measurement and Model Correlation of Specific Heat Capacity of Water-Based Nanofluids With Silica, Alumina and Copper Oxide Nanoparticles," 2011. Available: https://doi.org/10.1115/IMECE2011-62054
[124] T. Singh, I. W. Almanassra, A. Ghani Olabi, T. Al-Ansari, G. McKay, and M. Ali Atieh, "Performance investigation of multiwall carbon nanotubes based water/oil nanofluids for high pressure and high temperature solar thermal technologies for sustainable energy systems," *Energy Conversion and Management*, vol. 225, p. 113453, 2020/12/01/ 2020.
[125] Y. Gao, Y. Xi, Y. Zhenzhong, A. P. Sasmito, A. S. Mujumdar, and L. J. T. S. Wang, "Experimental investigation of specific heat of aqueous graphene oxide Al2O3 hybrid nanofluid," no. 00, pp. 381-381, 2019.
[126] M. Devarajan *et al.*, "Thermophysical properties of CNT and CNT/Al2O3 hybrid nanofluid," *Micro & Nano Letters*, https://doi.org/10.1049/mnl.2017.0029 vol. 13, no. 5, pp. 617-621, 2018/05/01 2018.
[127] I. Popa, G. Gillies, G. Papastavrou, and M. Borkovec, "Attractive and Repulsive Electrostatic Forces between Positively Charged Latex Particles in the Presence of Anionic Linear Polyelectrolytes," *The Journal of Physical Chemistry B*, vol. 114, no. 9, pp. 3170-3177, 2010/03/11 2010.
[128] M. Uematsu and E. U. Frank, "Static Dielectric Constant of Water and Steam," *Journal of Physical and Chemical Reference Data,* vol. 9, no. 4, pp. 1291-1306, 1980/10/01 1980.
[129] T. J. Choi, S. P. Jang, and M. A. Kedzierski, "Effect of surfactants on the stability and solar thermal absorption characteristics of water-based nanofluids with multi-walled carbon nanotubes," *International Journal of Heat and Mass Transfer*, vol. 122, pp. 483-490, 2018/07/01/ 2018.
[130] A. K. Tiwari, N. S. Pandya, Z. Said, S. H. Chhatbar, Y. A. Al-Turki, and A. R. Patel, "3S (sonication, surfactant, stability) impact on the viscosity of hybrid nanofluid with different base fluids: An experimental study," *Journal of Molecular Liquids*, p. 115455, 2021/01/23/ 2021.
[131] D. Wen and Y. Ding, "Effective Thermal Conductivity of Aqueous Suspensions of Carbon Nanotubes (Carbon Nanotube Nanofluids)," *Journal of Thermophysics and Heat Transfer,* vol. 18, no. 4, pp. 481-485, 2004/10/01 2004.

[132] R. Choudhary, D. Khurana, A. Kumar, and S. Subudhi, "Stability analysis of Al2O3/water nanofluids," *Journal of Experimental Nanoscience,* vol. 12, no. 1, pp. 140-151, 2017/01/01 2017.
[133] G. Colangelo, E. Favale, P. Miglietta, M. Milanese, and A. de Risi, "Thermal conductivity, viscosity and stability of Al2O3-diathermic oil nanofluids for solar energy systems," *Energy,* vol. 95, pp. 124-136, 2016/01/15/ 2016.
[134] S. U. Ilyas, R. Pendyala, and N. Marneni, "Preparation, Sedimentation, and Agglomeration of Nanofluids," *Chemical Engineering & Technology,* vol. 37, no. 12, pp. 2011-2021, 2014/12/01 2014.
[135] S. U. Ilyas, S. Ridha, and F. A. Abdul Kareem, "Dispersion stability and surface tension of SDS-Stabilized saline nanofluids with graphene nanoplatelets," *Colloids and Surfaces A: Physicochemical and Engineering Aspects,* vol. 592, p. 124584, 2020/05/05/ 2020.
[136] A. Gallego, K. Cacua, B. Herrera, D. Cabaleiro, M. M. Piñeiro, and L. Lugo, "Experimental evaluation of the effect in the stability and thermophysical properties of water-Al2O3 based nanofluids using SDBS as dispersant agent," *Advanced Powder Technology,* vol. 31, no. 2, pp. 560-570, 2020/02/01/ 2020.
[137] W. U. Rehman *et al.,* "Synthesis, characterization, stability and thermal conductivity of multi-walled carbon nanotubes (MWCNTs) and eco-friendly jatropha seed oil based nanofluid: An experimental investigation and modeling approach," *Journal of Molecular Liquids,* vol. 293, p. 111534, 2019/11/01/ 2019.
[138] S. U. Ilyas, R. Pendyala, M. Narahari, and L. Susin, "Stability, rheology and thermal analysis of functionalized alumina- thermal oil-based nanofluids for advanced cooling systems," *Energy Conversion and Management,* vol. 142, pp. 215-229, 2017/06/15/ 2017.
[139] L. Vandsburger, "Synthesis and covalent surface modification of carbon nanotubes for preparation of stabilized nanofluid suspensions," McGill University, 2009.
[140] Z. Said, "Thermophysical and optical properties of SWCNTs nanofluids," *International Communications in Heat and Mass Transfer,* vol. 78, pp. 207-213, 2016/11/01/ 2016.
[141] S. Bhattacharjee, "DLS and zeta potential – What they are and what they are not?," *Journal of Controlled Release,* vol. 235, pp. 337-351, 2016/08/10/ 2016.
[142] C. Anushree and J. Philip, "Assessment of long term stability of aqueous nanofluids using different experimental techniques," *Journal of Molecular Liquids,* vol. 222, pp. 350-358, 2016/10/01/ 2016.
[143] N. Navarrete, A. Gimeno-Furió, J. Forner-Escrig, J. E. Juliá, and R. Mondragón, "Colloidal stability of molten salt –based nanofluids: Dynamic Light Scattering tests at high temperature conditions," *Powder Technology,* vol. 352, pp. 1-10, 2019/06/15/ 2019.
[144] W. Chamsa-ard, S. Brundavanam, C. C. Fung, D. Fawcett, and G. Poinern, "Nanofluid Types, Their Synthesis, Properties and Incorporation in Direct Solar Thermal Collectors: A Review," *Nanomaterials,* vol. 7, no. 6, 2017.
[145] B. LotfizadehDehkordi, A. Ghadimi, and H. S. C. Metselaar, "Box–Behnken experimental design for investigation of stability and thermal conductivity of TiO2 nanofluids," *Journal of Nanoparticle Research,* vol. 15, no. 1, p. 1369, 2013/01/01 2013.
[146] R. Li, L. Zhang, L. Shi, and P. Wang, "MXene Ti3C2: An Effective 2D Light-to-Heat Conversion Material," *ACS Nano,* vol. 11, no. 4, pp. 3752-3759, 2017/04/25 2017.
[147] A. Ghadimi, R. Saidur, and H. S. C. Metselaar, "A review of nanofluid stability properties and characterization in stationary conditions," *International Journal of Heat and Mass Transfer,* vol. 54, no. 17, pp. 4051-4068, 2011/08/01/ 2011.

[148] D. C. Gregg, "Practical organic chemistry (Vogel, Arthur I.)," *J. Chem. Educ.*, vol. 29, p. 320, 1952.
[149] I. M. Mahbubul *et al.*, "Effect of Ultrasonication Duration on Colloidal Structure and Viscosity of Alumina–Water Nanofluid," *Industrial & Engineering Chemistry Research*, vol. 53, no. 16, pp. 6677-6684, 2014/04/23 2014.
[150] A. Asadi *et al.*, "Effect of sonication characteristics on stability, thermophysical properties, and heat transfer of nanofluids: A comprehensive review," *Ultrasonics Sonochemistry*, vol. 58, p. 104701, 2019/11/01/ 2019.
[151] A. Asadi, I. M. Alarifi, V. Ali, and H. M. Nguyen, "An experimental investigation on the effects of ultrasonication time on stability and thermal conductivity of MWCNT-water nanofluid: Finding the optimum ultrasonication time," *Ultrasonics Sonochemistry*, vol. 58, p. 104639, 2019/11/01/ 2019.
[152] A. Afzal, I. Nawfal, I. M. Mahbubul, and S. S. Kumbar, "An overview on the effect of ultrasonication duration on different properties of nanofluids," *Journal of Thermal Analysis and Calorimetry*, vol. 135, no. 1, pp. 393-418, 2019/01/01 2019.
[153] M. Kamalgharibi, F. Hormozi, S. A. H. Zamzamian, and M. M. Sarafraz, "Experimental studies on the stability of CuO nanoparticles dispersed in different base fluids: influence of stirring, sonication and surface active agents," *Heat and Mass Transfer*, vol. 52, no. 1, pp. 55-62, 2016/01/01 2016.
[154] Z. Chen, A. Shahsavar, A. A. A. A. Al-Rashed, and M. Afrand, "The impact of sonication and stirring durations on the thermal conductivity of alumina-liquid paraffin nanofluid: An experimental assessment," *Powder Technology*, vol. 360, pp. 1134-1142, 2020/01/15/ 2020.
[155] D. H. Fontes, G. Ribatski, and E. P. Bandarra Filho, "Experimental evaluation of thermal conductivity, viscosity and breakdown voltage AC of nanofluids of carbon nanotubes and diamond in transformer oil," *Diamond and Related Materials*, vol. 58, pp. 115-121, 2015/09/01/ 2015.
[156] B. Munkhbayar, M. R. Tanshen, J. Jeoun, H. Chung, and H. Jeong, "Surfactant-free dispersion of silver nanoparticles into MWCNT-aqueous nanofluids prepared by one-step technique and their thermal characteristics," *Ceramics International*, vol. 39, no. 6, pp. 6415-6425, 2013/08/01/ 2013.
[157] J. Boopathy, R. Pari, M. Kavitha, and P. C. Angelo, "Preparation of nano fluids by mechanical method," *AIP Conference Proceedings*, vol. 1461, no. 1, pp. 218-221, 2012/07/23 2012.
[158] S. Mukherjee, P. C. Mishra, and P. Chaudhuri, "Stability of Heat Transfer Nanofluids – A Review," *ChemBioEng Reviews*, vol. 5, no. 5, pp. 312-333, 2018/10/01 2018.
[159] B. M. Paramashivaiah and C. R. Rajashekhar, "Studies on effect of various surfactants on stable dispersion of graphene nano particles in simarouba biodiesel," *IOP Conference Series: Materials Science and Engineering*, vol. 149, p. 012083, 2016/09 2016.
[160] H. Vatanparast, F. Shahabi, A. Bahramian, A. Javadi, and R. Miller, "The Role of Electrostatic Repulsion on Increasing Surface Activity of Anionic Surfactants in the Presence of Hydrophilic Silica Nanoparticles," *Scientific Reports*, vol. 8, no. 1, p. 7251, 2018/05/08 2018.
[161] A. Amiri, M. Naraghi, G. Ahmadi, M. Soleymaniha, and M. Shanbedi, "A review on liquid-phase exfoliation for scalable production of pure graphene, wrinkled, crumpled and functionalized graphene and challenges," *FlatChem*, vol. 8, pp. 40-71, 2018/03/01/ 2018.

[162] D. Parviz, S. Das, H. S. T. Ahmed, F. Irin, S. Bhattacharia, and M. J. Green, "Dispersions of Non-Covalently Functionalized Graphene with Minimal Stabilizer," *ACS Nano,* vol. 6, no. 10, pp. 8857-8867, 2012/10/23 2012.
[163] A. Ghosh, K. V. Rao, S. J. George, and C. N. R. Rao, "Noncovalent Functionalization, Exfoliation, and Solubilization of Graphene in Water by Employing a Fluorescent Coronene Carboxylate," *Chemistry – A European Journal,* vol. 16, no. 9, pp. 2700-2704, 2010/03/01 2010.
[164] J. M. Englert *et al.*, "Soluble Graphene: Generation of Aqueous Graphene Solutions Aided by a Perylenebisimide-Based Bolaamphiphile," *Advanced Materials,* vol. 21, no. 42, pp. 4265-4269, 2009/11/13 2009.
[165] S. S. J. Aravind, P. Baskar, T. T. Baby, R. K. Sabareesh, S. Das, and S. Ramaprabhu, "Investigation of Structural Stability, Dispersion, Viscosity, and Conductive Heat Transfer Properties of Functionalized Carbon Nanotube Based Nanofluids," *The Journal of Physical Chemistry C,* vol. 115, no. 34, pp. 16737-16744, 2011/09/01 2011.
[166] H. S. Xue, J. R. Fan, Y. C. Hu, R. H. Hong, and K. F. Cen, "The interface effect of carbon nanotube suspension on the thermal performance of a two-phase closed thermosyphon," *Journal of Applied Physics,* vol. 100, no. 10, p. 104909, 2006/11/15 2006.
[167] A. Amiri *et al.*, "Pool boiling heat transfer of CNT/water nanofluids," *Applied Thermal Engineering,* vol. 71, no. 1, pp. 450-459, 2014/10/05/ 2014.
[168] M. Shanbedi, S. Zeinali Heris, M. Baniadam, and A. Amiri, "The Effect of Multi-Walled Carbon Nanotube/Water Nanofluid on Thermal Performance of a Two-Phase Closed Thermosyphon," *Experimental Heat Transfer,* vol. 26, no. 1, pp. 26-40, 2013/01/01 2013.
[169] M. N. A. W. M. Yazid, N. A. C. Sidik, R. Mamat, and G. Najafi, "A review of the impact of preparation on stability of carbon nanotube nanofluids," *International Communications in Heat and Mass Transfer,* vol. 78, pp. 253-263, 2016/11/01/ 2016.
[170] A. Amiri, M. Shanbedi, B. T. Chew, S. N. Kazi, and K. H. Solangi, "Toward improved engine performance with crumpled nitrogen-doped graphene based water–ethylene glycol coolant," *Chemical Engineering Journal,* vol. 289, pp. 583-595, 2016/04/01/ 2016.
[171] E. Ettefaghi, B. Ghobadian, A. Rashidi, G. Najafi, M. H. Khoshtaghaza, and S. Pourhashem, "Preparation and investigation of the heat transfer properties of a novel nanofluid based on graphene quantum dots," *Energy Conversion and Management,* vol. 153, pp. 215-223, 2017/12/01/ 2017.
[172] D. Lee, J.-W. Kim, and B. G. Kim, "A New Parameter to Control Heat Transport in Nanofluids: Surface Charge State of the Particle in Suspension," *The Journal of Physical Chemistry B,* vol. 110, no. 9, pp. 4323-4328, 2006/03/01 2006.
[173] H. Xie, H. Lee, W. Youn, and M. Choi, "Nanofluids containing multiwalled carbon nanotubes and their enhanced thermal conductivities," *Journal of Applied Physics,* vol. 94, no. 8, pp. 4967-4971, 2003/10/15 2003.
[174] P. I. P. Soares *et al.*, "Iron oxide nanoparticles stabilized with a bilayer of oleic acid for magnetic hyperthermia and MRI applications," *Applied Surface Science,* vol. 383, pp. 240-247, 2016/10/15/ 2016.
[175] S. Umar, F. Sulaiman, N. Abdullah, and S. N. Mohamad, "Investigation of the effect of pH adjustment on the stability of nanofluid," *AIP Conference Proceedings,* vol. 2031, no. 1, p. 020031, 2018/11/29 2018.
[176] B. Smith *et al.*, "Colloidal Properties of Aqueous Suspensions of Acid-Treated, Multi-Walled Carbon Nanotubes," *Environmental Science & Technology,* vol. 43, no. 3, pp. 819-825, 2009/02/01 2009.

[177] K. A. Wepasnick, B. A. Smith, J. L. Bitter, and D. Howard Fairbrother, "Chemical and structural characterization of carbon nanotube surfaces," *Analytical and Bioanalytical Chemistry,* vol. 396, no. 3, pp. 1003-1014, 2010/02/01 2010.
[178] A. Ghozatloo, M. Shariaty-Niasar, and A. M. Rashidi, "Preparation of nanofluids from functionalized Graphene by new alkaline method and study on the thermal conductivity and stability," *International Communications in Heat and Mass Transfer,* vol. 42, pp. 89-94, 2013/03/01/ 2013.
[179] Q. Yu, Y. J. Kim, and H. Ma, "Nanofluids with plasma treated diamond nanoparticles," *Applied Physics Letters,* vol. 92, no. 10, p. 103111, 2008/03/10 2008.
[180] K.-J. Park, D. Jung, and S. E. Shim, "Nucleate boiling heat transfer in aqueous solutions with carbon nanotubes up to critical heat fluxes," *International Journal of Multiphase Flow,* vol. 35, no. 6, pp. 525-532, 2009/06/01/ 2009.
[181] K. Birdi, *Handbook of surface and colloid chemistry*. CRC press, 2015.
[182] E. Piacenza, A. Presentato, and R. J. Turner, "Stability of biogenic metal(loid) nanomaterials related to the colloidal stabilization theory of chemical nanostructures," *Critical Reviews in Biotechnology,* Review vol. 38, no. 8, pp. 1137-1156, 2018.
[183] M. Shanbedi, S. Zeinali Heris, and A. Maskooki, "Experimental investigation of stability and thermophysical properties of carbon nanotubes suspension in the presence of different surfactants," *Journal of Thermal Analysis and Calorimetry,* vol. 120, no. 2, pp. 1193-1201, 2015/05/01 2015.
[184] Q. Y. Tang, I. Shafiq, Y. C. Chan, N. B. Wong, and R. Cheung, "Study of the Dispersion and Electrical Properties of Carbon Nanotubes Treated by Surfactants in Dimethylacetamide," *Journal of Nanoscience and Nanotechnology,* vol. 10, no. 8, pp. 4967-4974, // 2010.
[185] S. Biggs and T. W. Healy, "Electrosteric stabilisation of colloidal zirconia with low-molecular-weight polyacrylic acid. An atomic force microscopy study," *Journal of the Chemical Society, Faraday Transactions,* 10.1039/FT9949003415 vol. 90, no. 22, pp. 3415-3421, 1994.
[186] E. González, M. Paulis, and M. J. Barandiaran, "Effect of controlled length acrylic acid-based electrosteric stabilizers on latex film properties," *European Polymer Journal,* vol. 59, pp. 122-128, 2014/10/01/ 2014.
[187] K. Manojkumar, A. Sivaramakrishna, and K. Vijayakrishna, "A short review on stable metal nanoparticles using ionic liquids, supported ionic liquids, and poly(ionic liquids)," *Journal of Nanoparticle Research,* vol. 18, no. 4, p. 103, 2016/04/12 2016.
[188] H. J. Kong, S. G. Bike, and V. C. Li, "Electrosteric stabilization of concentrated cement suspensions imparted by a strong anionic polyelectrolyte and a non-ionic polymer," *Cement and Concrete Research,* vol. 36, no. 5, pp. 842-850, 2006/05/01/ 2006.
[189] R. Bandyopadhyaya, E. Nativ-Roth, O. Regev, and R. Yerushalmi-Rozen, "Stabilization of Individual Carbon Nanotubes in Aqueous Solutions," *Nano Letters,* vol. 2, no. 1, pp. 25-28, 2002/01/01 2002.
[190] S. Chakraborty, I. Sengupta, I. Sarkar, S. K. Pal, and S. Chakraborty, "Effect of surfactant on thermo-physical properties and spray cooling heat transfer performance of Cu-Zn-Al LDH nanofluid," *Applied Clay Science,* vol. 168, pp. 43-55, 2019/02/01/ 2019.
[191] J. Yu, N. Grossiord, C. E. Koning, and J. Loos, "Controlling the dispersion of multi-wall carbon nanotubes in aqueous surfactant solution," *Carbon,* vol. 45, no. 3, pp. 618-623, 2007/03/01/ 2007.
[192] L. Fedele, L. Colla, S. Bobbo, S. Barison, and F. Agresti, "Experimental stability analysis of different water-based nanofluids," *Nanoscale Research Letters,* vol. 6, no. 1, p. 300, 2011/04/06 2011.

[193] X. Li, D. Zhu, and X. Wang, "Evaluation on dispersion behavior of the aqueous copper nano-suspensions," *Journal of Colloid and Interface Science,* vol. 310, no. 2, pp. 456-463, 2007/06/15/ 2007.
[194] M. Iqbal *et al.*, "High temperature stability and low adsorption of sub-100nm magnetite nanoparticles grafted with sulfonated copolymers on Berea sandstone in high salinity brine," *Colloids and Surfaces A: Physicochemical and Engineering Aspects,* vol. 520, pp. 257-267, 2017/05/05/ 2017.
[195] H. Chen, S. Witharana, Y. Jin, C. Kim, and Y. Ding, "Predicting thermal conductivity of liquid suspensions of nanoparticles (nanofluids) based on rheology," *Particuology,* vol. 7, no. 2, pp. 151-157, 2009/04/01/ 2009.
[196] M. Hojjat, S. G. Etemad, R. Bagheri, and J. Thibault, "Rheological characteristics of non-Newtonian nanofluids: Experimental investigation," *International Communications in Heat and Mass Transfer,* vol. 38, no. 2, pp. 144-148, 2011/02/01/ 2011.
[197] V. Penkavova, J. Tihon, and O. Wein, "Stability and rheology of dilute TiO2-water nanofluids," *Nanoscale Research Letters,* vol. 6, no. 1, p. 273, 2011/03/31 2011.
[198] H. Chen, Y. Ding, and C. Tan, "Rheological behaviour of nanofluids," *New Journal of Physics,* vol. 9, no. 10, pp. 367-367, 2007/10/09 2007.
[199] P. C. Mishra, S. Mukherjee, S. K. Nayak, and A. Panda, "A brief review on viscosity of nanofluids," *International Nano Letters,* vol. 4, no. 4, pp. 109-120, 2014/12/01 2014.
[200] A. K. Sharma, A. K. Tiwari, and A. R. Dixit, "Rheological behaviour of nanofluids: A review," *Renewable and Sustainable Energy Reviews,* vol. 53, pp. 779-791, 2016/01/01/ 2016.
[201] C. T. Nguyen *et al.*, "Temperature and particle-size dependent viscosity data for water-based nanofluids – Hysteresis phenomenon," *International Journal of Heat and Fluid Flow,* vol. 28, no. 6, pp. 1492-1506, 2007/12/01/ 2007.
[202] D. P. Barai, B. A. Bhanvase, and V. K. Saharan, "Reduced Graphene Oxide-Fe3O4 Nanocomposite Based Nanofluids: Study on Ultrasonic Assisted Synthesis, Thermal Conductivity, Rheology, and Convective Heat Transfer," *Industrial & Engineering Chemistry Research,* vol. 58, no. 19, pp. 8349-8369, 2019/05/15 2019.
[203] A. V. Minakov, V. Y. Rudyak, and M. I. Pryazhnikov, "Systematic Experimental Study of the Viscosity of Nanofluids," *Heat Transfer Engineering,* pp. 1-17, 2020.
[204] V. Y. Rudyak and S. L. Krasnolutskii, "Dependence of the viscosity of nanofluids on nanoparticle size and material," *Physics Letters A,* vol. 378, no. 26, pp. 1845-1849, 2014/05/16/ 2014.
[205] V. Y. Rudyak and S. L. Krasnolutskii, "Simulation of the nanofluid viscosity coefficient by the molecular dynamics method," *Technical Physics,* vol. 60, no. 6, pp. 798-804, 2015/06/01 2015.
[206] C. T. Nguyen *et al.*, "Viscosity data for Al2O3–water nanofluid—hysteresis: is heat transfer enhancement using nanofluids reliable?," *International Journal of Thermal Sciences,* vol. 47, no. 2, pp. 103-111, 2008/02/01/ 2008.
[207] V. Y. Rudyak, S. V. Dimov, and V. V. Kuznetsov, "On the dependence of the viscosity coefficient of nanofluids on particle size and temperature," *Technical Physics Letters,* vol. 39, no. 9, pp. 779-782, 2013/09/01 2013.
[208] M. Jarahnejad *et al.*, "Experimental investigation on viscosity of water-based Al2O3 and TiO2 nanofluids," *Rheologica Acta,* vol. 54, no. 5, pp. 411-422, 2015/05/01 2015.
[209] H. D. Koca, S. Doganay, A. Turgut, I. H. Tavman, R. Saidur, and I. M. Mahbubul, "Effect of particle size on the viscosity of nanofluids: A review," *Renewable and Sustainable Energy Reviews,* vol. 82, pp. 1664-1674, 2018/02/01/ 2018.

[210] R. Sadri *et al.*, "An experimental study on thermal conductivity and viscosity of nanofluids containing carbon nanotubes," *Nanoscale Research Letters,* vol. 9, no. 1, p. 151, 2014/03/28 2014.
[211] T. X. Phuoc, M. Massoudi, and R.-H. Chen, "Viscosity and thermal conductivity of nanofluids containing multi-walled carbon nanotubes stabilized by chitosan," *International Journal of Thermal Sciences,* vol. 50, no. 1, pp. 12-18, 2011/01/01/ 2011.
[212] L. Wu, L. M. Keer, J. Lu, B. Song, and L. Gu, "Molecular dynamics simulations of the rheological properties of graphene–PAO nanofluids," *Journal of Materials Science,* vol. 53, no. 23, pp. 15969-15976, 2018/12/01 2018.
[213] W. H. Azmi, K. V. Sharma, R. Mamat, A. B. S. Alias, and I. I. Misnon, "Correlations for thermal conductivity and viscosity of water based nanofluids," *IOP Conference Series: Materials Science and Engineering,* vol. 36, p. 012029, 2012/09/18 2012.
[214] A. V. Minakov, V. Y. Rudyak, and M. I. Pryazhnikov, "Rheological behavior of water and ethylene glycol based nanofluids containing oxide nanoparticles," *Colloids and Surfaces A: Physicochemical and Engineering Aspects,* vol. 554, pp. 279-285, 2018/10/05/ 2018.
[215] J. Wang, J. Zhu, X. Zhang, and Y. Chen, "Heat transfer and pressure drop of nanofluids containing carbon nanotubes in laminar flows," *Experimental Thermal and Fluid Science,* vol. 44, pp. 716-721, 2013/01/01/ 2013.
[216] R. Mondragon, J. Enrique Julia, A. Barba, and J. C. Jarque, "Determination of the packing fraction of silica nanoparticles from the rheological and viscoelastic measurements of nanofluids," *Chemical Engineering Science,* vol. 80, pp. 119-127, 2012/10/01/ 2012.
[217] B. Aladag, S. Halelfadl, N. Doner, T. Maré, S. Duret, and P. Estellé, "Experimental investigations of the viscosity of nanofluids at low temperatures," *Applied Energy,* vol. 97, pp. 876-880, 2012/09/01/ 2012.
[218] M. A. K. Abdelhalim, M. M. Mady, and M. M. Ghannam, "Rheological and dielectric properties of different gold nanoparticle sizes," *Lipids in Health and Disease,* vol. 10, no. 1, p. 208, 2011/11/11 2011.
[219] J. Jeong, C. Li, Y. Kwon, J. Lee, S. H. Kim, and R. Yun, "Particle shape effect on the viscosity and thermal conductivity of ZnO nanofluids," *International Journal of Refrigeration,* vol. 36, no. 8, pp. 2233-2241, 2013/12/01/ 2013.
[220] H. Eshgarf and M. Afrand, "An experimental study on rheological behavior of non-Newtonian hybrid nano-coolant for application in cooling and heating systems," *Experimental Thermal and Fluid Science,* vol. 76, pp. 221-227, 2016/09/01/ 2016.
[221] J.-C. Yang, F.-C. Li, W.-W. Zhou, Y.-R. He, and B.-C. Jiang, "Experimental investigation on the thermal conductivity and shear viscosity of viscoelastic-fluid-based nanofluids," *International Journal of Heat and Mass Transfer,* vol. 55, no. 11, pp. 3160-3166, 2012/05/01/ 2012.
[222] M. Bahrami, M. Akbari, A. Karimipour, and M. Afrand, "An experimental study on rheological behavior of hybrid nanofluids made of iron and copper oxide in a binary mixture of water and ethylene glycol: Non-Newtonian behavior," *Experimental Thermal and Fluid Science,* vol. 79, pp. 231-237, 2016/12/01/ 2016.
[223] A. N. Omrani, E. Esmaeilzadeh, M. Jafari, and A. Behzadmehr, "Effects of multi walled carbon nanotubes shape and size on thermal conductivity and viscosity of nanofluids," *Diamond and Related Materials,* vol. 93, pp. 96-104, 2019/03/01/ 2019.
[224] K. Khanafer and K. Vafai, "A critical synthesis of thermophysical characteristics of nanofluids," *International Journal of Heat and Mass Transfer,* vol. 54, no. 19, pp. 4410-4428, 2011/09/01/ 2011.

[225] M. Corcione, "Empirical correlating equations for predicting the effective thermal conductivity and dynamic viscosity of nanofluids," *Energy Conversion and Management,* vol. 52, no. 1, pp. 789-793, 2011/01/01/ 2011.
[226] L. Syam Sundar, M. K. Singh, and A. C. M. Sousa, "Investigation of thermal conductivity and viscosity of Fe3O4 nanofluid for heat transfer applications," *International Communications in Heat and Mass Transfer,* vol. 44, pp. 7-14, 2013/05/01/ 2013.
[227] M. Hemmat Esfe, H. Rahimi Raki, M. R. Sarmasti Emami, and M. Afrand, "Viscosity and rheological properties of antifreeze based nanofluid containing hybrid nano-powders of MWCNTs and TiO2 under different temperature conditions," *Powder Technology,* vol. 342, pp. 808-816, 2019/01/15/ 2019.
[228] A. Einstein, "A new determination of molecular dimensions," *Ann. Phys.,* vol. 19, pp. 289-306, 1906 1906.
[229] H. C. Brinkman, "The viscosity of concentrated suspensions and solutions," *The Journal of Chemical Physics,* Article vol. 20, no. 4, p. 571, 1952.
[230] R. Roscoe, "The viscosity of suspensions of rigid spheres," *J. Appl. Phys.,* vol. 267, pp. 3-6, 1952.
[231] I. M. Krieger and T. J. Dougherty, "A Mechanism for Non-Newtonian Flow in Suspensions of Rigid Spheres," *Journal of Rheology,* Article vol. 3, no. 1, pp. 137-152, 1959.
[232] H. Brenner and D. W. Condiff, "Transport mechanics in systems of orientable particles. IV. convective transport," *Journal of Colloid and Interface Science,* vol. 47, no. 1, pp. 199-264, 1974/04/01/ 1974.
[233] D. J. Jeffrey and A. Acrivos, "The rheological properties of suspensions of rigid particles," *AIChE Journal,* Article vol. 22, no. 3, pp. 417-432, 1976.
[234] G. K. Batchelor, "The effect of Brownian motion on the bulk stress in a suspension of spherical particles," *Journal of Fluid Mechanics,* Article vol. 83, no. 1, pp. 97-117, 1977.
[235] A. L. Graham, "On the viscosity of suspensions of solid spheres," *Applied Scientific Research,* Article vol. 37, no. 3-4, pp. 275-286, 1981.
[236] H. Chang *et al.,* "Modeling study on the thermal performance of a modified cavity receiver with glass window and secondary reflector," *Energy Conversion and Management,* vol. 106, pp. 1362-1369, 2015/12/01/ 2015.
[237] M. J. Muhammad, I. A. Muhammad, N. A. Che Sidik, and M. N. A. W. Muhammad Yazid, "Thermal performance enhancement of flat-plate and evacuated tube solar collectors using nanofluid: A review," *International Communications in Heat and Mass Transfer,* vol. 76, pp. 6-15, 2016/08/01/ 2016.
[238] M. P. Islam and T. Morimoto, "Performance prediction of solar collector adsorber tube temperature using a nonlinear autoregressive model with eXogenous input," *Int. J. Comput. Appl.,* vol. 114, no. 12, pp. 24-32, 2015.
[239] K. M. Pandey and R. Chaurasiya, "A review on analysis and development of solar flat plate collector," *Renewable and Sustainable Energy Reviews,* vol. 67, pp. 641-650, 2017/01/01/ 2017.
[240] E. Natarajan and R. Sathish, "Role of nanofluids in solar water heater," *The International Journal of Advanced Manufacturing Technology,* 2009/07/01 2009.
[241] T. Yousefi, F. Veysi, E. Shojaeizadeh, and S. Zinadini, "An experimental investigation on the effect of Al2O3–H2O nanofluid on the efficiency of flat-plate solar collectors," *Renewable Energy,* vol. 39, no. 1, pp. 293-298, 2012/03/01/ 2012.

[242] S. K. Verma, A. K. Tiwari, S. Tiwari, and D. S. Chauhan, "Performance analysis of hybrid nanofluids in flat plate solar collector as an advanced working fluid," *Solar Energy*, vol. 167, pp. 231-241, 2018/06/01/ 2018.
[243] G. Colangelo and M. Milanese, "Numerical simulation of thermal efficiency of an innovative Al2O3 nanofluid solar thermal collector: Influence of nanoparticles concentration," *Thermal Science*, vol. 21, no. 6 Part B, pp. 2769-2779, 2017.
[244] N. Akram *et al.*, "Experimental investigations of the performance of a flat-plate solar collector using carbon and metal oxides based nanofluids," *Energy*, vol. 227, p. 120452, 2021/07/15/ 2021.
[245] M. Eltaweel, A. A. Abdel-Rehim, and A. A. A. Attia, "A comparison between flat-plate and evacuated tube solar collectors in terms of energy and exergy analysis by using nanofluid," *Applied Thermal Engineering*, vol. 186, p. 116516, 2021/03/05/ 2021.
[246] J. Ghaderian *et al.*, "Performance of copper oxide/distilled water nanofluid in evacuated tube solar collector (ETSC) water heater with internal coil under thermosyphon system circulations," *Applied Thermal Engineering*, vol. 121, pp. 520-536, 2017/07/05/ 2017.
[247] M. A. Sharafeldin and G. Gróf, "Efficiency of evacuated tube solar collector using WO3/Water nanofluid," *Renewable Energy*, vol. 134, pp. 453-460, 2019/04/01/ 2019.
[248] M. A. Sabiha, R. Saidur, S. Hassani, Z. Said, and S. Mekhilef, "Energy performance of an evacuated tube solar collector using single walled carbon nanotubes nanofluids," *Energy Conversion and Management*, vol. 105, pp. 1377-1388, 2015/11/15/ 2015.
[249] H. Kim, J. Kim, and H. Cho, "Experimental study on performance improvement of U-tube solar collector depending on nanoparticle size and concentration of Al2O3 nanofluid," *Energy*, vol. 118, pp. 1304-1312, 2017/01/01/ 2017.
[250] P. S. G. Natividade, G. de Moraes Moura, E. Avallone, E. P. Bandarra Filho, R. V. Gelamo, and J. C. d. S. I. Gonçalves, "Experimental analysis applied to an evacuated tube solar collector equipped with parabolic concentrator using multilayer graphene-based nanofluids," *Renewable Energy*, vol. 138, pp. 152-160, 2019/08/01/ 2019.
[251] S. Aberoumand, S. Ghamari, and B. Shabani, "Energy and exergy analysis of a photovoltaic thermal (PV/T) system using nanofluids: An experimental study," *Solar Energy*, vol. 165, pp. 167-177, 2018/05/01/ 2018.
[252] S. Alous, M. Kayfeci, and A. Uysal, "Experimental investigations of using MWCNTs and graphene nanoplatelets water-based nanofluids as coolants in PVT systems," *Applied Thermal Engineering*, vol. 162, p. 114265, 2019/11/05/ 2019.
[253] Y. L. Hewakuruppu *et al.*, "Limits of selectivity of direct volumetric solar absorption," *Solar Energy*, vol. 114, pp. 206-216, 2015/04/01/ 2015.
[254] M. Milanese, G. Colangelo, A. Cretì, M. Lomascolo, F. Iacobazzi, and A. de Risi, "Optical absorption measurements of oxide nanoparticles for application as nanofluid in direct absorption solar power systems – Part I: Water-based nanofluids behavior," *Solar Energy Materials and Solar Cells*, vol. 147, pp. 315-320, 2016/04/01/ 2016.
[255] M. Milanese, G. Colangelo, A. Cretì, M. Lomascolo, F. Iacobazzi, and A. de Risi, "Optical absorption measurements of oxide nanoparticles for application as nanofluid in direct absorption solar power systems – Part II: ZnO, CeO2, Fe2O3 nanoparticles behavior," *Solar Energy Materials and Solar Cells*, vol. 147, pp. 321-326, 2016/04/01/ 2016.
[256] X. Chen, P. Zhou, H. Yan, and M. Chen, "Systematically investigating solar absorption performance of plasmonic nanoparticles," *Energy*, vol. 216, p. 119254, 2021/02/01/ 2021.
[257] C. Guo, C. Liu, S. Jiao, R. Wang, and Z. Rao, "Introducing optical fiber as internal light source into direct absorption solar collector for enhancing photo-thermal conversion

performance of MWCNT-H2O nanofluids," *Applied Thermal Engineering*, vol. 173, p. 115207, 2020/06/05/ 2020.
[258] M. Karami, "Experimental investigation of first and second laws in a direct absorption solar collector using hybrid Fe3O4/SiO2 nanofluid," *Journal of Thermal Analysis and Calorimetry*, vol. 136, no. 2, pp. 661-671, 2019/04/01 2019.
[259] M. Karami, M. A. Akhavan-Bahabadi, S. Delfani, and M. Raisee, "Experimental investigation of CuO nanofluid-based Direct Absorption Solar Collector for residential applications," *Renewable and Sustainable Energy Reviews*, vol. 52, pp. 793-801, 2015/12/01/ 2015.
[260] S. Delfani, M. Karami, and M. A. A. Behabadi, "Performance characteristics of a residential-type direct absorption solar collector using MWCNT nanofluid," *Renewable Energy*, vol. 87, pp. 754-764, 2016/03/01/ 2016.
[261] Q. Li *et al.*, "Experimental and numerical investigation of volumetric versus surface solar absorbers for a concentrated solar thermal collector," *Solar Energy*, vol. 136, pp. 349-364, 2016/10/15/ 2016.
[262] H. Wang, X. Li, B. Luo, K. Wei, and G. Zeng, "The MXene/water nanofluids with high stability and photo-thermal conversion for direct absorption solar collectors: A comparative study," *Energy*, vol. 227, p. 120483, 2021/07/15/ 2021.
[263] A. Mwesigye and İ. H. Yılmaz, "Thermal and thermodynamic benchmarking of liquid heat transfer fluids in a high concentration ratio parabolic trough solar collector system," *Journal of Molecular Liquids*, vol. 319, p. 114151, 2020/12/01/ 2020.
[264] A. Menbari, A. A. Alemrajabi, and A. Rezaei, "Heat transfer analysis and the effect of CuO/Water nanofluid on direct absorption concentrating solar collector," *Applied Thermal Engineering*, vol. 104, pp. 176-183, 2016/07/05/ 2016.
[265] A. A. Hachicha, Z. Said, S. M. A. Rahman, and E. Al-Sarairah, "On the thermal and thermodynamic analysis of parabolic trough collector technology using industrial-grade MWCNT based nanofluid," *Renewable Energy*, vol. 161, pp. 1303-1317, 2020/12/01/ 2020.
[266] E. C. Okonkwo, E. A. Essien, E. Akhayere, M. Abid, D. Kavaz, and T. A. H. Ratlamwala, "Thermal performance analysis of a parabolic trough collector using water-based green-synthesized nanofluids," *Solar Energy*, vol. 170, pp. 658-670, 2018/08/01/ 2018.
[267] T. V. R. Sekhar, R. Prakash, G. Nandan, and M. Muthuraman, "Performance enhancement of a renewable thermal energy collector using metallic oxide nanofluids," *Micro & Nano Letters*, https://doi.org/10.1049/mnl.2017.0410 vol. 13, no. 2, pp. 248-251, 2018/02/01 2018.
[268] J. Subramani, P. K. Nagarajan, S. Wongwises, S. A. El-Agouz, and R. Sathyamurthy, "Experimental study on the thermal performance and heat transfer characteristics of solar parabolic trough collector using Al2O3 nanofluids," *Environmental Progress & Sustainable Energy*, https://doi.org/10.1002/ep.12767 vol. 37, no. 3, pp. 1149-1159, 2018/05/01 2018.
[269] S. E. Ghasemi and A. A. Ranjbar, "Thermal performance analysis of solar parabolic trough collector using nanofluid as working fluid: A CFD modelling study," *Journal of Molecular Liquids*, vol. 222, pp. 159-166, 2016/10/01/ 2016.
[270] S. K. Verma, A. K. Tiwari, and D. S. Chauhan, "Experimental evaluation of flat plate solar collector using nanofluids," *Energy Conversion and Management*, vol. 134, pp. 103-115, 2017/02/15/ 2017.
[271] W. S. Sarsam, S. N. Kazi, and A. Badarudin, "Thermal performance of a flat-plate solar collector using aqueous colloidal dispersions of multi-walled carbon nanotubes with different outside diameters," *Experimental Heat Transfer*, pp. 1-24, 2020.

[272] S. Choudhary, A. Sachdeva, and P. Kumar, "Time-based assessment of thermal performance of flat plate solar collector using magnesium oxide nanofluid," *International Journal of Sustainable Energy,* pp. 1-17, 2020.
[273] M. S. Gad and M. Said, "Effect of different nanofluids on performance analysis of flat plate solar collector," *Journal of Dispersion Science and Technology,* pp. 1-12, 2020.
[274] L. S. Sundar, E. V. Ramana, Z. Said, V. Punnaiah, K. V. V. Chandra Mouli, and A. C. M. Sousa, "Properties, heat transfer, energy efficiency and environmental emissions analysis of flat plate solar collector using nanodiamond nanofluids," *Diamond and Related Materials,* vol. 110, p. 108115, 2020/12/01/ 2020.
[275] M. Moravej *et al.*, "Enhancing the efficiency of a symmetric flat-plate solar collector via the use of rutile TiO2-water nanofluids," *Sustainable Energy Technologies and Assessments,* vol. 40, p. 100783, 2020/08/01/ 2020.
[276] A. M. Alklaibi, L. S. Sundar, and A. C. M. Sousa, "Experimental analysis of exergy efficiency and entropy generation of diamond/water nanofluids flow in a thermosyphon flat plate solar collector," *International Communications in Heat and Mass Transfer,* vol. 120, p. 105057, 2021/01/01/ 2021.
[277] Y. Tong, X. Chi, W. Kang, and H. Cho, "Comparative investigation of efficiency sensitivity in a flat plate solar collector according to nanofluids," *Applied Thermal Engineering,* vol. 174, p. 115346, 2020/06/25/ 2020.
[278] A. Allouhi and M. Benzakour Amine, "Heat pipe flat plate solar collectors operating with nanofluids," *Solar Energy Materials and Solar Cells,* vol. 219, p. 110798, 2021/01/01/ 2021.
[279] S. Choudhary, A. Sachdeva, and P. Kumar, "Time-based analysis of stability and thermal efficiency of flat plate solar collector using iron oxide nanofluid," *Applied Thermal Engineering,* vol. 183, p. 115931, 2021/01/25/ 2021.
[280] S. M. S. Hosseini and M. Shafiey Dehaj, "Assessment of TiO2 water-based nanofluids with two distinct morphologies in a U type evacuated tube solar collector," *Applied Thermal Engineering,* vol. 182, p. 116086, 2021/01/05/ 2021.
[281] I. M. Mahbubul, M. M. A. Khan, N. I. Ibrahim, H. M. Ali, F. A. Al-Sulaiman, and R. Saidur, "Carbon nanotube nanofluid in enhancing the efficiency of evacuated tube solar collector," *Renewable Energy,* vol. 121, pp. 36-44, 2018/06/01/ 2018.
[282] A. Ozsoy and V. Corumlu, "Thermal performance of a thermosyphon heat pipe evacuated tube solar collector using silver-water nanofluid for commercial applications," *Renewable Energy,* vol. 122, pp. 26-34, 2018/07/01/ 2018.
[283] R. Daghigh and P. Zandi, "Improving the performance of heat pipe embedded evacuated tube collector with nanofluids and auxiliary gas system," *Renewable Energy,* vol. 134, pp. 888-901, 2019/04/01/ 2019.
[284] M. A. Sharafeldin, G. Gróf, E. Abu-Nada, and O. Mahian, "Evacuated tube solar collector performance using copper nanofluid: Energy and environmental analysis," *Applied Thermal Engineering,* vol. 162, p. 114205, 2019/11/05/ 2019.
[285] M. S. Dehaj and M. Z. Mohiabadi, "Experimental investigation of heat pipe solar collector using MgO nanofluids," *Solar Energy Materials and Solar Cells,* vol. 191, pp. 91-99, 2019/03/01/ 2019.
[286] G. Sadeghi, S. Nazari, M. Ameri, and F. Shama, "Energy and exergy evaluation of the evacuated tube solar collector using Cu2O/water nanofluid utilizing ANN methods," *Sustainable Energy Technologies and Assessments,* vol. 37, p. 100578, 2020/02/01/ 2020.
[287] A. H. A. Al-Waeli, K. Sopian, M. T. Chaichan, H. A. Kazem, H. A. Hasan, and A. N. Al-Shamani, "An experimental investigation of SiC nanofluid as a base-fluid for a

photovoltaic thermal PV/T system," *Energy Conversion and Management,* vol. 142, pp. 547-558, 2017/06/15/ 2017.
[288] A. N. Al-Shamani, K. Sopian, S. Mat, H. A. Hasan, A. M. Abed, and M. H. Ruslan, "Experimental studies of rectangular tube absorber photovoltaic thermal collector with various types of nanofluids under the tropical climate conditions," *Energy Conversion and Management,* vol. 124, pp. 528-542, 2016/09/15/ 2016.
[289] G. Rajendiran, V. B. Kuppusamy, and S. Shanmugasundaram, "Experimental investigation of the effects of sonication time and volume concentration on the performance of PVT solar collector," *IET Renewable Power Generation,* https://doi.org/10.1049/iet-rpg.2018.5283 vol. 12, no. 12, pp. 1375-1381, 2018/09/01 2018.
[290] I. Wole-Osho, H. Adun, M. Adedeji, E. C. Okonkwo, D. Kavaz, and M. Dagbasi, "Effect of hybrid nanofluids mixture ratio on the performance of a photovoltaic thermal collector," *International Journal of Energy Research,* https://doi.org/10.1002/er.5619 vol. 44, no. 11, pp. 9064-9081, 2020/09/01 2020.
[291] X. Li *et al.*, "Numerical analysis of photothermal conversion performance of MXene nanofluid in direct absorption solar collectors," *Energy Conversion and Management,* vol. 226, p. 113515, 2020/12/15/ 2020.
[292] M. Esmaeili, M. Karami, and S. Delfani, "Performance enhancement of a direct absorption solar collector using copper oxide porous foam and nanofluid," *International Journal of Energy Research,* https://doi.org/10.1002/er.5305 vol. 44, no. 7, pp. 5527-5544, 2020/06/10 2020.
[293] K. Wang *et al.*, "Significant photothermal conversion enhancement of nanofluids induced by Rayleigh-Bénard convection for direct absorption solar collectors," *Applied Energy,* vol. 254, p. 113706, 2019/11/15/ 2019.
[294] A. A. Minea and W. M. El-Maghlany, "Influence of hybrid nanofluids on the performance of parabolic trough collectors in solar thermal systems: Recent findings and numerical comparison," *Renewable Energy,* vol. 120, pp. 350-364, 2018/05/01/ 2018.
[295] M. A. Ehyaei, A. Ahmadi, M. E. H. Assad, A. A. Hachicha, and Z. Said, "Energy, exergy and economic analyses for the selection of working fluid and metal oxide nanofluids in a parabolic trough collector," *Solar Energy,* vol. 187, pp. 175-184, 2019/07/15/ 2019.
[296] M. S. Bretado de los Rios, C. I. Rivera-Solorio, and A. J. García-Cuéllar, "Thermal performance of a parabolic trough linear collector using Al2O3/H2O nanofluids," *Renewable Energy,* vol. 122, pp. 665-673, 2018/07/01/ 2018.
[297] M. A. Rehan *et al.*, "Experimental performance analysis of low concentration ratio solar parabolic trough collectors with nanofluids in winter conditions," *Renewable Energy,* vol. 118, pp. 742-751, 2018/04/01/ 2018.
[298] O. Z. Sharaf, R. A. Taylor, and E. Abu-Nada, "On the colloidal and chemical stability of solar nanofluids: From nanoscale interactions to recent advances," *Physics Reports,* vol. 867, pp. 1-84, 2020/06/25/ 2020.
[299] M. Faizal, R. Saidur, S. Mekhilef, A. Hepbasli, and I. M. Mahbubul, "Energy, economic, and environmental analysis of a flat-plate solar collector operated with SiO2 nanofluid," *Clean Technologies and Environmental Policy,* vol. 17, no. 6, pp. 1457-1473, 2015/08/01 2015.
[300] S. Fotowat, S. Askar, M. Ismail, and A. Fartaj, "A study on corrosion effects of a water based nanofluid for enhanced thermal energy applications," *Sustainable Energy Technologies and Assessments,* vol. 24, pp. 39-44, 2017/12/01/ 2017.

[301] K. Elsaid, A. G. Olabi, T. Wilberforce, M. A. Abdelkareem, and E. T. Sayed, "Environmental impacts of nanofluids: A review," *Science of The Total Environment*, vol. 763, p. 144202, 2021/04/01/ 2021.
[302] I. Carrillo-Berdugo *et al.*, "Interface-inspired formulation and molecular-level perspectives on heat conduction and energy storage of nanofluids," *Scientific Reports*, vol. 9, no. 1, p. 7595, 2019/05/20 2019.